



CrossMark

2021 Census of Interstellar, Circumstellar, Extragalactic, Protoplanetary Disk, and Exoplanetary Molecules

Brett A. McGuire^{1,2,3} ¹ Department of Chemistry, Massachusetts Institute of Technology, Cambridge, MA 02139, USA² National Radio Astronomy Observatory, Charlottesville, VA 22903, USA³ Harvard-Smithsonian Center for Astrophysics, Cambridge, MA 02138, USA

Received 2021 June 30; revised 2021 September 24; accepted 2021 September 24; published 2022 March 14

Abstract

To date, 241 individual molecular species, composed of 19 different elements, have been detected in the interstellar and circumstellar medium by astronomical observations. These molecules range in size from two atoms to 70 and have been detected across the electromagnetic spectrum from centimeter wavelengths to the ultraviolet. This census presents a summary of the first detection of each molecular species, including the observational facility, wavelength range, transitions, and enabling laboratory spectroscopic work, as well as listing tentative and disputed detections. Tables of molecules detected in interstellar ices, external galaxies, protoplanetary disks, and exoplanetary atmospheres are provided. A number of visual representations of these aggregate data are presented and briefly discussed in context.

Unified Astronomy Thesaurus concepts: [Astrochemistry \(75\)](#); [Interstellar molecules \(849\)](#)

1. Introduction

Since the detection of the methylidyne (CH), the first molecule identified in the interstellar medium (ISM) (Dunham 1937; Swings & Rosenfeld 1937; McKellar 1940), observations of molecules have played crucial roles in a wide range of applications, from broadening our understanding of interstellar chemical evolution (Herbst & van Dishoeck 2009) and the formation of planets (Öberg et al. 2011) to providing exceptional astrophysical probes of physical conditions and processes (Friesen et al. 2013). Beginning in the early 1960s, the advent of radio astronomy has enabled a boom in the detection of new molecules, a trend that has continued at a nearly linear rate ever since.

Yet, despite the remarkably steady (and perhaps even accelerating) pace of new molecular detections, the number of as yet unidentified spectral features attributable to molecules is staggering. Indeed, these mysteries extend across the electromagnetic spectrum. In the radio, high-sensitivity, broadband spectral line surveys continue to reveal hundreds of features not assignable to transitions of molecules in spectroscopic databases (Cernicharo et al. 2013a), although there is evidence that a nontrivial number of these features may be due to transitions of vibrationally excited or rare isotopic species that have not been completely cataloged (Fortman et al. 2012).

At shorter wavelengths, the presence of the unidentified infrared emission bands (UIRs)—sharp, distinct emission features ubiquitous in ultraviolet (UV)-irradiated regions in our galaxy as well as seen in dozens of external galaxies—continues to elude conclusive molecular identification. A substantial body of literature now seems to favor the assignment of these emission features to polycyclic aromatic hydrocarbons (PAHs) (Tielens 2008), or at the very least sp^2 -hybridized aromatic carbon structures. The possibility that these features arise from mixed aromatic/aliphatic organic

nanoparticles has also been raised (Kwok & Zhang 2013). Regardless, it remains that no individual molecule has been definitely identified from UIR features, although three PAHs (1-cyanonaphthalene, 2-cyanonaphthalene, and indene) have now been detected at radio frequencies (Burkhardt et al. 2021; McGuire et al. 2021; Cernicharo et al. 2021a).

A yet older mystery are the diffuse interstellar bands (DIBs), first discovered by Mary Lea Heger in 1922 (McCall & Griffin 2013). Despite nearly a century of observation and laboratory work, these sharp features seen from the IR to the UV remain nearly completely unassigned. Campbell et al. (2015) recently reported the first attribution of a molecular carrier to a DIB that has not been disputed in the literature, that of C_{60}^+ . Yet hundreds of DIBs remain to be identified.

In the following sections, known, tentatively detected, and disputed interstellar, circumstellar, extragalactic, and exoplanetary molecules are cataloged and presented. The major lists in this paper are as follows (names are in-document hyperlinks in most PDF viewers):

1. [List of known interstellar and circumstellar molecules](#)
 - (a) [List of tentative detections](#)
 - (b) [List of disputed detections](#)
2. [List of molecules detected in external galaxies](#)
3. [List of molecules detected in interstellar ices](#)
4. [List of molecules detected in protoplanetary disks](#)

The primary list is that of the known interstellar and circumstellar molecules, and for each species in this list, a best-effort attempt was made to locate the first reported detection or detections of the species in the literature. The detection source or sources and instrument are given, and for some species a short description of any particularly noteworthy attributes is given as well. When available, a reference to the enabling laboratory spectroscopy work cited in the detection paper is provided. In the cases where the detection paper uses frequencies without apparent attribution to the laboratory spectroscopy, the most recent effort in the literature that would reasonably have been available at the time of publication of the detection is provided on a best-effort basis.



Original content from this work may be used under the terms of the [Creative Commons Attribution 4.0 licence](#). Any further distribution of this work must maintain attribution to the author(s) and the title of the work, journal citation and DOI.

Table 1
Commonly Used Facility Abbreviations

Abbreviation	Description
ALMA	Atacama Large Millimeter/submillimeter Array
APEX	Atacama Pathfinder Experiment
ARO	Arizona Radio Observatory
ATCA	Australian Telescope Compact Array
BIMA	Berkeley-Illinois-Maryland Array
CSO	Caltech Submillimeter Observatory
FCRAO	Five College Radio Astronomy Observatory
FUSE	Far Ultraviolet Spectroscopic Explorer
GBT	Green Bank Telescope
IRAM	Institut de Radioastronomie Millimétrique
IRTF	Infrared Radio Telescope Facility
ISO	Infrared Space Observatory
KPNO	Kitt Peak National Observatory
MWO	Millimeter-wave Observatory
NRAO	National Radio Astronomy Observatory
OVRO	Owens Valley Radio Observatory
PdBI	Plateau de Bure Interferometer
SEST	Swedish-ESO Submillimeter Telescope
SMA	Sub-millimeter Array
SMT	Sub-millimeter Telescope
SOFIA	Stratospheric Observatory for Infrared Astronomy
UKIRT	United Kingdom Infrared Telescope

The classification of a molecule as detected, tentatively detected, or disputed was made as agnostically as possible. Molecules are listed as detected if a literature source has claimed that detection and did not self-identify that detection as tentative and no subsequent literature could be found that disputes that claim. Tentative detections are listed only if the source has claimed the detection as such. Detections are considered disputed until a literature source has claimed that dispute has been resolved.

Subsets of the lists presented in this work are available both online and in numerous publications. Three exceptional web-based resources are of particular note with respect to the list of interstellar and circumstellar detections: the Cologne Database for Molecular Spectroscopy’s *List of Molecules in Space* (H.S. P. Müller),⁴ the *Astrochymist’s A Bibliography of Astromolecules* (D. Woon),⁵ and the list of M. Araki.⁶ As of the time of publication, these resources are providing the most frequently updated lists of known interstellar and circumstellar species. This publication is intended as a complement, rather than a supplement, to these resources.⁷

A Python 3 package, `astromol`, updated more frequently than this paper, contains the latest information regarding the census, as well as utilities to recreate all figures from the main text. It is accessible at <https://github.com/bmcguir2/astromol>. A brief description of the script and some of its function is provided in Appendix B. Immediately following this section is a list of updates since the prior 2018 census (McGuire 2018).

A list of commonly used abbreviations for facilities is given in Table 1. Tables 2 and 3 summarize the current list of known interstellar and circumstellar molecules. The column headers and individual molecule entries are active in-document hyperlinks in most PDF viewers. In Section 11, some aggregate

⁴ <https://www.astro.uni-koeln.de/cdms/molecules>

⁵ http://www.astrochymist.org/astrochymist_ism.html

⁶ http://www.rs.kagu.tus.ac.jp/tsukilab/research_seikanlist.html

⁷ Suggested updates, corrections, and comments can be directed to brettmc@mit.edu.

analysis of the data is presented. All figures can be recreated, and customized, using the provided `astromol` package.

2. Changes since 2018 Census

2.1. Content Updates

Since the 2018 census release, a number of new detections of molecules in the interstellar and circumstellar media, protoplanetary disks, external galaxies, and exoplanetary atmospheres have been added. These reflect new detections published in the literature as of 1 June 2021. Where necessary, detections have been moved out of “tentative” or “disputed.” All figures, tables, and graphs have been updated to reflect new detections. References to numbers, percentages, and so forth throughout the text have been updated to reflect new values. All figures and tables have been updated to reflect the new values. Finally, the previous set of Python scripts has been retired. These have been replaced by the `astromol` package. All figures and nearly all tables in the manuscript have been generated using this package.

2.2. 2018–2021 Highlights

The 2021 update adds a number of noteworthy new discoveries to the census, a few of which are highlighted below:

1. Thirty-five new ISM/circumstellar medium (CSM) detections have been reported.
2. Of these, more than half (22) were reported in TMC-1, primarily by observations with the GBT and the Yebes 40 m telescopes.
3. Seven new sulfur-bearing species have been identified, accounting for $\sim 25\%$ of all known sulfur-bearing species.
4. Seven new molecules with rings in their structures have been identified, nearly doubling the total number known.
5. Three individual PAH molecules have been identified in space, the first individual PAHs discovered outside the solar system.

3. Detection Techniques

As will be seen in the following pages, the vast majority of new molecule detections ($\sim 90\%$) have been made using radio astronomy techniques in the centimeter, millimeter, and submillimeter wavelength ranges. The manuscript, and indeed this section, is therefore inherently biased toward radio astronomy. To understand this bias, it is helpful to review the techniques, and their limitations, used to detect molecules across various wavelength ranges. In the end, it comes down to the energy required, and that which is available, to populate molecular energy levels for undergoing transitions at various wavelengths. This in turn dictates the environments and sight lines in which detections can be accomplished.

3.1. Radio Astronomy

Here, radio astronomical observations are roughly defined as those stretching from centimeter to far-infrared (hundreds of micrometers) wavelengths, or below ~ 2 THz (in frequency). The primary molecular signal arising in these regions is that of the rotational motion of molecules. For a linear molecule (symmetric and asymmetric tops follow similar, if more complex patterns), the rotational energy levels J are given, to first order, by

Table 2
List of Detected Interstellar Molecules with Two to Seven Atoms, Categorized by Number of Atoms, and Vertically Ordered by Detection Year

2 Atoms		3 Atoms		4 Atoms		5 Atoms		6 Atoms	7 Atoms
CH	NH	H ₂ O	MgCN	NH ₃	SiC ₃	HC ₃ N	C ₄ H ⁻	CH ₃ OH	CH ₃ CHO
CN	SiN	HCO ⁺	H ₃ ⁺	H ₂ CO	CH ₃	HCOOH	CNCHO	CH ₃ CN	CH ₃ CCH
CH ⁺	SO ⁺	HCN	SiCN	HNCO	C ₃ N ⁻	CH ₂ NH	HNCNH	NH ₂ CHO	CH ₃ NH ₂
OH	CO ⁺	OCS	AlNC	H ₂ CS	PH ₃	NH ₂ CN	CH ₃ O	CH ₃ SH	CH ₂ CHCN
CO	HF	HNC	SiNC	C ₂ H ₂	HCNO	H ₂ CCO	NH ₃ D ⁺	C ₂ H ₄	HC ₅ N
H ₂	N ₂	H ₂ S	HCP	C ₃ N	HOCN	C ₄ H	H ₂ NCO ⁺	C ₅ H	C ₆ H
SiO	CF ⁺	N ₂ H ⁺	CCP	HNCS	HSCN	SiH ₄	NCCNH ⁺	CH ₃ CN	c-C ₂ H ₄ O
CS	PO	C ₂ H	AlOH	HOCO ⁺	HOOH	c-C ₃ H ₂	CH ₃ Cl	HC ₂ CHO	CH ₂ CHOH
SO	O ₂	SO ₂	H ₂ O ⁺	C ₃ O	1-C ₃ H ⁺	CH ₂ CN	MgC ₃ N	H ₂ C ₄	C ₆ H ⁻
SiS	AlO	HCO	H ₂ Cl ⁺	1-C ₃ H	HMgNC	C ₅	HC ₃ O ⁺	C ₅ S	CH ₃ NCO
NS	CN ⁻	HNO	KCN	HCNH ⁺	HCCO	SiC ₄	NH ₂ OH	HC ₃ NH ⁺	HC ₅ O
C ₂	OH ⁺	HCS ⁺	FeCN	H ₃ O ⁺	CNCN	H ₂ CCC	HC ₃ S ⁺	C ₅ N	HOCH ₂ CN
NO	SH ⁺	HOC ⁺	HO ₂	C ₃ S	HONO	CH ₄	H ₂ CCS	HC ₄ H	HC ₄ NC
HCl	HCl ⁺	SiC ₂	TiO ₂	c-C ₃ H	MgCCH	HCCNC	C ₄ S	HC ₄ N	H ₃ HNH
NaCl	SH	C ₂ S	CCN	HC ₂ N	HCCS	HNCCC	CHOSH	c-H ₂ C ₃ O	c-C ₃ HCC
AlCl	TiO	C ₃	SiCSi	H ₂ CN		H ₂ COH ⁺		CH ₂ CNH	
KCl	ArH ⁺	CO ₂	S ₂ H					C ₅ N ⁻	
AlF	NS ⁺	CH ₂	HCS					HNCHCN	
PN	HeH ⁺	C ₂ O	HSC					SiH ₃ CN	
SiC	VO	MgNC	NCO					MgC ₄ H	
CP		NH ₂	CaNC					CH ₃ CO ⁺	
		NaCN	NCS					H ₂ CCCS	
		N ₂ O						CH ₂ CCH	

Note. Column headers and molecule formulas are in-document hyperlinks in most PDF viewers.

Table 3
List of Detected Interstellar Molecules with Eight or More Atoms, Categorized by Number of Atoms, and Vertically Ordered by Detection Year

8 Atoms	9 Atoms	10 Atoms	11 Atoms	12 Atoms	13 Atoms	PAHs	Fullerenes
HCOOCH ₃	CH ₃ OCH ₃	CH ₃ COCH ₃	HC ₉ N	C ₆ H ₆	C ₆ H ₅ CN	1-C ₁₀ H ₇ CN	C ₆₀
CH ₃ C ₃ N	CH ₃ CH ₂ OH	HOCH ₂ CH ₂ OH	CH ₃ C ₆ H	n-C ₃ H ₇ CN	HC ₁₁ N	2-C ₁₀ H ₇ CN	C ₆₀ ⁺
C ₇ H	CH ₃ CH ₂ CN	CH ₃ CH ₂ CHO	C ₂ H ₅ OCHO	i-C ₃ H ₇ CN		C ₉ H ₈	C ₇₀
CH ₃ COOH	HC ₇ N	CH ₃ C ₅ N	CH ₃ COOCH ₃	1-C ₅ H ₅ CN			
H ₂ C ₆	CH ₃ C ₄ H	CH ₃ CHCH ₂ O	CH ₃ COCH ₂ OH	2-C ₅ H ₅ CN			
CH ₂ OHCHO	C ₈ H	CH ₃ CH ₂ OH	C ₅ H ₆				
HC ₆ H	CH ₃ CONH ₂						
CH ₂ CHCHO	C ₈ H ⁻						
CH ₂ CCHCN	CH ₂ CHCH ₃						
NH ₂ CH ₂ CN	CH ₃ CH ₂ SH						
CH ₃ CHNH	HC ₇ O						
CH ₃ SiH ₃	CH ₃ NHCHO						
NH ₂ CONH ₂	H ₂ CCCHCCH						
HCCCH ₂ CN	HCCCHCHCN						
CH ₂ CHCCH	H ₂ CCHC ₃ N						

Note. Column headers and molecule formulas are in-document hyperlinks in most PDF viewers.

Equation (1):

$$E_J = BJ(J + 1), \quad (1)$$

where B is the rotational constant of the molecule; B is inversely proportional to the moment of inertia of the molecule (I):

$$B = \frac{h^2}{8\pi^2 I}, \quad (2)$$

where I is related to the reduced mass of the molecule (μ) and the radial extent of the mass (r):

$$I = \mu r^2. \quad (3)$$

Thus, lighter, smaller molecules will have large values of B (e.g., B [NH] = 490 GHz; Klaus et al. 1997), and heavier, larger molecules will have very small values of B (e.g., B [HC₉N] = 0.29 GHz; McCarthy et al. 2000). The frequencies of rotational transitions are given by the difference in energy levels (Equation (1)). Small molecules with large values of B , and correspondingly widely spaced energy levels, will have transitions at higher frequencies. Larger molecules, with smaller values of B , have closely spaced energy levels with transitions at lower frequencies.

Assuming NH and HC₉N are reasonable examples of the range of sizes of typical interstellar molecules, the ground-state rotational transitions ($J = 1 \rightarrow 0$) therefore fall between ~ 1

THz (NH) and ~ 500 MHz (HC_3N). As a result, observations of the pure rotational transitions of molecules are most often (nearly exclusively) conducted with radio astronomy facilities.

The absolute energies of these rotational levels also dictate the manner and environments in which they may be observed. The equivalent kT energy of most rotational levels of interstellar species is typically < 1000 K. In sufficiently dense environments, the distribution of energy between these levels is governed by collisions with other gas particles, a condition commonly referred to as local thermodynamic equilibrium (LTE), and is thus proportional (or equal) to the kinetic temperature of the gas. For warm regions such as hot cores, sufficient energy is available to produce a population distribution (excitation temperature, T_{ex}) well above the background radiation field, permitting the observation of emission from molecules undergoing rotational transitions (see, e.g., Belloche et al. 2013). Even in very cold regions, like TMC-1 ($T_{\text{ex}} = 5\text{--}10$ K), sufficient energy is still present to populate the lowest few rotational energy levels, and emission can still be seen (see, e.g., Kaifu et al. 2004). Conversely, when T_{ex} is below the background radiation field temperature (typically black-/graybody dust emission), molecules can be observed in absorption against this continuum (see, e.g., SH; Neufeld et al. 2012). Thus, a major advantage of radio observations is the ability to observe molecules in virtually any source, either in emission (due to the low energy needed to populate rotational levels) or in absorption against background continuum.

The major weakness of this technique is that it is blind to completely symmetric molecules (and largely blind to those that are highly symmetric). The strength of a rotational transition is proportional to the square of the permanent electric dipole moment of the molecule, and thus highly symmetric molecules often possess either very weak or no allowed pure rotational transitions (e.g., CH_4). Further, as the molecules increase in size and complexity, the number of accessible energy levels increases substantially, and thus the partitioning of population among these levels results in the number of molecules emitting/absorbing at a given frequency being decreased dramatically. Finally, molecules trapped in the condensed phase cannot undergo free rotation, making their detection by rotational spectroscopy in the radio impossible.

3.2. Infrared Astronomy

Pure rotational transitions of molecules in the radio occur within a single vibrational state of a molecule. This is often, but not exclusively, the ground vibrational state (see, e.g., Goldsmith et al. 1983). Transitions can also occur between vibrational states, the energies of which normally fall between 100 and many 1000 cm^{-1} (see, e.g., CO_2 ; Stull et al. 1962), and the resulting wavelengths of light between a few and a few hundred micrometers (i.e., the near- to far-infrared). Because these energy levels are substantially higher than those of pure rotational transitions, observations of emission from vibrational transitions usually require exceptionally warm regions or a radiative pumping mechanism to populate the levels. A common example of this effect is the aforementioned UIR features, which are often attributed to the infrared vibrational transitions of PAHs that have been pumped by an external, enhanced UV radiation field (Tielens 2008).

Absent these extraordinary excitation conditions, however, observation of vibrational transitions of molecules in the IR requires a background radiation source for the molecules to be

seen against in absorption. This places a number of limitations on the breadth of environments that can be probed with IR astronomy, as these sight lines must not only fortuitously contain a background source but also be optically thin enough to allow for the transmission of that light through the source. Even given these limitations, IR astronomy has been an extraordinarily useful tool for molecular astrophysics, particularly in the identification of molecules that are highly symmetric and lack strong or nonzero permanent dipole moments.

Beyond the identification of new species, however, a substantial benefit of IR astronomy is the ability to observe molecules condensed into interstellar ices. While condensed-phase molecules cannot undergo free rotation, their vibrational transitions remain accessible. These are largely seen in absorption, as the energy required to excite a transition into emission is likely to simply cause the molecule to desorb into the gas phase. As well, the vibrational motions are not unaffected by the condensed-phase environment. Both the physical structure of the solid and the molecular content of the surrounding material can alter the frequencies and line shapes of vibrational modes in small and large ways (see, e.g., Cooke et al. 2016). That said, these changes are often readily observable and quantifiable in the laboratory, and as a result, IR astronomy has provided a unique window into the molecular content of condensed-phase materials in the ISM.

3.3. Visible and UV Astronomy

The least well-represented wavelength ranges are the visible and UV. Transitions arising in these regions typically involve population transfer between electronic levels of molecules and atoms (see, e.g., N_2 ; Lofthus & Krupenie 1977). As with vibrational transitions in the infrared, no permanent dipole moment is required, enabling the detection of species otherwise blind to radio astronomy. The energy requirements for driving electronic transitions into emission are great enough that they are typically seen only in stellar atmospheres and other extremely energetic environments (see, e.g., emission from atomic Fe in Eta Carinae; Aller 1966). In these conditions, many molecules will simply dissociate into their constituent atoms.

Thus, like the infrared, the most likely avenue of molecular detection in the visible and UV is through absorption spectroscopy against a background source. This imposes similar restrictions to the infrared, but with the added challenge of the comparatively higher opacity of interstellar clouds at these wavelengths. As a result, the few detections in these ranges have all been in diffuse, line-of-sight (LOS) clouds to bright background continuum sources.

3.4. Summary

In summary, the detections presented below will be heavily biased toward radio astronomy. The primary molecular signal arising in the radio is that of transitions between rotational energy levels. The energetics of the environments in which most molecules are found is very well matched to that required to populate these rotational energy levels, as opposed to the vibrational and especially electronic levels dominating the IR and UV/Vis regimes. The resulting ability to observe in both emission and absorption, over a wide range of environments, substantially increases the opportunities for detection.

4. Known Interstellar Molecules

This section covers those species with published detections that have not been disputed. This list includes tentative detections and disputed detections that were later confirmed. Molecules are ordered first by number of atoms, then by year detected. A common name is provided after the molecular formula for most species. Note that for simplicity, due to differences in beam sizes, pointing centers, and nomenclature through time, detections toward subregions within the Sgr B2 and Orion sources have not been differentiated here. The exception to this is the Orion Bar photon-dominated/photo-dissociation region (PDR).

4.1. Two-Atom Molecules

4.1.1. CH (Methylidyne)

Swings & Rosenfeld (1937) suggested that an observed line at $\lambda = 4300 \text{ \AA}$ by Dunham (1937) using the Mount Wilson Observatory in diffuse gas toward a number of supergiant B stars might have been due to the ${}^2\Delta \leftarrow {}^2\Pi$ transition of CH, reported in the laboratory by Jevons (1932). McKellar (1940) later identified several additional transitions in observational data. The first radio identification was reported by Rydbeck et al. (1973) at 3335 MHz with the Onsala telescope toward more than a dozen sources using estimated fundamental rotational transition frequencies from Shklovskii (1953), Goss (1966), and Baird & Bredohl (1971). The first direct measurement of the CH rotational spectrum was reported by Brazier & Brown (1983).

4.1.2. CN (Cyano Radical)

Lines of CN were first reported using the Mount Wilson Observatory around $\lambda = 3875 \text{ \AA}$ by McKellar (1940) and Adams (1941) based on the laboratory work of Jenkins & Wooldridge (1938). Later, Jefferts et al. (1970) reported the first detection of rotational emission from CN by observation of the $J = 1 - 0$ transition at 113.5 GHz in Orion and W51 using the NRAO 36 foot (ft) telescope. Identification was made prior to laboratory observation of the rotational transitions of CN and was based on rotational constants derived from electronic transitions measured by Poletto & Rigutti (1965) and dipole moments measured by Thomson & Dalby (1968). The laboratory rotational spectra were first measured 7 years later by Dixon & Woods (1977).

4.1.3. CH⁺ (Methylidyne Cation)

Swings & Rosenfeld (1937) suggested that a set of three lines at $\lambda = 4233, 3958, \text{ and } 3745 \text{ \AA}$ seen with the Mount Wilson Observatory in diffuse gas belonged to a diatomic cation. Douglas & Herzberg (1941) confirmed the assignment to CH⁺ by laboratory observation of these lines in the ${}^1\Pi \leftarrow {}^1\Sigma$ transition. The first observation of rotational transitions of CH⁺ was reported by Cernicharo et al. (1997) toward NGC 7027 using ISO and based on rotational constants derived from rovibronic transitions measured by Carrington & Ramsay (1982).

4.1.4. OH (Hydroxyl Radical)

Weinreb et al. (1963) reported the first detection of OH through observation of its ground state, ${}^2\Pi_{3/2}$, $J = 3/2$, Λ -

doubled, $F = 2 \rightarrow 2$ and $F = 1 \rightarrow 1$ hyperfine transitions at 1666 MHz toward Cas A using the Millstone Hill Observatory. The frequencies were measured in the laboratory by Ehrenstein et al. (1959).

4.1.5. CO (Carbon Monoxide)

Wilson et al. (1970) reported the observation of the $J = 1 \rightarrow 0$ transition of CO toward Orion using the NRAO 36 ft telescope at a (velocity-shifted) frequency of 115,267.2 MHz, based on a rest frequency of 115,271.2 MHz from Cord et al. (1968).

4.1.6. H₂ (Molecular Hydrogen)

Molecular hydrogen was reported by Carruthers & Carruthers (1970) toward ξ Per using a spectrograph on an Aerobee-150 rocket launched from White Sands Missile Range. The $B^1\Sigma_u \leftarrow X^1\Sigma_g$ Lyman series in the range of 1000–1400 Å was observed and identified by direct comparison to an absorption cell observed with the same instrument used for the rocket observations.

4.1.7. SiO (Silicon Monoxide)

The $J = 3 \rightarrow 2$ transition of SiO at 130,246 MHz was observed by Wilson et al. (1971) toward Sgr B2 using the NRAO 36 ft telescope. The transition frequency was calculated based on the laboratory work of Raymonda (1970) and Törring (1968). SiO was the first confirmed silicon-containing species in the ISM.

4.1.8. CS (Carbon Monosulfide)

Penzias et al. (1971) reported the detection of the $J = 3 \rightarrow 2$ transition of CS at 146,969 MHz toward Orion, W51, IRC +10216, and DR21 using the NRAO 36 ft telescope. The laboratory microwave spectrum was first reported by Mockler & Bird (1955). CS was the first confirmed sulfur-containing species in the ISM.

4.1.9. SO (Sulfur Monoxide)

An unidentified line in NRAO 36 ft observations of Orion was assigned to the $J_K = 3_2 \rightarrow 2_1$ transition of SO by Gottlieb & Ball (1973) based on laboratory data from Winnewisser et al. (1964). The authors subsequently observed SO emission toward numerous other sources, as well as identifying the $4_3 \rightarrow 3_2$ transition using the 16 ft telescope at McDonald Observatory. SO was the first molecule detected in space in a ${}^3\Sigma$ ground electronic state via radio astronomy.

4.1.10. SiS (Silicon Monosulfide)

Morris et al. (1975) reported the detection of the $J = 6 \rightarrow 5$ and $5 \rightarrow 4$ transitions of SiS at 108,924.6 MHz and 90,771.85 MHz, respectively, based on the laboratory work of Hoefl (1965). The observations were conducted toward IRC+10216 using the NRAO 36 ft telescope.

4.1.11. NS (Nitrogen Sulfide)

Gottlieb et al. (1975) and Kuiper et al. (1975) simultaneously and independently reported the detection of NS. Gottlieb et al. (1975) observed the $J = 5/2 \rightarrow 3/2$ transition in the ${}^2\Pi_{1/2}$ electronic state at 115,154 MHz (Amano et al. 1969) toward

Sgr B2 using the 16 ft antenna at the University of Texas Millimeter Wave Observatory over three periods in 1973–1974 and confirmed the detection using the NRAO 36 ft telescope in May 1975. Kuiper et al. (1975) observed the same transitions toward Sgr B2 using the NRAO 36 ft telescope in February 1975.

4.1.12. C_2 (Dicarbon)

The detection of C_2 was reported by Souza & Lutz (1977) toward Cygnus OB2 No. 12 using the Smithsonian Institution’s Mount Hopkins Observatory. The detected lines at 10140 Å were measured in the laboratory by Phillips (1948).

4.1.13. NO (Nitric Oxide)

Liszt & Turner (1978) reported the identification of NO in the ISM toward Sgr B2 using the NRAO 36 ft telescope. The detection was based on the laboratory analysis of the hyperfine splitting in the $^2\Pi_{1/2} J = 3/2 \rightarrow 1/2$ transition near 150.1 GHz as reported in Gallagher & Johnson (1956).

4.1.14. HCl (Hydrogen Chloride)

Interstellar $H^{35}Cl$ was reported by Blake et al. (1985), who used the Kuiper Airborne Observatory to observe the $J = 1 \rightarrow 0$ transition at 625,918.8 MHz toward Orion. The laboratory transition frequencies were reported in De Lucia et al. (1971).

4.1.15. $NaCl$ (Sodium Chloride)

The detection of $NaCl$ was reported by Cernicharo et al. (1987a) toward IRC+10216 using IRAM 30 m observations of six transitions between 91 and 169 GHz, as well as the $J = 8 \rightarrow 7$ transition of $Na^{37}Cl$ at 101,961.9 MHz. The laboratory frequencies were obtained from Lovas & Tiemann (1974).

4.1.16. $AlCl$ (Aluminum Chloride)

The detection of $AlCl$ was reported by Cernicharo et al. (1987a) toward IRC+10216 using IRAM 30 m observations of four transitions between 87 and 160 GHz, as well as the $J = 10 \rightarrow 9$ and $11 \rightarrow 10$ transitions of $Al^{37}Cl$ at 142,322.5 MHz and 156,546.8 MHz, respectively. The laboratory frequencies were obtained from Lovas & Tiemann (1974).

4.1.17. KCl (Potassium Chloride)

The detection of KCl was reported by Cernicharo et al. (1987a) toward IRC+10216 using IRAM 30 m observations of six transitions between 100 and 161 GHz. The laboratory frequencies were obtained from Lovas & Tiemann (1974).

4.1.18. AlF (Aluminum Fluoride)

Cernicharo et al. (1987a) claimed a tentative detection of AlF toward IRC+10216 using IRAM 30 m observations of three transitions between 99 and 165 GHz. The laboratory frequencies were obtained from Lovas & Tiemann (1974). The detection was confirmed by Ziurys et al. (1994b) using CSO observations of IRC+10216. Three additional lines, the $J = 7 \rightarrow 6$, $8 \rightarrow 7$, and $10 \rightarrow 9$, were observed at 230,793, 263,749, and 329,642 MHz, respectively, based on laboratory data from Wyse et al. (1970).

4.1.19. PN (Phosphorous Mononitride)

Sutton et al. (1985) first suggested that a feature observed in their line survey data using the OVRO 10.4 m telescope toward Orion at 234,936 MHz could be attributed to the $J = 5 \rightarrow 4$ transition of PN , using the laboratory data reported in Wyse et al. (1972). Turner and Bally (1987) and Ziurys (1987) later simultaneously confirmed the detection of PN . Turner and Bally (1987) observed the $2 \rightarrow 1$, $3 \rightarrow 2$, and $5 \rightarrow 4$ transitions at 93,980, 140,968, and 234,936 MHz, respectively, toward Orion, W51, and Sgr B2 using the NRAO 12 m telescope. Ziurys (1987) observed the $2 \rightarrow 1$, $3 \rightarrow 2$, and $5 \rightarrow 4$ transitions toward Orion using the FCRAO 14 m telescope and the $6 \rightarrow 5$ using the NRAO 12 m telescope. The $2 \rightarrow 1$ transition was also observed toward Sgr B2 and W51. PN was the first phosphorous-containing molecule detected in the ISM.

4.1.20. SiC (Silicon Carbide)

Cernicharo et al. (1989) reported the detection of the SiC radical in IRC+10216 using the IRAM 30 m telescope. Fine structure and Λ -doubled lines were detected in the $J = 2 \rightarrow 1$, $4 \rightarrow 3$, and $6 \rightarrow 5$ transitions in the $^3\Pi$ electronic ground state near 81, 162, and 236 GHz, respectively, based on laboratory data presented in the same manuscript. The authors make note of unidentified lines suggestive of the SiC radical in earlier data toward IRC+10216 beginning in 1976, both in their own observations and in those of I. Dubois (unpublished) using the NRAO 36 ft telescope.

4.1.21. CP (Carbon Monophosphide)

Saito et al. (1989) measured the rotational spectrum of CP in the laboratory and conducted an astronomical search for the $N = 1 \rightarrow 0$ and $2 \rightarrow 1$ transitions at 48 and 96 GHz, respectively, using the Nobeyama 45 m telescope across several sources, resulting in nondetections. Guélin et al. (1990) subsequently reported the successful detection of the $2 \rightarrow 1$ and $5 \rightarrow 4$ (239 GHz) transitions toward IRC+10216 using the IRAM 30 m telescope.

4.1.22. NH (Imidogen Radical)

Meyer & Roth (1991) reported the detection of the $A^3\Pi - X^3\Sigma (0,0) R_1(0)$ line of NH in absorption toward ξ Per and HD 27778 at 3358 Å using the KPNO 4 m telescope. The laboratory rest frequencies were obtained from Dixon (1959). The earliest reported detection of rotational transitions of NH appears to be that of Cernicharo et al. (2000), who observed the $N_J = 2_3 \rightarrow 1_2$ transition at 974 GHz toward Sgr B2 with ISO. Although no laboratory reference is given, the frequencies used were presumably those of Klaus et al. (1997).

4.1.23. SiN (Silicon Nitride)

Turner (1992b) reported the detection of the $N = 2 \rightarrow 1$ and $6 \rightarrow 5$ transitions of SiN at 87 and 262 GHz, respectively, toward IRC+10216 using the NRAO 12 m telescope. The $2 \rightarrow 1$ transition was measured by Saito et al. (1983), and the frequency for the $6 \rightarrow 5$ was calculated from the constants given therein.

4.1.24. SO^+ (Sulfur Monoxide Cation)

The detection of SO^+ was reported by Turner (1992a) toward IC 443G using the NRAO 12 m telescope. The Λ -doubled ${}^2\Pi_{1/2}$, $J = 5/2 \rightarrow 3/2$ and $9/2 \rightarrow 7/2$ transitions at 116 and 209 GHz, respectively, were observed. The frequencies of the $5/2 \rightarrow 3/2$ transitions were measured by Amano et al. (1991), while those of the $9/2 \rightarrow 7/2$ transitions were calculated from the constants given therein.

4.1.25. CO^+ (Carbon Monoxide Cation)

CO^+ was first observed toward M17SW and NGC 7027 using the NRAO 12 m telescope by Latter et al. (1993). The $N = 2 \rightarrow 1$, $J = 3/2 \rightarrow 1/2$ and $5/2 \rightarrow 3/2$ near 236 GHz and the $3 \rightarrow 2$, $5/2 \rightarrow 3/2$ were observed based on the laboratory work of Sastry et al. (1981b). An earlier reported detection of the $2 \rightarrow 1$, $5/2 \rightarrow 3/2$ transition in Orion by Erickson et al. (1981), based on the laboratory data of Dixon & Woods (1975), was later definitely assigned to transitions of ${}^{13}CH_3OH$ by Blake et al. (1984).

4.1.26. HF (Hydrogen Fluoride)

Neufeld et al. (1997) reported the detection of the $J = 2 \rightarrow 1$ transition of HF at 2.5 THz toward Sgr B2 using ISO. The rest frequencies were measured in the laboratory by Nolt et al. (1987).

4.1.27. N_2 (Nitrogen)

Knauth et al. (2004) observed the $c'_4 {}^1\Sigma_u^+ - X^1\Sigma_g^+$ and $c'_3 {}^1\Sigma_u^+ - X^1\Sigma_g^+$ transitions of N_2 at 958.6 and 960.3 Å, respectively, using FUSE observations toward HD 124314. The oscillator strengths of the $c'_4 {}^1\Sigma_u^+ - X^1\Sigma_g^+$ transition were obtained from Stark et al. (2000), and the $c'_3 {}^1\Sigma_u^+ - X^1\Sigma_g^+$ transition from a private communication with G. Stark.

4.1.28. CF^+ (Fluoromethylidinium Cation)

The detection of CF^+ was reported by Neufeld et al. (2006) using IRAM 30 m and APEX 12 m observations of the $J = 1 \rightarrow 0$, $2 \rightarrow 1$, and $3 \rightarrow 2$ transitions at 102.6, 205.2, and 307.7 GHz, respectively, toward the Orion Bar. The laboratory frequencies were reported by Plummer et al. (1986).

4.1.29. PO (Phosphorous Monoxide)

Tenenbaum et al. (2007) reported the detection of the Λ -doubled $J = 11/2 \rightarrow 9/2$ and $13/2 \rightarrow 11/2$ transitions of PO at 240 and 284 GHz, respectively, using SMT 10 m observations of VY Canis Majoris. Although not cited, the frequencies were presumably obtained from the laboratory work of Kawaguchi et al. (1983) and Bailleux et al. (2002).

4.1.30. O_2 (Oxygen)

A tentative detection of molecular oxygen was reported by Goldsmith et al. (2002) in SWAS observations of ρ Oph, although more sensitive observations of the region by Pagani et al. (2003) using the Odin satellite could not confirm the detection and set an upper limit 3 times lower than that of Goldsmith et al. (2002). O_2 was only definitely detected several years later by Larsson et al. (2007) using observations of the $N_J = 1_1 \rightarrow 1_0$ transition at 118,750 MHz, again with the Odin satellite toward ρ Oph A. Although no citation is provided, the

frequencies were presumably obtained from the laboratory work of Endo & Mizushima (1982). Later, Goldsmith et al. (2011) reported the observation of the $N_J = 3_3 \rightarrow 1_2$, $5_4 \rightarrow 3_4$, and $7_6 \rightarrow 5_6$ transitions at 487, 774, and 1121 GHz, respectively, using Herschel/HIFI observations of Orion. Although there appears to be no citation to the laboratory data, these transition frequencies were likely taken from Drouin et al. (2010).

4.1.31. AlO (Aluminum Monoxide)

Tenenbaum & Ziurys (2009) reported the detection of the $N = 7 \rightarrow 6$, $6 \rightarrow 5$, and $4 \rightarrow 3$ transitions of AlO at 268, 230, and 153 GHz, respectively, toward VY Canis Majoris using the SMT 10 m telescope. The laboratory frequencies were reported in Yamada et al. (1990).

4.1.32. CN^- (Cyanide Anion)

The detection of CN^- was reported by Agúndez et al. (2010) in observations of IRC+10216 using the IRAM 30 m telescope. The $J = 1 \rightarrow 0$, $2 \rightarrow 1$, and $3 \rightarrow 2$ lines at 112.3, 224.5, and 336.8 GHz were observed, based on the laboratory work of Amano (2008b).

4.1.33. OH^+ (Hydroxyl Cation)

OH^+ was detected by Wyrowski et al. (2010) using APEX 12 m observations of Sgr B2. The $N = 1 \rightarrow 0$, $J = 0 \rightarrow 1$ transitions were detected in absorption at 909 GHz based on the laboratory work of Bekooy et al. (1985). Nearly simultaneously, Benz et al. (2010) reported the detection of the $1 \rightarrow 0$, $3/2 \rightarrow 1/2$ transitions at 1033 GHz toward W3 IRS5 using Herschel/HIFI, and Gerin et al. (2010) reported a detection along the LOS to W31C, also with Herschel/HIFI.

4.1.34. SH^+ (Sulfanylium Cation)

Benz et al. (2010) reported the detection of the $N_J = 1_2 \rightarrow 0_1$ transition of SH^+ at 526 GHz using Herschel/HIFI observations of W3. Although only a reference to the CDMS database is given, the frequency was almost certainly based on the laboratory work of Hovde & Saykally (1987) and Brown & Müller (2009). Although published after Benz et al. (2010), the first *submitted* detection appears to be that of Menten et al. (2011), who reported the detection of SH^+ in absorption toward Sgr B2, using the APEX 12 m telescope. The $N_J = 1_1 \rightarrow 0_1$ transition at 683 GHz was observed based on the laboratory work of Hovde & Saykally (1987) and Brown & Müller (2009). Benz et al. (2010) acknowledge the earlier submission of Menten et al. (2011) in their work.

4.1.35. HCl^+ (Hydrogen Chloride Cation)

The detection of HCl^+ was reported by De Luca et al. (2012) in Herschel/HIFI observations of W31C and W49N. Hyperfine and Λ -doubling structure was observed in the ${}^2\Pi_{3/2}$ $J = 5/2 \rightarrow 3/2$ transition of $H^{35}Cl^+$ at 1.444 THz toward both sources, and the same transition of $H^{37}Cl^+$ was also observed toward W31C. The laboratory work was described in Gupta et al. (2012).

4.1.36. SH (Mercapto Radical)

Neufeld et al. (2012) reported the detection of the ${}^2\Pi_{3/2}$ $J = 5/2 \rightarrow 3/2$ Λ -doubled transition of SH at 1383 GHz along the LOS to W49A using the GREAT instrument on SOFIA. The transition frequencies relied upon the work of Morino & Kawaguchi (1995) and Klisch et al. (1996).

4.1.37. TiO (Titanium Monoxide)

TiO was detected in VY Canis Majoris by Kamiński et al. (2013) using a combination of SMA and PdBI observations. Several fine structure components in the $J = 11 \rightarrow 10$, $J = 10 \rightarrow 9$, $J = 9 \rightarrow 8$, and $J = 7 \rightarrow 6$ transitions were observed between 221 and 352 GHz based on the laboratory work of Namiki et al. (1998).

4.1.38. ArH⁺ (Argonium)

Although a feature was initially observed in several Herschel data sets near 618 GHz (Neill et al. 2014), the attribution to ${}^{36}\text{ArH}^+$ was not readily apparent. On Earth, ${}^{40}\text{Ar}$ is 300 times more abundant than ${}^{36}\text{Ar}$ (Lee et al. 2006), and as no signal from ${}^{40}\text{ArH}^+$ was visible, ${}^{36}\text{ArH}^+$ seemed an unlikely carrier. Barlow et al. (2013), however, recognized that ${}^{36}\text{Ar}$ is the dominant isotope in the ISM (Cameron 1973) and identified the $J = 1 \rightarrow 0$ and $2 \rightarrow 1$ rotational lines of ${}^{36}\text{ArH}^+$ at 617.5 and 1234.6 GHz, respectively, in the Herschel/SPIRE spectra of the Crab Nebula. A citation is only given to the CDMS database, as no laboratory data appeared to exist for ${}^{36}\text{ArH}^+$. Instead, it is derived in the database to observational accuracy using isotopic scaling factors from other isotopologues.

4.1.39. NS⁺ (Nitrogen Sulfide Cation)

Cernicharo et al. (2018) reported both the laboratory spectroscopy and astronomical identification of NS⁺. The $J = 2 \rightarrow 1$ line has been observed with the IRAM 30 m telescope toward numerous sight lines, with confirming observations of the $3 \rightarrow 2$ and $5 \rightarrow 4$ in several.

4.1.40. HeH⁺ (Helium Hydride Cation)

Güsten et al. (2019) reported the astronomical identification of HeH⁺ in SOFIA observations of NGC 7027. The $J = 1 \rightarrow 0$ line was observed to have the same velocity profile as the CO $J = 11 \rightarrow 10$ in the same source. The identification was made based on the laboratory work of Perry et al. (2014).

4.1.41. VO (Vanadium Oxide)

Humphreys et al. (2019) reported the detection of VO in the circumstellar material of VY Canis Majoris using Hubble Space Telescope observations. They identify bandheads of the B⁴Π–X⁴Σ electronic transition around 7900 Å and 8600 Å based on the laboratory work of Cheung et al. (1994) and Adam et al. (1995).

4.2. Three-Atom Molecules

4.2.1. H₂O (Water)

Cheung et al. (1969) reported the detection of the $J_{K_a, K_c} = 6_{1,6} \rightarrow 5_{2,3}$ transition of H₂O at 22.2 GHz using the Hat Creek Observatory toward Sgr B2, Orion, and W49. No citation to the laboratory data appears to be given but

presumably was obtained from the work of Golden et al. (1948).

4.2.2. HCO⁺ (Formylium Cation)

Buhl & Snyder (1970) first reported the discovery of a bright emission feature at 89,190 MHz toward Orion, W51, W3(OH), L134, and Sgr A in observations with the NRAO 36 ft telescope and named the carrier “X-ogen.” Shortly thereafter, Klemperer (1970) suggested the attribution of this line to HCO⁺. The detection and attribution were confirmed by the laboratory observation of HCO⁺ by Woods et al. (1975).

4.2.3. HCN (Hydrogen Cyanide)

The first reported detection of HCN was that of Snyder & Buhl (1971), who observed the ground state $J = 1 \rightarrow 0$ transition at 88.6 GHz toward W3(OH), Orion, Sgr A, W49, W51, and DR 21 using the NRAO 36 ft telescope. The enabling laboratory spectroscopy was reported by Delucia & Gordy (1969).

4.2.4. OCS (Carbonyl Sulfide)

Emission from the $J = 9 \rightarrow 8$ transition of OCS at 109,463 MHz toward Sgr B2 was reported by Jefferts et al. (1971) using the NRAO 36 ft telescope. The laboratory spectroscopy was reported in King & Gordy (1954).

4.2.5. HNC (Hydrogen Isocyanide)

Both Zuckerman et al. (1972) and Snyder & Buhl (1972a) observed unidentified emission signal at 90.7 GHz using the NRAO 36 ft telescope toward W51 and NGC 2264, respectively. Snyder & Buhl (1972a) suggested this line to be due to HNC, which was confirmed 4 years later with the first laboratory measurement of the $J = 1 \rightarrow 0$ transition in the laboratory by Blackman et al. (1976).

4.2.6. H₂S (Hydrogen Sulfide)

Thaddeus et al. (1972) reported the detection of the $J_{K_a, K_c} = 1_{1,0} \rightarrow 1_{0,1}$ transition of *ortho*-H₂S at 168.7 GHz toward a number of sources with the NRAO 36 ft telescope. The laboratory transition frequencies were measured by Cupp et al. (1968).

4.2.7. N₂H⁺ (Protonated Nitrogen)

Turner (1974) first reported an unidentified emission line at 93.174 GHz with the NRAO 36 ft telescope toward a number of sources, including Sgr B2, DR 21(OH), NGC 2264, and NGC 6334N. In a companion letter, Green et al. (1974) suggested the carrier was N₂H⁺, based on theoretical calculations. Thaddeus & Turner (1975) claim the following year to have confirmed the detection by observing an exceptional match to the predicted ¹⁴N hyperfine splitting. Laboratory work by Saykally et al. (1976) solidified the detection.

4.2.8. C₂H (Ethyne Radical)

The detection of C₂H was reported by Tucker et al. (1974) through observation of four λ -doubled, hyperfine components of the $N = 1 \rightarrow 0$ transition near 87.3 GHz in NRAO 36 ft telescope observations of Orion and numerous other sources.

The assignment was made based on a calculated rotational constant under the assumption that the C–H and C≡C bonds had the same length as those already known in acetylene (C₂H₂). A linear structure was assumed based on the laboratory work of Cochran et al. (1964) and Graham et al. (1974). The confirming laboratory microwave spectroscopy was later reported by Sastry et al. (1981a).

4.2.9. SO₂ (Sulfur Dioxide)

SO₂ was reported in NRAO 36 ft telescope observations toward Orion and Sgr B2 by Snyder et al. (1975). The $J_{K_a, K_c} = 8_{1,7} \rightarrow 8_{0,8}$, $8_{3,5} \rightarrow 9_{2,8}$, and $7_{3,5} \rightarrow 8_{2,6}$ transitions at 83.7, 86.6, and 97.7 GHz, respectively, were observed in emission. The enabling laboratory microwave spectroscopy work was performed by Steenbeckeliers (1968) with additional computation analysis performed by Kirchhoff (1972).

4.2.10. HCO (Formyl Radical)

Snyder et al. (1976) reported the detection of the $N_{K_-, K_+} = 1_{0,1} - 0_{0,0}$, $J = 3/2 \rightarrow 1/2$, $F = 2 \rightarrow 1$ transition of HCO at 86,671 MHz toward W3, NGC 2024, W51, and K3-50 using the NRAO 36 ft telescope. The laboratory microwave spectroscopy was reported by Saito (1972).

4.2.11. HNO (Nitroxyl Radical)

The detection of HNO was first reported by Ulich et al. (1977), who observed the $J_{K_a, K_c} = 1_{0,1} \rightarrow 0_{0,0}$ transition at 81,477 MHz toward Sgr B2 and NGC 2024 using the NRAO 36 ft telescope. The laboratory frequency was measured by Saito & Takagi (1973). The initial detection was subject to significant controversy in the literature (see Snyder et al. 1993). Subsequent observation of additional lines by Hollis et al. (1991) and Ziurys et al. (1994c) confirmed the initial detection, aided by the laboratory work of Sastry et al. (1984).

4.2.12. HCS⁺ (Protonated Carbon Monosulfide)

Thaddeus et al. (1981) reported the detection of four harmonically spaced, unidentified lines in NRAO 36 ft and Bell 7 m telescope observations of Orion and Sgr B2. Based on the harmonic pattern, the lines were assigned to the $J = 2 \rightarrow 1$, $3 \rightarrow 2$, $5 \rightarrow 4$, and $6 \rightarrow 5$ transitions of HCS⁺ at 85, 128, 213, and 256 GHz, respectively. The confirming laboratory measurements were presented in a companion letter by Gudeman et al. (1981).

4.2.13. HOC⁺ (Hydroxymethylumylidene)

HOC⁺ was reported by Woods et al. (1983) in FCRAO and Onsala observations toward Sgr B2. The $J = 1 \rightarrow 0$ transition at 89,478 MHz was identified based on the laboratory work of Gudeman & Woods (1982). The detection was confirmed by Ziurys & Apponi (1995), who observed the $J = 2 \rightarrow 1$, and $3 \rightarrow 2$ transitions at 179 and 268 GHz, respectively.

4.2.14. c-SiC₂ (Silacyclopropynylidene)

Thaddeus et al. (1984) reported the detection of c-SiC₂ in NRAO 36 ft and Bell 7 m telescope observations of IRC +10216. Nine transitions between 93 and 171 GHz were observed and assigned based on the laboratory work of Michalopoulos et al. (1984), who derived rotational constants

from rotationally resolved optical transitions. Thaddeus et al. (1984) note that a number of these transitions had previously been observed in IRC+10216 and classified as unidentified by various other researchers as early as 1976. Suenram et al. (1989) and Gottlieb et al. (1989) subsequently reported the laboratory observation of the pure rotational spectrum. c-SiC₂ was the first molecular ring molecule identified in the ISM.

4.2.15. C₂S (Dicarbon Sulfide)

The detection of C₂S (³Σ⁻) was reported toward TMC-1 and Sgr B2 by Saito et al. (1987) using the Nobeyama 45 m telescope. The laboratory measurements were also performed by Saito et al. (1987). Although published a month earlier than Saito et al. (1987), Cernicharo et al. (1987d) reported the detection of C₂S in IRC+10216 using the laboratory results of Saito et al. (1987) from a preprint article.

4.2.16. C₃ (Tricarbon)

Hinkle et al. (1988) reported the detection of C₃ in KPNO 4 m telescope observations of IRC+10216. The ν_3 band of C₃ was observed and assigned based on combination differences from the work of Gausset et al. (1965) near 2030 cm⁻¹.

4.2.17. CO₂ (Carbon Dioxide)

D'Hendecourt & Jourdain de Muizon (1989) reported the observation of the ν_2 bending mode of CO₂ ice in absorption at 15.2 μm using archival spectra from the IRAS database toward AFGL 961, AFGL 989, and AFGL 890. The assignment was based on laboratory spectroscopy of mixed CO₂ ices (D'Hendecourt & Allamandola 1986). Gas-phase CO₂ was later observed toward numerous sight lines with ISO as a sharp absorption feature near 15 μm superimposed on a broad solid-phase absorption feature near the same frequency (van Dishoeck et al. 1996). The frequencies were obtained from Paso et al. (1980), while the band strengths used were taken from Reichle & Young (1972).

4.2.18. CH₂ (Methylene)

CH₂ was first detected by Hollis et al. (1989) in NRAO 12 m telescope observations of Orion. Several hyperfine components of the $N_{K_a, K_c} = 4_{0,4} \rightarrow 3_{1,3}$ transition were observed at 68 and 71 GHz and were assigned based on the laboratory work of Lovas et al. (1983). The detection was later confirmed by Hollis et al. (1995).

4.2.19. C₂O (Dicarbon Monoxide)

The detection of C₂O was reported by Ohishi et al. (1991) toward TMC-1 using the Nobeyama 45 m telescope. The $N_J = 1_2 \rightarrow 0_1$ and $2_3 \rightarrow 1_2$ transitions at 22 and 46 GHz, respectively, were assigned based on the laboratory data of Yamada et al. (1985).

4.2.20. MgNC (Magnesium Isocyanide)

Kawaguchi et al. (1993) successfully assigned a series of three unidentified harmonically spaced doublet emission lines detected by Guélin et al. (1986) in IRAM 30 m observations of IRC+10216 to the $N = 7 \rightarrow 6$, $8 \rightarrow 7$, and $9 \rightarrow 8$ transitions of MgNC based on their own laboratory spectroscopy of the

species. MgNC was the first magnesium-containing molecule to be detected in the ISM.

4.2.21. NH_2 (Amidogen Radical)

The detection of NH_2 was reported by van Dishoeck et al. (1993) toward Sgr B2 using CSO observations of five components of the $J = 3/2 \rightarrow 3/2$, $1/2 \rightarrow 1/2$, and $3/2 \rightarrow 1/2$ transitions at 426, 469, and 461 GHz, respectively, based on the laboratory work of Burkholder et al. (1988) and Charo et al. (1981). Some hyperfine splitting was resolved.

4.2.22. NaCN (Sodium Cyanide)

The detection of NaCN was reported by Turner et al. (1994) using NRAO 12 m telescope observations of IRC+10216. The $J_{K_a, K_c} = 5_{0,5} \rightarrow 4_{0,4}$, $6_{0,6} \rightarrow 5_{0,5}$, $7_{0,7} \rightarrow 6_{0,6}$, and $9_{0,9} \rightarrow 8_{0,8}$ transitions at 78, 93, 108, and 139 GHz, respectively, were observed. The assignments were based on predictions from the rotational constants derived in van Vaals et al. (1984).

4.2.23. N_2O (Nitrous Oxide)

Ziurys et al. (1994a) reported the detection of the $J = 3 \rightarrow 2$, $4 \rightarrow 3$, $5 \rightarrow 4$, and $6 \rightarrow 5$ transitions of N_2O at 75, 100, 125, and 150 GHz, respectively, in NRAO 12 m observations toward Sgr B2. The laboratory frequencies were obtained from Lovas (1978).

4.2.24. MgCN (Magnesium Cyanide Radical)

The detection of the MgCN radical was reported by Ziurys et al. (1995) in NRAO 12 m and IRAM 30 m observations of IRC+10216. The $N = 11 \rightarrow 10$, $10 \rightarrow 9$, and $9 \rightarrow 8$ transitions were observed, some with resolved spin-rotation splitting, based on the accompanying laboratory work of Anderson et al. (1994).

4.2.25. H_3^+

First suggested as a possible interstellar molecule in Martin et al. (1961), H_3^+ was detected 35 years later in absorption toward GL 2136 and W33A by Geballe & Oka (1996) using UKIRT to observe three transitions of the ν_2 fundamental band near 3.7 μm . The laboratory work was performed by Oka (1980).

4.2.26. SiCN (Silicon Monocyanide Radical)

Guélin et al. (2000) reported the detection of the SiCN radical in IRAM 30 m observations of IRC+10216. Three Λ -doubled transitions at 83, 94, and 105 GHz were detected based on the laboratory work by Apponi et al. (2000).

4.2.27. AlNC (Aluminum Isocyanide)

The detection of AlNC toward IRC+10216 with the IRAM 30 m telescope was reported by Ziurys et al. (2002). Five transitions between 132 and 251 GHz were assigned based on the laboratory work of Robinson et al. (1997).

4.2.28. SiNC (Silicon Monoisocyanide Radical)

Guélin et al. (2004) reported the detection of the SiNC radical in IRAM 30 m telescope observations of IRC+10216. Four rotational transitions between 83 and 134 GHz were

observed and assigned based on the laboratory work of Apponi et al. (2000).

4.2.29. HCP (Phosphaethyne)

Agúndez et al. (2007) reported the detection of four transitions ($J = 4 \rightarrow 3$ through $7 \rightarrow 6$) of HCP toward IRC+10216 using the IRAM 30 m telescope. The enabling laboratory work was performed by Bizzocchi et al. (2001) and references therein.

4.2.30. CCP (Dicarbon Phosphide Radical)

The detection of the CCP radical in ARO 12 m observations of IRC+10216 was reported by Halfen et al. (2008). Five transitions with partially resolved hyperfine splitting were identified and assigned based on laboratory work described in the same manuscript.

4.2.31. AlOH (Aluminum Hydroxide)

AlOH was detected in ARO 12 m and SMT observations of VY Canis Majoris by Tenenbaum & Ziurys (2010). The $J = 9 \rightarrow 8$, $7 \rightarrow 6$, and $5 \rightarrow 4$ transitions at 283, 220, and 157 GHz, respectively, were identified based on the enabling laboratory work of Apponi et al. (1993).

4.2.32. H_2O^+ (Oxidaniumyl Cation)

H_2O^+ was identified in Herschel/HIFI spectra toward DR21, Sgr B2, and NGC 6334 by Ossenkopf et al. (2010). Six hyperfine components of the $N_{K_a, K_c} = 1_{1,1} \rightarrow 0_{0,0}$, $J = 3/2 \rightarrow 1/2$ transition in the 2B_1 electronic ground state at 1.115 THz were observed. The assignments were based on a synthesis, reanalysis, and extrapolation of the laboratory work by Strahan et al. (1986) and Mürtz et al. (1998). Nearly simultaneously, Gerin et al. (2010) reported the observation of H_2O^+ along the LOS to W31C, also using Herschel/HIFI.

4.2.33. H_2Cl^+ (Chloronium Cation)

Lis et al. (2010) reported the observation of the $J_{K_a, K_c} = 2_{1,2} \rightarrow 1_{0,1}$ transitions of *ortho*- H^{35}Cl^+ and *ortho*- H^{35}Cl^+ near 781 GHz and the $J_{K_a, K_c} = 1_{1,1} \rightarrow 0_{0,0}$ transition of *para*- H^{35}Cl^+ near 485 GHz in absorption toward NGC 6334I and Sgr B2 using Herschel/HIFI. The frequencies were derived from the rotational constants determined in the laboratory work of Araki et al. (2001).

4.2.34. KCN (Potassium Cyanide)

The detection of KCN was reported by Pulliam et al. (2010) using ARO 12 m, IRAM 30 m, and SMT observations of IRC+10216. More than a dozen transitions between 85 and 250 GHz were assigned based on the laboratory work of Törring et al. (1980).

4.2.35. FeCN (Iron Cyanide)

Zack et al. (2011) reported the detection of six transitions of FeCN between 84 and 132 GHz in ARO 12 m observations of IRC+10216. The enabling laboratory spectroscopy was reported in Flory & Ziurys (2011), which was not yet published at the time of the publication of Zack et al. (2011).

4.2.36. HO_2 (Hydroperoxyl Radical)

The detection of HO_2 was reported in IRAM 30 m and APEX observations toward ρ Oph A by Parise et al. (2012). Several hyperfine components were observed in the $N_{K_a, K_c} = 2_{0,2} \rightarrow 1_{0,1}$ and $4_{0,4} \rightarrow 3_{0,3}$ transitions at 130 and 261 GHz, respectively. The laboratory work was performed by Beers & Howard (1975), Saito (1977), and Charo & De Lucia (1982).

4.2.37. TiO_2 (Titanium Dioxide)

TiO_2 was detected by Kamiński et al. (2013) in SMA and PdBI observations of VY Canis Majoris. More than two dozen transitions of TiO_2 were observed between 221 and 351 GHz based on the laboratory work of Brünken et al. (2008) and Kania et al. (2011).

4.2.38. CCN (Cyanomethylidyne)

Anderson & Ziurys (2014) reported the detection of CCN in ARO 12 m and SMT observations of IRC+10216. The $J = 9/2 \rightarrow 7/2$, $13/2 \rightarrow 11/2$, and $19/2 \rightarrow 17/2$ Λ -doubled transitions near 106, 154, and 225 GHz, respectively, were identified and assigned based on the laboratory work of Anderson et al. (2015), which was published several months later.

4.2.39. SiCSi (Disilicon Carbide)

A total of 112 transitions of SiCSi were observed in IRAM 30 m telescope observations of IRC+10216 between 80 and 350 GHz as reported by Cernicharo et al. (2015). The transition frequencies were derived based on the contemporaneous laboratory work of McCarthy et al. (2015).

4.2.40. S_2H (Hydrogen Disulfide)

Fuente et al. (2017) reported the detection of S_2H in IRAM 30 m observations of the Horsehead PDR region. Although Fuente et al. (2017) do not provide quantum numbers, they detect four lines corresponding to the unresolved hyperfine doublets of the $J_{K_a, K_c} = 6_{0,6} \rightarrow 5_{0,5}$ and $7_{0,7} \rightarrow 6_{0,6}$ transitions near 94 and 110 GHz, respectively. The laboratory analysis was described in Tanimoto et al. (2000).

4.2.41. HCS (Thioformyl Radical)

The detection of HCS was reported by Agúndez et al. (2018b) in IRAM 30 m observations of L483. Five resolved hyperfine components of the $N_{K_a, K_c} = 2_{0,2} \rightarrow 1_{0,1}$ transition of HCS near 81 GHz were identified based on the laboratory work of Habara et al. (2002).

4.2.42. HSC (Sulfhydryl Carbide Radical)

The detection of HSC was reported by Agúndez et al. (2018b) in IRAM 30 m observations of L483. Two resolved hyperfine components of the $N_{K_a, K_c} = 2_{0,2} \rightarrow 1_{0,1}$ transition of HSC near 81 GHz were identified based on the laboratory work of Habara & Yamamoto (2000).

4.2.43. NCO (Isocyanate Radical)

Marcelino et al. (2018) reported the detection of the NCO radical in IRAM 30 m observations of L483. Several hyperfine components of the $J = 7/2 \rightarrow 5/2$ and $9/2 \rightarrow 7/2$ transitions

near 81.4 and 104.6 GHz were identified and assigned based on the laboratory work of Saito & Amano (1970) and Kawaguchi et al. (1985).

4.2.44. CaNC (Calcium Isocyanide)

Cernicharo et al. (2019a) reported the detection of CaNC in IRAM 30 m observations of IRC+10216, the first calcium-bearing molecule detected in interstellar or circumstellar media. A total of nine doublets between 72.9 and 169.9 GHz corresponding to transitions between $N = 9 \rightarrow 8$ and $N = 21 \rightarrow 20$, some severely blended, were identified and assigned based on the laboratory work of Steimle et al. (1993) and Scurlock et al. (1994) and using a dipole moment from Steimle et al. (1992).

4.2.45. NCS (Thiocyanogen)

The detection of NCS in Yebes 40 m observations of TMC-1 was reported by Cernicharo et al. (2021f). Three hyperfine-split components of the $J = 5/2 \rightarrow 3/2$ transition of NCS at 42.7 GHz were identified and assigned based on the laboratory work of Amano & Amano (1991), McCarthy et al. (2003), and Maeda et al. (2007).

4.3. Four-Atom Molecules

4.3.1. NH_3 (Ammonia)

The first detection of NH_3 was reported by Cheung et al. (1968) by observation of its $(J, K) = (1, 1)$ and $(2, 2)$ inversion transitions in the Galactic center using a 20 m radio telescope located at Hat Creek Observatory. No references to the laboratory data are given, but the frequencies were likely derived from the accumulated works of Cleeton & Williams (1934), Gunther-Mohr et al. (1954), Kukolich (1965), and Kukolich (1967).

4.3.2. H_2CO (Formaldehyde)

Snyder et al. (1969) reported the detection of H_2CO in NRAO 140 ft telescope observations of more than a dozen interstellar sources. The $J_{K_a, K_c} = 1_{1,1} \rightarrow 1_{1,0}$ transition at 4830 MHz was observed without hyperfine splitting, based on the laboratory data of Shigenari (1967).

4.3.3. HNCO (Isocyanic Acid)

HNCO was observed in NRAO 36 ft observations of Sgr B2 by Snyder & Buhl (1972b). The $J_{K_a, K_c} = 4_{0,4} \rightarrow 3_{0,3}$ transition at 87,925 MHz was detected and assigned based on the laboratory work of Kewley et al. (1963). The detection was confirmed in a companion article with the observation of the $1_{0,1} \rightarrow 0_{0,0}$ transition by Buhl et al. (1972).

4.3.4. H_2CS (Thioformaldehyde)

Sinclair et al. (1973) reported the detection of H_2CS through Parkes 64 m observations of the Sgr B2. The $J_{K_a, K_c} = 2_{1,1} \rightarrow 2_{1,2}$ transition at 3139 MHz was identified and assigned based on the laboratory work of Johnson & Powell (1970).

4.3.5. C_2H_2 (Acetylene)

The detection of C_2H_2 was reported by Ridgway et al. (1976) in Mayall 4 m telescope observations of IRC+10216. The $\nu_1 + \nu_5$ combination band of acetylene at 4091 cm^{-1} was identified based on the laboratory work of Baldacci et al. (1973).

4.3.6. C_3N (Cyanoethynyl Radical)

Guélin & Thaddeus (1977) reported the tentative detection of C_3N in NRAO 36 ft observations of IRC+10216. They observed two sets of doublet transitions, with the center frequencies at 89 and 99 GHz. Based on calculated rotational constants, they tentatively assigned the emission to C_3N . Friberg et al. (1980) later confirmed the detection by observing the predicted $N = 3 \rightarrow 2$ transitions near 30 GHz. The laboratory spectra were subsequently measured by Gottlieb et al. (1983).

4.3.7. HNCS (Isothiocyanic Acid)

HNCS was detected by observation of the $J = 11 \rightarrow 10$, $9 \rightarrow 8$, and $8 \rightarrow 7$ transitions, among others, at 192, 106, and 94 GHz, respectively, in Bell 7 m and NRAO 36 ft telescope observations of Sgr B2 by Frerking et al. (1979). The laboratory frequencies were measured by Kewley et al. (1963).

4.3.8. $HOCO^+$ (Protonated Carbon Dioxide)

Thaddeus et al. (1981) reported the observation of a series of three lines in Bell 7 m observations of Sgr B2 they assigned to the $J = 6 \rightarrow 5$, $5 \rightarrow 4$, and $4 \rightarrow 3$ transitions of $HOCO^+$ at 128, 107, and 86 GHz, respectively, based on ab initio calculations by Green et al. (1976). The detection was later confirmed by laboratory observation of the rotational spectrum by Bogey et al. (1984).

4.3.9. C_3O (Tricarbon Monoxide)

The detection of C_3O was reported by Matthews et al. (1984) through NRAO 140 ft telescope observations of TMC-1. The $J = 2 \rightarrow 1$ transition at 19,244 MHz was observed and assigned based on laboratory work by Brown et al. (1983). Three further transitions up to $J = 9 \rightarrow 8$ were observed in a follow-up study in the same source by Brown et al. (1985b). The detection was confirmed by Kaifu et al. (2004) with the observation of numerous additional lines in Nobeyama 45 m observations of TMC-1.

4.3.10. $l\text{-}C_3H$ (Propynylidyne Radical)

The $l\text{-}C_3H$ radical was detected toward TMC-1 and IRC +10216 through a combination of observations with the Bell 7 m, University of Massachusetts 14 m, NRAO 36 ft, and Onsala 20 m telescopes as reported in Thaddeus et al. (1985a). A number of transitions between 33 and 103 GHz were identified based on the accompanying laboratory work of Gottlieb et al. (1985).

4.3.11. $HCNH^+$ (Protonated Hydrogen Cyanide)

$HCNH^+$ was reported in NRAO 12 m and MWO 4.9 m telescope observations of Sgr B2 by Ziurys & Turner (1986). The $J = 1 \rightarrow 0$, $2 \rightarrow 1$, and $3 \rightarrow 2$ transitions were targeted at 74, 148, and 222 GHz, respectively, based on frequencies estimated from the laboratory work of Altman et al. (1984) and

confirmed during the course of publication by the laboratory work of Bogey et al. (1985b).

4.3.12. H_3O^+ (Hydronium Cation)

Wootten et al. (1986) and Hollis et al. (1986) nearly simultaneously reported the detection of H_3O^+ . Wootten et al. (1986) used the NRAO 12 m telescope to search for the $J_K = 1_1 \rightarrow 2_1$ transition at 307.2 GHz in Orion and Sgr B2, reporting a detection in each. Hollis et al. (1986) also observed the same transition in both Orion and Sgr B2 with the NRAO 12 m telescope. Later, Wootten et al. (1991) reported the detection of a confirming line in Orion and Sgr B2 with the identification of the $3_2 \rightarrow 2_2$ transition of *ortho*- H_3O^+ using the CSO. These detections were based on the laboratory work of Plummer et al. (1985), Bogey et al. (1985a), and Liu & Oka (1985).

4.3.13. C_3S (Tricarbon Monosulfide Radical)

The detection of C_3S was reported by Yamamoto et al. (1987a). The authors measured the laboratory rotational spectrum of the molecule and assigned the $^1\Sigma J = 4 \rightarrow 3$, $7 \rightarrow 6$, and $8 \rightarrow 7$ lines at 23, 40, and 46 GHz, respectively, to previously unidentified lines in the observations of Kaifu et al. (1987) toward TMC-1 using the Nobeyama 45 m telescope.

4.3.14. $c\text{-}C_3H$ (Cyclopropenylidene Radical)

Yamamoto et al. (1987b) reported the detection of the hyperfine components of the $J = 5/2 \rightarrow 3/2$ and $3/2 \rightarrow 1/2$ transitions at 91.5 and 91.7 GHz, respectively, in Nobeyama 45 m observations of TMC-1. The enabling laboratory spectroscopy was presented in the same manuscript.

4.3.15. HC_2N (Cyanocarbene Radical)

Guélin & Cernicharo (1991) reported the detection of nine lines of HC_2N in IRAM 30 m observations of IRC+10216 between 72 and 239 GHz. The enabling laboratory work was presented in Saito et al. (1984) and Brown et al. (1990).

4.3.16. H_2CN (Methylene Amidogen Radical)

The detection of H_2CN was reported in NRAO 12 m observations of TMC-1 by Ohishi et al. (1994), who observed two hyperfine components of the $N_{K_a, K_c} = 1_{0,1} \rightarrow 0_{0,0}$ transition at 73.3 GHz. The laboratory spectroscopy was conducted by Yamamoto & Saito (1992).

4.3.17. SiC_3 (Silicon Tricarbide)

Apponi et al. (1999a) reported the detection of SiC_3 in NRAO 12 m observations of IRC+10216. Nine transitions of SiC_3 between 81 and 103 GHz were observed and assigned based on laboratory work by the same group, published shortly thereafter in McCarthy et al. (1999) and Apponi et al. (1999b).

4.3.18. CH_3 (Methyl Radical)

The detection of CH_3 was reported by Feuchtgruber et al. (2000) using ISO observations of the ν_2 Q -branch line at $16.5\ \mu\text{m}$ and the $R(0)$ line at $16.0\ \mu\text{m}$ toward Sgr A*. The enabling laboratory work was performed by Yamada et al. (1981). The first ground-based detection of CH_3 was described later by Knez et al. (2009).

4.3.19. C_3N^- (Cyanoethynyl Anion)

Both the laboratory spectroscopy and astronomical detection of C_3N^- were presented in Thaddeus et al. (2008). The anion was detected in IRAM 30 m observations of IRC+10216 in the $J = 10 \rightarrow 9$, $11 \rightarrow 10$, $14 \rightarrow 13$, and $15 \rightarrow 14$ transitions at 97, 107, 136, and 146 GHz, respectively.

4.3.20. PH_3 (Phosphine)

Agúndez et al. (2008) and Tenenbaum & Ziurys (2008) simultaneously and independently reported the tentative detection of PH_3 . Tenenbaum & Ziurys (2008) observed emission from the $J_K = 1_0 \rightarrow 0_0$ transition at 267 GHz toward IRC+10216 and CRL 2688 using the SMT telescope. Agúndez et al. (2008) observed the same transition toward IRC+10216 using the IRAM 30 m telescope and searched for the $J = 3 \rightarrow 2$ transition at 801 GHz using the CSO, unsuccessfully. These detections were confirmed by Agúndez et al. (2014a) through successful observation of the 534 GHz $J = 2 \rightarrow 1$ line toward IRC+10216 with Herschel/HIFI. The laboratory spectroscopy was presented in Cazzoli & Puzzarini (2006), Sousa-Silva et al. (2013), and Müller (2013).

4.3.21. $HCNO$ (Fulminic Acid)

The discovery of $HCNO$ was reported by Marcelino et al. (2009) through observation of the $J = 5 \rightarrow 4$ and $4 \rightarrow 3$ transitions at 92 and 115 GHz, respectively, in IRAM 30 m observations of TMC-1, L1527, B1-b, L1544, and L183. The laboratory rotational spectra were reported in Winnewisser & Winnewisser (1971).

4.3.22. $HOCN$ (Cyanic Acid)

The laboratory rotational spectrum and tentative astronomical identification of $HOCN$ were reported by Brünken et al. (2009a) toward Sgr B2 using archival survey data. The $J_{K_a, K_c} = 5_{0,5} \rightarrow 4_{0,4}$ and $6_{0,6} \rightarrow 5_{0,5}$ transitions at 104.9 and 125.8 GHz, respectively, were observed in Bell 7 m observations by Cummins et al. (1986). The $4_{0,4} \rightarrow 3_{0,3}$ transition at 83.9 GHz was observed in the survey of Turner (1989) using the NRAO 36 ft telescope but misassigned in that work to a transition of CH_3OD . These detections were confirmed shortly thereafter by Brünken et al. (2010) using IRAM 30 m observations of Sgr B2 to self-consistently observe the $4_{0,4} \rightarrow 3_{0,3}$ through $8_{0,8} \rightarrow 7_{0,7}$ transitions.

4.3.23. $HSCN$ (Thiocyanic Acid)

Halfen et al. (2009) reported the detection of $HSCN$ in ARO 12 m observations of Sgr B2. Six lines between 69 and 138 GHz were observed and assigned to the $J_{K_a, K_c} = 6_{0,6} \rightarrow 5_{0,5}$ through $12_{0,12} \rightarrow 11_{0,11}$ transitions based on the laboratory work of Brünken et al. (2009b).

4.3.24. $HOOH$ (Hydrogen Peroxide)

The detection of $HOOH$ was reported by Bergman et al. (2011) in APEX 12 m observations toward ρ Oph A. Three lines corresponding to the $J_{K_a, K_c} = 3_{0,3} \rightarrow 2_{1,1}$, $\tau = 4 \rightarrow 2$, $6_{1,5} \rightarrow 5_{0,5}$, $2 \rightarrow 4$, and $5_{0,5} \rightarrow 4_{1,3}$, $4 \rightarrow 2$ torsion-rotation transitions at 219, 252, and 318 GHz, respectively, were assigned based on the laboratory work of Helminger et al. (1981) and Petkie et al. (1995).

4.3.25. $l-C_3H^+$ (Cyclopropynylidinium Cation)

Pety et al. (2012) first reported the detection of a series of eight harmonically spaced unidentified lines in IRAM 30 m observations of the Horsehead PDR region, which seemed to correspond to the $J = 4 \rightarrow 3$ through $12 \rightarrow 11$ transitions of a linear or quasi-linear molecule. Based on the comparison of their derived rotational constants to ab initio values calculated by Ikuta (1997), they tentatively assigned the carrier of these lines to the $l-C_3H^+$ cation. Using the derived spectroscopic parameters, McGuire et al. (2013a) subsequently detected the $1 \rightarrow 0$ and $2 \rightarrow 1$ transitions at 22.5 and 45 GHz, respectively, in absorption toward Sgr B2 using the GBT 100 m telescope. Contemporaneously, Huang et al. (2013) and Fortenberry et al. (2013) challenged the attribution to $l-C_3H^+$, suggesting that the C_3H^- anion was a more likely candidate based on better agreement between the distortion constants from their high-level quantum chemical calculations to those derived by Pety et al. (2012). This assertion was challenged by McGuire et al. (2014), who argued that the formation and destruction chemistry in the high-UV environments in which the molecule was found strongly favored $l-C_3H^+$ over C_3H^- . The assignment to $l-C_3H^+$ was shortly thereafter confirmed by the laboratory observation and characterization of the rotational spectrum of the cation by Brünken et al. (2014).

4.3.26. $HMgNC$ (Hydromagnesium Isocyanide)

Cabezas et al. (2013) reported the laboratory and astronomical identification of $HMgNC$ in IRAM 30 m observations of IRC+10216. The $J = 8 \rightarrow 7$ through $13 \rightarrow 12$ transitions between 88 and 142 GHz were observed and assigned based on predicted values from the laboratory observations of the hyperfine-split $1 \rightarrow 0$ and $2 \rightarrow 1$ transitions at 11 and 22 GHz, respectively.

4.3.27. $HCCO$ (Ketenyl Radical)

The detection of $HCCO$ was reported by Agúndez et al. (2015a) using IRAM 30 m observations of Lupus-1A and L483. Four fine and hyperfine components of the $N = 4 \rightarrow 3$ transition of $HCCO$ were resolved near 86.7 GHz and assigned based on the laboratory work of Endo & Hirota (1987) and Ohshima & Endo (1993).

4.3.28. $CNCN$ (Isocyanogen)

Agúndez et al. (2018a) reported the detection of $CNCN$ in L483 using IRAM 30 m observations. The $J = 8 \rightarrow 7$, $9 \rightarrow 8$, $10 \rightarrow 9$ transitions at 82.8, 93.1, and 103.5 GHz, respectively, were observed and assigned based on the laboratory work of Winnewisser et al. (1992) and Gerry et al. (1990). A tentative detection in TMC-1 was also reported in the same work.

4.3.29. $HONO$ (Nitrous Acid)

Coutens et al. (2019) reported the detection of $HONO$ in IRAS 16293 using ALMA observations. Twelve lines between 329 and 362 GHz were observed and assigned based on the laboratory work of Guilmot et al. (1993b, 1993a) and Dehayem-Kamadjeu et al. (2005).

4.3.30. MgCCH (Magnesium Monoacetylide)

Agúndez et al. (2014b) reported the tentative detection of MgCCH in IRAM 30 m observations of IRC+10216. They identified and assigned two sets of features corresponding to l -doubled transitions of the $^2\Sigma^+$ ground electronic state of MgCCH at 89 and 99 GHz based on the laboratory work of Brewster et al. (1999). The detection was confirmed in Cernicharo et al. (2019b) using IRAM 30 m and Yebes 40 m observations of the same source.

4.3.31. HCCS (Thioketenyl Radical)

The detection of HCCS was reported in Yebes 40 m observations of TMC-1 by Cernicharo et al. (2021f). They identify and assign the $F = 4 \rightarrow 3$ and $F = 3 \rightarrow 2$ hyperfine components of the $J = 7/2 \rightarrow 5/2$ transition of HCCS at 41.1 GHz based on the laboratory work of Kim et al. (2002) and Vrtilek et al. (1992).

4.4. Five-Atom Molecules

4.4.1. HC₃N (Cyanoacetylene)

Turner (1971) reported the detection of the $F = 2 \rightarrow 1$ and $1 \rightarrow 1$ hyperfine components of the $J = 1 \rightarrow 0$ transition of HC₃N at 9098 and 9097 MHz, respectively, in NRAO 140 ft telescope observations of Sgr B2. The assignment was based on the laboratory work of Tyler & Sheridan (1963). The detection was confirmed the following year by Dickinson (1972) through observation of two hyperfine components of the $J = 2 \rightarrow 1$ transition at 18 GHz in Haystack Observatory 120 ft telescope observations of Sgr B2.

4.4.2. HCOOH (Formic Acid)

The detection of HCOOH was reported by Zuckerman et al. (1971) in Sgr B2 using the NRAO 140 ft telescope. The $J_{K_a, K_c} = 1_{1,1} \rightarrow 1_{1,0}$ transition at 1639 MHz was identified and assigned based on laboratory work presented in the same manuscript. Later, Winnewisser & Churchwell (1975) confirmed the detection by observation of the $2_{1,1} \rightarrow 2_{1,2}$ transition at 4.9 GHz in Sgr B2 using the MPIfR 100 m telescope. This identification was based on the laboratory work of Bellet et al. (1971b) and Bellet et al. (1971a) (in French).

4.4.3. CH₂NH (Methanimine)

Godfrey et al. (1973) reported the detection of CH₂NH in Sgr B2 using the Parkes 64 m telescope. The $J = 1_{1,0} \rightarrow 1_{1,1}$ transition at 5.2 GHz was observed and assigned based on laboratory work presented in the same manuscript and building on the earlier laboratory efforts of Johnson & Lovas (1972). CH₂NH is also referred to as methylenimine.

4.4.4. NH₂CN (Cyanamide)

Turner et al. (1975) described the detection of NH₂CN in Sgr B2 by observation of its $J_{K_a, K_c} = 5_{1,4} \rightarrow 4_{1,3}$ and $4_{1,3} \rightarrow 3_{1,2}$ transitions at 100.6 and 80.5 GHz, respectively, using the NRAO 36 ft telescope. The assignment was based on the work of Lide (1962), Millen et al. (1962), and Tyler et al. (1972) and subsequently confirmed in the laboratory by Johnson et al. (1976).

4.4.5. H₂CCO (Ketene)

The detection of H₂CCO was reported by Turner (1977) in NRAO 36 ft telescope observations of Sgr B2. The $J_{K_a, K_c} = 5_{1,4} \rightarrow 4_{1,3}$, $5_{1,5} \rightarrow 4_{1,4}$, and $4_{1,3} \rightarrow 3_{1,2}$ transitions at 102, 100, and 82 GHz, respectively, were observed and assigned based on the laboratory work of Johnson & Strandberg (1952) and Johns et al. (1972).

4.4.6. C₄H (Butadiynyl Radical)

Guélin et al. (1978) reported the tentative detection of C₄H using NRAO 36 ft observations of IRC+10216 in combination with the previously published observations of Scoville & Solomon (1978) and Liszt (1978) in complementary frequency ranges. In total, four sets of spin doublet lines were observed between 86 and 114 GHz and assigned to the $N = 9 \rightarrow 8$ through $N = 12 \rightarrow 11$ transitions of C₄H based on comparison with the theoretical rotational constants calculated by Wilson & Green (1977). The detection was subsequently confirmed through the laboratory efforts of Gottlieb et al. (1983).

4.4.7. SiH₄ (Silane)

The detection of SiH₄ was reported by Goldhaber & Betz (1984) in IRTF observations toward IRC+10216. Thirteen absorption lines in the ν_4 band near 917 cm⁻¹ were assigned based on laboratory work described in the same manuscript.

4.4.8. *c*-C₃H₂ (Cyclopropenylidene)

The laboratory spectroscopy and interstellar detection of *c*-C₃H₂ were described in a pair of papers by Thaddeus et al. (1985b) and Vrtilek et al. (1987). After the report of Thaddeus et al. (1985b), the molecule began to be detected in numerous sources, with the best detections, as reported in Vrtilek et al. (1987), being in Sgr B2, Orion, and TMC-1 with the Bell 7 m telescope. A total of 11 transitions between 18 and 267 GHz were initially assigned.

4.4.9. CH₂CN (Cyanomethyl Radical)

Irvine et al. (1988b) reported the detection of the CH₂CN radical in TMC-1 and Sgr B2 using a combination of observations from the FCRAO 14 m, NRAO 140 ft, Onsala 20 m, and Nobeyama 45 m telescopes. Numerous hyperfine-resolved components of the $N_{K_a, K_c} = 1_{0,1} \rightarrow 0_{0,0}$ and $2_{0,2} \rightarrow 1_{0,1}$ transitions at 20 and 40 GHz, respectively, were observed in TMC-1, as well as an unresolved detection of the $4_{0,4} \rightarrow 4_{0,3}$ transition at 101 GHz. The assignments were made based on laboratory work presented in a companion paper from Saito et al. (1988). Five partially resolved components were also detected in Sgr B2 between 40 and 101 GHz.

4.4.10. C₅ (Pentacarbon)

The detection of C₅ was reported by Bernath et al. (1989) in KPNO 4 m telescope observations of IRC+10216. More than a dozen *P*- and *R*-branch transitions of the ν_3 asymmetric stretching mode near 2164 cm⁻¹ were detected, guided by the laboratory work of Vala et al. (1989).

4.4.11. SiC₄ (Silicon Tetracarbide)

Ohishi et al. (1989) reported the detection of SiC₄ in Nobeyama 45 m observations of IRC+10216. Their search was

initially guided by quantum chemical calculations they carried out, the results of which led to the assignment of five astronomically observed features between 37 and 89 GHz to the $J = 12 \rightarrow 11$, $13 \rightarrow 12$, $14 \rightarrow 13$, $16 \rightarrow 15$, and $28 \rightarrow 27$ transitions of SiC₄. In the same work, they confirmed the detection by conducting laboratory microwave spectroscopy of the $J = 42 \rightarrow 41$ through $48 \rightarrow 47$ transitions.

4.4.12. H₂CCC (Propadienylidene)

The detection of H₂CCC was reported by Cernicharo et al. (1991a) in IRAM 30 m telescope observations and archival Effelsberg 100 m telescope observations (Cernicharo et al. 1987b) of TMC-1. The $J_{K_a, K_c} = 1_{0,1} \rightarrow 0_{0,0}$ transition of *para*-H₂CCC at 21 GHz and three transitions of *ortho*-H₂CCC between 103 and 147 GHz were identified based on the laboratory work of Vrtilek et al. (1990).

4.4.13. CH₄ (Methane)

CH₄ was detected in both the gas phase and solid phase in IRTF observations toward NGC 7538 IRS 9 by Lacy et al. (1991). The gas-phase $R(0)$ line and two blended $R(2)$ lines at 1311.43, 1322.08, and 1322.16 cm⁻¹ were observed and assigned based on the laboratory work of Champion et al. (1989). The solid-phase absorption of the ν_4 mode near 7.7 μm was observed and assigned based on the laboratory work of D'Hendecourt & Allamandola (1986).

4.4.14. HCCNC (Isocyanoacetylene)

Kawaguchi et al. (1992a) reported the detection of HCCNC, also known as isocyanoethyne and ethynyl isocyanide, in Nobeyama 45 m observations of TMC-1. The $J = 4 \rightarrow 3$, $5 \rightarrow 4$, and $9 \rightarrow 8$ transitions at 40, 50, and 89 GHz, respectively, were identified and assigned based on the laboratory work of Krueger et al. (2010).

4.4.15. HNCCC

Kawaguchi et al. (1992b) reported both the laboratory spectroscopy and astronomical identification of HNCCC in Nobeyama 45 m telescope observations of TMC-1. The $J = 3 \rightarrow 2$, $4 \rightarrow 3$, and $5 \rightarrow 4$ transitions at 28, 37, and 47 GHz, respectively, were assigned and identified.

4.4.16. H₂COH⁺ (Protonated Formaldehyde)

The detection of H₂COH⁺ was reported by Ohishi et al. (1996) in Nobeyama 45 m and NRAO 12 m telescope observations of Sgr B2, Orion, and W51. Six transitions between 32 and 174 GHz were observed and assigned based on the laboratory work of Chomiak et al. (1994).

4.4.17. C₄H⁻ (Butadiynyl Anion)

Cernicharo et al. (2007) reported the detection of C₄H⁻ in IRAM 30 m observations of IRC+10216 through observation of five transitions between 84 and 140 GHz. The detection was enabled by the laboratory work of Gupta et al. (2007).

4.4.18. CNCHO (Cyanoformaldehyde)

CNCHO was detected in GBT 100 m observations of Sgr B2(N) by Remijan et al. (2008a). A total of seven transitions between 2.1 and 41 GHz were identified and assigned based on

the laboratory work of Bogey et al. (1988b) and Bogey et al. (1995). CNCHO is also referred to as formyl cyanide.

4.4.19. HNCNH (Carbodiimide)

McGuire et al. (2012) reported the detection of HNCNH in GBT 100 m observations of Sgr B2. Four sets of transitions were identified to arise from maser action, while several other stronger transitions incapable of masing were not observed. The assignments were made based on the laboratory work of Birk et al. (1989), Wagener et al. (1995), and Jabs et al. (1997).

4.4.20. CH₃O (Methoxy Radical)

The detection of CH₃O was reported in IRAM 30 m observations of B1-b by Cernicharo et al. (2012). Several hyperfine components of the $N = 1 \rightarrow 0$ transition near 82.4 GHz were identified and assigned based on the laboratory work of Endo et al. (1984) and Momose et al. (1988). Components of the $2 \rightarrow 1$ transition are shown, but no frequency information is provided other than that the transitions are at 2 mm.

4.4.21. NH₃D⁺ (Deuterated Ammonium Cation)

The detection of NH₃D⁺ was reported toward Orion and B1-b in IRAM 30 m observations by Cernicharo et al. (2013b). A single line with unresolved hyperfine structure was observed and assigned to the $J_K = 1_0 \rightarrow 0_0$ transition of NH₃D⁺ based on laboratory results presented in the same manuscript. A companion article by Domenech et al. (2013) detailed the laboratory results.

4.4.22. H₂NCO⁺ (Protonated Isocyanic Acid)

Gupta et al. (2013) reported a tentative detection of H₂NCO⁺ in GBT 100 m observations of Sgr B2. Based on laboratory work presented in the same manuscript, they identified and assigned the $J_{K_a, K_c} = 0_{0,0} \rightarrow 1_{0,1}$ and $1_{1,0} \rightarrow 2_{1,1}$ transitions of *para*- and *ortho*-H₂NCO⁺ at 20.2 and 40.8 GHz, respectively. The detection was confirmed by Marcelino et al. (2018) in IRAM 30 m observations of L483. They observed six additional transitions of H₂NCO⁺ between 80 and 116 GHz.

4.4.23. NCCNH⁺ (Protonated Cyanogen)

Agúndez et al. (2015b) reported the detection of NCCNH⁺ in TMC-1 and L483 using IRAM 30 m and Yerbes 40 m observations. The $J = 5 \rightarrow 4$ and $10 \rightarrow 9$ transitions at 44.3 and 88.8 GHz, respectively, were identified and assigned based on the laboratory work of Amano & Scappini (1991) and Gottlieb et al. (2000).

4.4.24. CH₃Cl (Chloromethane)

CH₃Cl, also called methyl chloride, was detected in ALMA observations of IRAS 16293 and in ROSINA mass spectrometry measurements of comet 67P/Churyumov-Gerasimenko by Fayolle et al. (2017). Both the ³⁵Cl and ³⁷Cl isotopologues were detected through observation and assignment of the $J_K = 13_K \rightarrow 12_K$ $K = 0$ to 4 transitions between 340 and 360 GHz. The laboratory work was presented by Wlodarczak et al. (1986).

4.4.25. MgC_3N (Magnesium Cyanoethynyl Radical)

Cernicharo et al. (2019b) reported the detection of MgC_3N in IRAM 30 m and Yebes 40 m observations of IRC+10216. A series of doublet lines between 33 and 111 GHz were identified and assigned based on quantum chemical calculations. To date, there has been no laboratory confirmation of these assignments.

4.4.26. HC_3O^+ (Protonated Tricarbon Monoxide)

The detection of HC_3O^+ was reported by Cernicharo et al. (2020b) in IRAM 30 m and Yebes 40 m observations of TMC-1. They identify and assign four lines in their spectra to the $J = 4 \rightarrow 3$, $J = 5 \rightarrow 4$, $J = 10 \rightarrow 9$, and $J = 11 \rightarrow 10$ transitions between 35.6 and 98.1 GHz. The initial assignment was based on quantum chemical calculations in the same paper, as well as from Thorwirth et al. (2020). Laboratory spectroscopy presented in the same paper confirms the detection.

4.4.27. NH_2OH (Hydroxylamine)

Rivilla et al. (2020) reported the detection of NH_2OH in IRAM 30 m observations of G+0.693-0.027. Based on the laboratory work of Tsunekawa (1972) and Morino et al. (2000), they identified and assigned approximately 10 largely unblended rotational transitions between 100.7–201.6 GHz.

4.4.28. HC_3S^+ (Protonated Tricarbon Monosulfide)

The detection of HC_3S^+ was reported by Cernicharo et al. (2021b) in Yebes 40 m observations of TMC-1. They identify and assign four lines in their spectra to the $J = 6 \rightarrow 5$, $J = 7 \rightarrow 6$, $J = 8 \rightarrow 7$, and $J = 9 \rightarrow 8$ transitions between 32.8 and 49.2 GHz. The initial assignment was based on quantum chemical calculations in the same paper, as well as from Thorwirth et al. (2020). Laboratory spectroscopy presented in the same paper confirms the detection.

4.4.29. H_2CCS (Thioketene)

Cernicharo et al. (2021f) reported the detection of H_2CCS in Yebes 40 m observations of TMC-1. They identify and assign the $3_{1,2} - 2_{1,1}$, $3_{1,3} - 2_{1,2}$, $4_{1,3} - 3_{1,2}$, $4_{1,4} - 3_{1,3}$, $3_{0,3} - 2_{0,2}$, and $4_{0,4} - 3_{0,3}$ transitions between 33.4 and 44.8 GHz based on laboratory work by Georgiou et al. (1979); Winnewisser & Schäfer (1980), and McNaughton et al. (1996).

4.4.30. C_4S (Tetracarbon Monosulfide)

The detection of C_4S was reported by Cernicharo et al. (2021f) in Yebes 40 m observations of TMC-1. They identify and assign the $N_J = 10_{11} \rightarrow 9_{10}$, $N_J = 11_{12} \rightarrow 10_{11}$, $N_J = 12_{13} \rightarrow 11_{12}$, and $N_J = 13_{14} \rightarrow 12_{13}$ transitions between 32.6 and 41.5 GHz based on the laboratory work of Hirahara et al. (1993) and Gordon et al. (2001). The dipole moment was taken from the work of Lee (1997).

4.4.31. $CHOSH$ (Monothioformic Acid)

Rodríguez-Almeida et al. (2021) reported the detection of $CHOSH$ in IRAM 30 m and Yebes 40 m observations of G+0.693-0.027. Based on the laboratory work of Hocking & Winnewisser (1976), they identify and assign nine largely unblended a -type transitions between 34.2 and 93.5 GHz.

4.5. Six-Atom Molecules

4.5.1. CH_3OH (Methanol)

Ball et al. (1970) reported the detection of CH_3OH in NRAO 140 ft observations of Sgr A and Sgr B2. The $J_{K_a, K_c} = 1_{1,0} \rightarrow 1_{1,1}$ transition at 834 MHz was observed and assigned based on laboratory work described in the same manuscript.

4.5.2. CH_3CN (Methyl Cyanide)

CH_3CN was detected by Solomon et al. (1971) in Sgr B2 and Sgr A using the NRAO 36 ft telescope. Two fully resolved and two blended K components of the $J = 6 \rightarrow 5$ transition near 110.4 GHz were identified and assigned based on the laboratory data cataloged in Cord et al. (1968). It is likely that the frequencies listed in Cord et al. (1968) were obtained from, or relied heavily upon, the prior work by Kessler et al. (1950). CH_3CN is also referred to as acetonitrile.

4.5.3. NH_2CHO (Formamide)

The detection of NH_2CHO was reported by Rubin et al. (1971) in NRAO 140 ft observations of Sgr B2. The $J_{K_a, K_c} = 2_{1,1} \rightarrow 2_{1,2}$, $F = 2 \rightarrow 2$, and $1 \rightarrow 1$ hyperfine components were resolved, while the $3 \rightarrow 3$ was detected as part of a blend with the H112 α transition. The enabling laboratory spectroscopy was reported in the same manuscript. NH_2CHO was the first interstellar molecule detected containing H, C, N, and O.

4.5.4. CH_3SH (Methyl Mercaptan)

Linke et al. (1979) reported the detection of CH_3SH in Bell 7 m telescope observations of Sgr B2. Six transitions between 76 and 102 GHz were identified and assigned based on the laboratory work of Kilb (1955) and unpublished data of D. R. Johnson. This latter data set was analyzed and formed the foundation of the more extensive work of Lees & Mohammadi (1980).

4.5.5. C_2H_4 (Ethylene)

The detection of C_2H_4 was reported by Betz (1981) toward IRC+10216 using the 1.5 m McMath Solar Telescope. Three rotationally resolved rovibrational transitions were observed in the ν_7 state: the $J_{K_a, K_c} = 5_{1,5} \rightarrow 5_{0,5}$ at 28.5 THz was assigned based on the laboratory work of Lambeau et al. (1980), while the $1_{1,0} \rightarrow 0_{0,0}$ and $8_{0,8} \rightarrow 8_{1,8}$ were assigned based on laboratory work described in Betz (1981).

4.5.6. C_5H (Pentynylidyne Radical)

A tentative detection of C_5H was reported by Cernicharo et al. (1986b) in IRAM 30 m observations of IRC+10216. They identify a series of lines that could be assigned to a radical species in a $^2\Pi$ ground state with quantum numbers $J = 31/2 \rightarrow 29/2$ and $35/2 \rightarrow 33/2$ through $43/2 \rightarrow 41/2$ between 74 and 103 GHz. Based on comparison of the derived rotational constant ($B_0 = 2387$ MHz) to a calculated rotational constant ($B_0 = 2375$ MHz) described in the same manuscript, they tentatively assigned the emission to the C_5H radical. The subsequent laboratory work by Gottlieb et al. (1986) confirmed the assignment, and the interstellar identifications were

extended shortly thereafter by Cernicharo et al. (1986a) and Cernicharo et al. (1987c).

4.5.7. CH_3NC (Methyl Isocyanide)

A tentative detection of CH_3NC was reported by Cernicharo et al. (1988) in IRAM 30 m observations of Sgr B2. Somewhat blended signal was observed near the frequencies corresponding to the $J = 4 \rightarrow 3$, $5 \rightarrow 4$, and $7 \rightarrow 6$ transitions at 80.4, 100.5, and 140.7 GHz, respectively. Although no reference is given for these frequencies, they were presumably enabled by the laboratory work of Kukolich (1972) and Ring et al. (1947). The detection was confirmed nearly two decades later in GBT 100 m observations of Sgr B2 by Remijan et al. (2005), who observed the $J_K = 1_0 \rightarrow 0_0$ transition in absorption at 20.1 GHz, and by Gratier et al. (2013), who observed three lines in the $J = 5 \rightarrow 4$ transition at 100.5 GHz with the IRAM 30 m toward the Horsehead PDR.

4.5.8. HC_2CHO (Propynal)

Irvine et al. (1988a) reported the detection of HC_2CHO in NRAO 140 ft and Nobeyama 45 m observations of TMC-1. The $J_{K_a, K_c} = 2_{0,2} \rightarrow 1_{0,1}$ and $4_{0,4} \rightarrow 3_{0,3}$ transitions at 18.7 and 37.3 GHz, respectively, were assigned based on the laboratory work of Winnewisser (1973).

4.5.9. H_2C_4 (Butatrienylidene)

Cernicharo et al. (1991b) reported the detection of the H_2C_4 carbene molecule in IRAM 30 m observations of IRC+10216. Eight transitions with J values between 8 and 15 were identified and assigned between 80 and 135 GHz based on the laboratory spectroscopy of Killian et al. (1990).

4.5.10. C_5S (Pentacarbon Monosulfide Radical)

The C_5S radical was tentatively detected by Bell et al. (1993) in NRAO 140 ft telescope observations of IRC+10216. A weak line corresponding to the $J = 13 \rightarrow 12$ transition of C_5S was identified near 23,960 MHz based on the laboratory work of Kasai et al. (1993). The detection was confirmed in Agúndez et al. (2014b) with IRAM 30 m observations of IRC+10216. The $J = 44 \rightarrow 43$, $45 \rightarrow 44$, and $46 \rightarrow 45$ transitions at 81.2, 83.0, and 84.9 GHz, respectively, were identified and assigned based on the laboratory work of Gordon et al. (2001).

4.5.11. HC_3NH^+ (Protonated Cyanoacetylene)

Kawaguchi et al. (1994) reported the detection of HC_3NH^+ in Nobeyama 45 m observations of TMC-1. The $J = 4 \rightarrow 3$ and $5 \rightarrow 4$ transitions at 34.6 and 43.3 GHz, respectively, were identified and assigned based on the frequencies reported by Lee & Amano (1987) from infrared difference frequency laser spectroscopy. Using the astronomically detected pure rotational lines as a guide, the rotational spectrum was then measured in the laboratory by Gottlieb et al. (2000).

4.5.12. C_5N (Cyanobutadienyl Radical)

The C_5N radical was detected by Guélin et al. (1998) in Effelsberg 100 m and IRAM 30 m observations of TMC-1. Two sets of hyperfine components of the $J = 17/2 \rightarrow 15/2$ and $65/2 \rightarrow 63/2$ transitions of C_5N at 25.2 and 89.8 GHz,

respectively, were identified and assigned based on the laboratory work of Kasai et al. (1997).

4.5.13. HC_4H (Diacetylene)

Cernicharo et al. (2001) reported the detection of HC_4H in ISO observations of CRL 618 near 15.9 μm . The observed absorption signal was identified and assigned to the ν_8 fundamental bending mode of HC_4H based on the laboratory work of Arié & Johns (1992).

4.5.14. HC_4N

The HC_4N radical was detected by Cernicharo et al. (2004) in IRAM 30 m observations of IRC+10216. A dozen transitions between 83–97 GHz were identified and assigned based on the laboratory work of Tang et al. (1999).

4.5.15. $c\text{-H}_2\text{C}_3\text{O}$ (Cyclopropenone)

Hollis et al. (2006b) reported the detection of $c\text{-H}_2\text{C}_3\text{O}$ in GBT 100 m observations of Sgr B2. Six transitions between 9.3 and 44.6 GHz were identified and assigned based on the laboratory work of Benson et al. (1973) and Guillemin et al. (1990).

4.5.16. CH_2CNH (Ketenimine)

The detection of CH_2CNH was reported by Lovas et al. (2006a) using GBT 100 m telescope observations of Sgr B2. The $J_{K_a, K_c} = 9_{1,8} \rightarrow 10_{0,10}$, $8_{1,7} \rightarrow 9_{0,9}$, and $7_{1,6} \rightarrow 8_{0,8}$ transitions at 4.9, 23.2, and 41.5 GHz, respectively, were identified and assigned based on the laboratory work of Rodler et al. (1984) and Rodler et al. (1986).

4.5.17. C_5N^- (Cyanobutadienyl Anion)

Cernicharo et al. (2008) reported the detection of C_5N^- in IRAM 30 m observations of IRC+10216. They identify and assign 11 lines to the $J = 29 \rightarrow 28$ through $40 \rightarrow 39$ transitions of C_5N^- by comparison to the calculated rotational constants presented in Botschwina & Oswald (2008). To date, there does not appear to be a published pure rotational laboratory spectrum of this species.

4.5.18. HNCHCN (E-cyanomethanimine)

HNCHCN was detected in GBT 100 m telescope observations of Sgr B2 as reported by Zaleski et al. (2013). Nine transitions between 9.6 and 47.8 GHz were identified and assigned based on laboratory spectroscopy presented in the same manuscript.

4.5.19. SiH_3CN (Silyl Cyanide)

The tentative detection of SiH_3CN was reported by Agúndez et al. (2014b) in IRAM 30 m observations of IRC+10216 through the identification of three weak emission features that they assign to the $J = 9 \rightarrow 8$, $10 \rightarrow 9$, and $11 \rightarrow 10$ transitions of SiH_3CN at 89.5, 99.5, and 109.4 GHz, respectively, based on the laboratory work of Priem et al. (1998). The detection was confirmed by Cernicharo et al. (2017) through the detection of additional, higher-frequency transitions in this source.

4.5.20. MgC_4H (Magnesium Butadiynyl Radical)

Cernicharo et al. (2019b) reported the detection of MgC_4H in IRAM 30 m and Yebes 40 m observations of IRC+10216. A series of doublet lines between 71.8 and 110.5 GHz were identified and assigned based on quantum chemical calculations and comparison to constants derived from electronic spectra reported by Forthomme et al. (2010). To date, there has been no laboratory confirmation of these assignments by pure rotational spectroscopy.

4.5.21. CH_3CO^+ (Acetyl Cation)

The detection of CH_3CO^+ was reported by Cernicharo et al. (2021e) in IRAM 30 m and Yebes 40 m observations of TMC-1, L483, L1527, and L1544. Four lines corresponding to the $J = 2 \rightarrow 1$, $J = 4 \rightarrow 3$, $J = 5 \rightarrow 4$, and $J = 6 \rightarrow 5$ transitions of CH_3CO^+ at 36.5, 73.1, 91.3, and 109.6 GHz, respectively, were identified and assigned based on laboratory spectroscopy presented in the same paper.

4.5.22. H_2CCCS (Propadienethione)

Cernicharo et al. (2021f) reported the detection of H_2CCCS in Yebes 40 m observations of TMC-1. They identify and assign nine transitions between 35.3 and 45.5 GHz based on the laboratory work from Brown et al. (1988).

4.5.23. CH_2CCH (Propargyl Radical)

The detection of CH_2CCH was reported by Agúndez et al. (2021) in Yebes 40 m observations of TMC-1. Based on the laboratory work of Tanaka et al. (1997), they identify and assigned six hyperfine components of the $2_{0,2} - 1_{0,1}$ transition near 37.5 GHz.

4.6. Seven-Atom Molecules

4.6.1. CH_3CHO (Acetaldehyde)

The detection of the $J_{K_a, K_c} = 1_{1,1} \rightarrow 1_{1,0}$ transition of CH_3CHO at 1065 MHz was reported by Gottlieb (1973) in NRAO 140 ft observations of Sgr B2 and Sgr A. The assignment was made based on the laboratory work of Kilb et al. (1957) and Souter & Wood (1970). Fourikis et al. (1974a) reported a confirming observation of the $2_{1,1} \rightarrow 2_{1,2}$ transition in Parkes 64 m observations of Sgr B2 at 3195 MHz.

4.6.2. CH_3CCH (Methyl Acetylene)

Buhl & Snyder (1973) reported the detection of the $J_K = 5_0 \rightarrow 4_0$ transition of CH_3CCH at 85.4 GHz in NRAO 36 ft telescope observations of Sgr B2. Although no reference to the source of the frequency is given, it was presumably obtained from the laboratory work of Trambarulo & Gordy (1950). Subsequent confirming transitions were observed at higher frequencies by Hollis et al. (1981) and Kuiper et al. (1984).

4.6.3. CH_3NH_2 (Methylamine)

The detection of CH_3NH_2 was simultaneously reported by Fourikis et al. (1974b) and Kaifu et al. (1974). Kaifu et al. (1974) used the Mitaka 6 m and NRAO 36 ft telescopes to observe CH_3NH_2 toward Sgr B2 and Orion. The a , $J_{K_a, K_c} = 5_{1,5} \rightarrow 5_{0,5}$ and s , $4_{1,4} \rightarrow 4_{0,4}$ transitions at 73 and 86 GHz, respectively, were assigned based on the laboratory

work of Takagi & Kojima (1973). Using the same laboratory work, Fourikis et al. (1974b) reported the detection of the a , $2_{0,2} \rightarrow 1_{1,0}$ transition at 8.8 GHz using the Parkes 64 m telescope, also toward Sgr B2 and Orion.

4.6.4. CH_2CHCN (Vinyl Cyanide)

CH_2CHCN , also known as acrylonitrile, was detected by Gardner & Winnewisser (1975) in Parkes 64 m observations of Sgr B2. The $J_{K_a, K_c} = 2_{1,1} \rightarrow 2_{1,2}$ transition at 1372 MHz was identified and assigned based on the laboratory work of Gerry & Winnewisser (1973). Several additional confirming transitions were later observed in NRAO 140 ft telescope observations of TMC-1 by Matthews & Sears (1983).

4.6.5. HC_5N (Cyanodiacetylene)

Avery et al. (1976) reported the detection of HC_5N in Algonquin Radio Observatory 46 m telescope observations of Sgr B2. They observed and assigned the $J = 4 \rightarrow 3$ transition at 10,651 MHz based on the laboratory work of Alexander et al. (1976). Later that year, Broten et al. (1976) observed the $1 \rightarrow 0$ and $8 \rightarrow 7$ transitions with the same facility, also in Sgr B2.

4.6.6. C_6H (Hexatriynyl Radical)

The first detection of the C_6H radical was made by Suzuki et al. (1986) in Nobeyama 45 m observations of TMC-1. The authors observed three sets of doublet transitions at 23.6, 40.2, and 43.0 GHz, which they assigned to the hyperfine-split, Λ -doubled $J = 17/2 \rightarrow 15/2$, $29/2 \rightarrow 27/2$, and $31/2 \rightarrow 29/2$ transitions, respectively, of C_6H based on a comparison to the quantum chemical work of Murakami et al. (1987). The detection was confirmed the following year with the measurement of the laboratory rotational spectrum by Pearson et al. (1988).

4.6.7. $c-C_2H_4O$ (Ethylene Oxide)

Dickens et al. (1997) reported the detection of $c-C_2H_4O$ in Nobeyama 45 m, Haystack 140 ft, and SEST 15 m telescope observations of Sgr B2. Nine transitions between 39.6 and 254.2 GHz were identified and assigned based on the laboratory rotational spectroscopy performed by Hirose (1974).

4.6.8. CH_2CHOH (Vinyl Alcohol)

Turner & Apponi (2001) reported the detection of both *syn*- and *anti*-vinyl alcohol in NRAO 12 m observations of Sgr B2. The *syn* conformer of CH_2CHOH is the more stable, but only two lines, the $J_{K_a, K_c} = 2_{1,2} \rightarrow 1_{0,1}$ and $3_{1,3} \rightarrow 2_{0,2}$ transitions at 86.6 and 103.7 GHz, respectively, were identified and assigned based on the laboratory work of Kaushik (1977). In contrast, five transitions of the *anti* conformer were identified between 71.8 and 154.5 GHz based on the laboratory work of Rodler (1985).

4.6.9. C_6H^- (Hexatriynyl Anion)

The first molecular anion to be detected in the ISM, McCarthy et al. (2006) described both the observation and laboratory spectroscopic identification of C_6H^- . More than a decade prior, Kawaguchi et al. (1995) had noted the presence of a series of unidentified, harmonically spaced emission features in their Nobeyama 45 m survey of IRC+10216 dubbed

B1377. Based on their laboratory work, McCarthy et al. (2006) successfully assigned the carrier of these transitions to C_6H^- . They also identified the $J = 4 \rightarrow 3$ and $5 \rightarrow 4$ transitions at 11.0 and 13.8 GHz, respectively, in GBT 100 m telescope observations of TMC-1.

4.6.10. CH_3NCO (Methyl Isocyanate)

The detection of CH_3NCO was reported by Halfen et al. (2015) in ARO 12 m and SMT observations of Sgr B2. They observed 17 uncontaminated emission lines of CH_3NCO between 68 and 116 GHz and assigned them based on laboratory work described in the same manuscript. The following year, Cernicharo et al. (2016) reported the detection of the molecule in IRAM 30 m and ALMA data toward Orion, as well as extending the laboratory spectroscopy.

4.6.11. HC_5O (Butadiynylformyl Radical)

McGuire et al. (2017a) reported the detection of HC_5O in GBT 100 m observations of TMC-1. Four hyperfine-resolved components of the $J = 17/2 \rightarrow 15/2$ transition at 21.9 GHz were detected and assigned based on the laboratory work of Mohamed et al. (2005).

4.6.12. $HOCH_2CN$ (Glycolonitrile)

Zeng et al. (2019) reported the detection of $HOCH_2CN$ in ALMA observations of IRAS 16293. A total of 15 unblended transitions were identified and assigned based on the laboratory work of Margulès et al. (2017). $HOCH_2CN$ is also known as hydroxyacetonitrile.

4.6.13. H_3HNH (Propargylimine)

Bizzocchi et al. (2020) reported the detection of H_3HNH in IRAM 30 m observations of G+0.639-0.027. A total of 18 transitions of the Z-conformer were identified and assigned in the observational data between 73 and 111 GHz based on laboratory work described in the same paper as well as that of Kroto et al. (1984), Sugie et al. (1985), and McNaughton et al. (1988a).

4.6.14. HC_4NC (Isocyanoacetylene)

The detection of HC_4NC in TMC-1 was nearly simultaneously reported by Xue et al. (2020) using GBT 100 m observations and Cernicharo et al. (2020a) using Yebes 40 m observations. Xue et al. (2020) reported the detection of the $J = 8 \rightarrow 7$, $J = 9 \rightarrow 8$, and $J = 10 \rightarrow 9$ transitions, as well as an overall detection significance of 10.5σ based on spectral stacking and matched filtering analyses. Cernicharo et al. (2020a) reported the detection of the higher-lying $J = 12 \rightarrow 11$, $J = 13 \rightarrow 12$, $J = 14 \rightarrow 13$, $J = 15 \rightarrow 14$, and $J = 16 \rightarrow 15$ transitions. Both studies relied on the laboratory work of Botschwina et al. (1998).

4.6.15. $c-C_3HCCH$ (Ethinyl Cyclopropenylidene)

Cernicharo et al. (2021a) reported the detection of $c-C_3HCCH$ in Yebes 40 m observations of TMC-1. Based on the laboratory work of Travers et al. (1997) they identify and assign 10 largely unblended transitions and a number of others, between 31.5 and 44.0 GHz to $c-C_3HCCH$.

4.7. Eight-Atom Molecules

4.7.1. $HCOOCH_3$ (Methyl Formate)

Brown et al. (1975a) reported the detection of $cis-HCOOCH_3$ in Parkes 64 m telescope observations of Sgr B2. Based on laboratory work presented in the same paper, they identified and assigned the A-state $J_{K_a, K_c} = 1_{1,0} \rightarrow 1_{1,1}$ transition of $cis-HCOOCH_3$ at 1610.25 MHz. Several months later, Churchwell & Winnewisser (1975) confirmed the detection of the A-state line and additionally observed the E-state line of the same transition at 1610.9 MHz using the Effelsberg 100 m telescope. Nearly three decades later, Neill et al. (2012) reported the tentative identification of the higher-energy *trans* conformer of $HCOOCH_3$ in GBT 100 m telescope observations of Sgr B2, based on laboratory spectroscopy presented in the same work. A total of seven transitions between 9.1 and 27.4 GHz were observed.

4.7.2. CH_3C_3N (Methylcyanoacetylene)

The detection of CH_3C_3N was reported by Broten et al. (1984) in NRAO 140 ft observations of TMC-1. A total of seven components of the $J = 5 \rightarrow 4$ through $8 \rightarrow 7$ transitions of CH_3C_3N between 20.7 and 33.1 GHz were resolved and assigned based on the laboratory work of Moises et al. (1982).

4.7.3. C_7H (Heptatriynylidyne Radical)

Guélin et al. (1997) reported the detection of the C_7H radical in IRAM 30 m telescope observations of IRC+10216. Based on the laboratory spectroscopy of Travers et al. (1996a), they identified and assigned five rotational transitions between 83 and 86.6 GHz.

4.7.4. CH_3COOH (Acetic Acid)

The detection of CH_3COOH was reported by Mehringer et al. (1997) in BIMA and OVRO observations of Sgr B2. The $J_{K_a, K_c} = 8_{*,8} \rightarrow 7_{*,7}$ A- and E-state lines of CH_3COOH around 90.2 GHz and the $9_{*,9} \rightarrow 8_{*,8}$ E-state line at 100.9 GHz were identified and assigned based on the work of Tabor (1957) and Wlodarczak & Demaison (1988).

4.7.5. H_2C_6 (Hexapentaenylidene)

Langer et al. (1997) reported the detection of H_2C_6 in Goldstone 70 m telescope observations of TMC-1. The $J_{K_a, K_c} = 7_{1,7} \rightarrow 6_{1,6}$ and $8_{1,8} \rightarrow 7_{1,7}$ transitions of H_2C_6 at 18.8 and 21.5 GHz, respectively, were identified and assigned based on the laboratory work of McCarthy (1997).

4.7.6. CH_2OHCHO (Glycolaldehyde)

The detection of CH_2OCHO was reported by Hollis et al. (2000) in NRAO 12 m observations of Sgr B2. A total of five transitions between 71.5 and 103.7 GHz were identified and assigned based on the laboratory work of Marstokk & Møllendal (1973). Despite numerous claims in the astronomical literature, glycolaldehyde is not a true sugar and is instead a diose, a 2-carbon monosaccharide, making it the simplest sugar-related molecule.

4.7.7. HC_6H (Triacetylene)

Cernicharo et al. (2001) reported the detection of HC_6H in ISO observations of CRL 618. The ν_{11} fundamental bending mode of HC_6H at $16.1 \mu\text{m}$ was observed and assigned based on the laboratory work of Haas et al. (1994).

4.7.8. CH_2CHCHO (Propenal)

A tentative detection of CH_2CHCHO was reported by Dickens et al. (2001) in NRAO 12 m and SEST 15 m observations of G327.3-0.6 and Sgr B2. They tentatively assigned six emission lines between 88.5 and 107.5 GHz to CH_2CHCHO , based on the laboratory work of Winnewisser et al. (1975). The detection was confirmed by Hollis et al. (2004b) in GBT 100 m telescope observations of Sgr B2. They observed and assigned the $J_{K_a, K_c} = 2_{1,1} \rightarrow 1_{1,0}$ and $3_{1,3} \rightarrow 2_{1,2}$ transitions at 18.2 and 26.1 GHz, respectively, based on the laboratory work of Blom et al. (1984). CH_2CHCHO is also referred to as acrolein.

4.7.9. CH_2CCHCN (Cyanoallene)

Lovas et al. (2006b) reported the detection of CH_2CCHCN in GBT 100 m observations of TMC-1. Four transitions between 20.2 and 25.8 GHz with partially resolved hyperfine structure were identified and assigned based on the laboratory work of Bouchy et al. (1973) and Schwahn et al. (1986).

4.7.10. $\text{NH}_2\text{CH}_2\text{CN}$ (Aminoacetonitrile)

The detection of $\text{NH}_2\text{CH}_2\text{CN}$ was reported by Belloche et al. (2008) in IRAM 30 m, PdBI, and ATCA observations of Sgr B2. A total of 51 emission features between 80 and 116 GHz were identified and assigned to transitions of $\text{NH}_2\text{CH}_2\text{CN}$ based on the laboratory work of Bogey et al. (1990). As part of their work, Belloche et al. (2008) refined the spectroscopic fit for the molecule based on the work of Bogey et al. (1990) and references therein.

4.7.11. CH_3CHNH (Ethanimine)

Loomis et al. (2013) reported the detection of CH_3CHNH in GBT 100 m observations of Sgr B2. More than two dozen transitions of the molecule between 13.0 and 47.2 GHz were identified and assigned based on laboratory spectroscopy work presented in the same manuscript.

4.7.12. CH_3SiH_3 (Methyl Silane)

The detection of CH_3SiH_3 was reported by Cernicharo et al. (2017) in IRAM 30 m observations of IRC+10216. Ten transitions between 80 and 350 GHz were identified and assigned based on the laboratory work of Meerts & Ozier (1982) and Wong et al. (1983).

4.7.13. $(\text{NH}_2)_2\text{CO}$ (Urea)

Belloche et al. (2019) reported the detection of $(\text{NH}_2)_2\text{CO}$ in ALMA observations of Sgr B2(N1S). They identify a substantial number of transitions between 84.1 and 114.4 GHz, of which nine are claimed to be largely free of contamination from other species. Remijan et al. (2014) had earlier reported on the evidence for a tentative detection of $(\text{NH}_2)_2\text{CO}$ in the same source. These studies relied on

laboratory data from Brown et al. (1975b), Kasten & Dreizler (1986), Kretschmer et al. (1996), and Godfrey et al. (1997).

4.7.14. HCCCH_2CN (Propargyl Cyanide)

The detection of HCCCH_2CN was reported by McGuire et al. (2020) in GBT 100 m observations of TMC-1. The $4_{1,3} - 3_{1,2}$, $5_{1,5} - 4_{1,4}$, $5_{0,5} - 4_{0,4}$, and $5_{1,4} - 4_{1,3}$ transitions, with hyperfine structure, were observed and assigned based on laboratory work presented in the same paper as well as the work of Jones & Sheridan (1982), Demaison et al. (1985), McNaughton et al. (1988b), and Jager et al. (1990). An 18.0σ detection was claimed based on a spectral matched filtering analysis.

4.7.15. CH_2CHCCH (Vinyl Acetylene)

Cernicharo et al. (2021d) reported the detection of CH_2CHCCH in Yebes 40 m observations of TMC-1. They identify and assign seven transitions between 35.5 and 46.4 GHz based on the laboratory work of Sobolev et al. (1961), Thorwirth & Lichau (2003), and Thorwirth et al. (2004b).

4.8. Nine-Atom Molecules

4.8.1. CH_3OCH_3 (Dimethyl Ether)

Snyder et al. (1974) reported the detection of CH_3OCH_3 in NRAO 36 ft and Maryland Point Observatory NRL 85 ft observations of Orion. The $J_{K_a, K_c} = 6_{0,6} \rightarrow 5_{1,5}$, $2_{1,1} \rightarrow 2_{0,2}$, and $2_{2,0} \rightarrow 2_{1,1}$ transitions at 90.2, 31.1, and 88.2 GHz, respectively, were observed and assigned based on the laboratory work of Kasai & Myers (1959) and Blukis et al. (1963).

4.8.2. $\text{CH}_3\text{CH}_2\text{OH}$ (Ethanol)

The detection of *trans*- $\text{CH}_3\text{CH}_2\text{OH}$ was reported by Zuckerman et al. (1975) in NRAO 36 ft telescope observations of Sgr B2. The $J_{K_a, K_c} = 6_{0,6} \rightarrow 5_{1,5}$, $4_{1,4} \rightarrow 3_{0,3}$, and $5_{1,5} \rightarrow 4_{0,4}$ transitions at 85.3, 90.1, and 104.8 GHz, respectively, were identified and assigned based on the laboratory work of Takano et al. (1968). The *gauche* substates of $\text{CH}_3\text{CH}_2\text{OH}$ were later identified as the carriers of 14 previously unidentified emission features in the Nobeyama 45 m observations of Orion presented in Ohishi et al. (1988) based on the laboratory work of Pearson et al. (1997).

4.8.3. $\text{CH}_3\text{CH}_2\text{CN}$ (Ethyl Cyanide)

Johnson et al. (1977) reported the detection of $\text{CH}_3\text{CH}_2\text{CN}$ in NRAO 36 ft observations of Orion and weakly in Sgr B2. Two dozen emission features between 88 and 116 GHz were identified and assigned to $\text{CH}_3\text{CH}_2\text{CN}$ in Orion. The foundational laboratory spectroscopy was reported by Heise et al. (1974), Mäder et al. (1974), and Laurie (1959). Based on this work, additional higher-frequency lines were measured and assigned in Johnson et al. (1977).

4.8.4. HC_7N (Cyanotriacetylene)

Reports of the detection of HC_7N were made nearly simultaneously by Little et al. (1978) (January 4) and Kroto et al. (1978) (February 1), although the former acknowledges an earlier report by Kroto et al. (1977) (June 13). A few months

later (October 5), Winnewisser & Walmsley (1978) also reported the detection of HC₇N.

The observations of Kroto et al. (1977) and Kroto et al. (1978) were conducted toward TMC-1 using both the Algonquin 46 m and Haystack 36.6 m telescopes. Kroto et al. (1977) reported the observation of the $J = 9 \rightarrow 8$ transition at 10.2 GHz, while Kroto et al. (1978) additionally observed the $21 \rightarrow 20$ transition at 23.7 GHz. The assignments were based on laboratory work carried out by a subset of the authors of Kroto et al. (1978), which they would later report in Kirby et al. (1980).

Little et al. (1978) used the SRC Appleton Laboratory 25 m telescope to observe the $22 \rightarrow 21$ transition at 24.8 GHz in both TMC-1 and TMC-2. The rotational constants required for the detection were provided by H. W. Kroto.

The work of Winnewisser & Walmsley (1978) was presumably carried out independently, as there were no references to the previous three manuscripts in this paper. They reported the detection of the $21 \rightarrow 20$ transition in IRC +10216. Although the facility used for the observations is not named in the main portion of the manuscript, the authors acknowledge the operators of Effelsberg and cite a beam size of 40'' near 24 GHz, which is reasonably close to that of a 100 m telescope. There is also no reference given to the source of the rotational transition frequency, nor is a frequency actually given.

4.8.5. CH₃C₄H (Methyldiacetylene)

The detection of CH₃C₄H was nearly simultaneously reported by Walmsley et al. (1984) (March 22) and MacLeod et al. (1984) (July 15). Later that year, Loren et al. (1984) (November 1) also reported an independent detection, having received word of the earlier work during the publication process.

Walmsley et al. (1984) reported the detection in observations of TMC-1 using the Effelsberg 100 m telescope. They observed and assigned the $K = 0$ and $K = 1$ components of the $J = 6 \rightarrow 5$ and $5 \rightarrow 4$ transitions at 24.4 and 20.3 GHz, respectively. Their assignments were based on the laboratory work of Heath et al. (1955), although they suggest the astronomical observations might be used to refine those measurements moving forward.

Both MacLeod et al. (1984) and Loren et al. (1984) observed the same transitions in TMC-1, with the former using the Haystack 36.6 m and NRAO 140 ft telescopes and the latter using solely the NRAO 140 ft.

4.8.6. C₈H (Octatriynyl Radical)

Cernicharo & Guélin (1996) reported the detection of the C₈H radical in IRAM 30 m observations of IRC+10216, as well as in the archival Nobeyama 45 m observations of Kawaguchi et al. (1995). They identified and assigned 10 transitions between 31.1 and 83.9 GHz based on comparison to calculated rotational constants from Pauzat et al. (1991). The detection and assignment were confirmed in an accompanying letter by the laboratory work of McCarthy et al. (1996).

4.8.7. CH₃CONH₂ (Acetamide)

The detection of CH₃CONH₂ was reported toward Sgr B2 by Hollis et al. (2006a) using the GBT 100 m telescope. A total of eight transitions between 9.3 and 47.4 GHz were identified and

assigned based on the laboratory work of Suenram et al. (2001) and Ilyushin et al. (2004).

4.8.8. C₈H⁻ (Octatriynyl Anion)

Brünken et al. (2007b) and Remijan et al. (2007) simultaneously reported the detection of C₈H⁻. Both detections were made with the GBT 100 m telescope; the former described the detection in TMC-1, while the latter was toward IRC+10216. Remijan et al. (2007) detected the $J = 22 \rightarrow 21$ and $35 \rightarrow 34$ through $38 \rightarrow 37$ transitions between 25.7 and 44.3 GHz based on the laboratory work of Gupta et al. (2007). Brünken et al. (2007b) observed the $11 \rightarrow 10$ through $13 \rightarrow 12$, and the $16 \rightarrow 15$ transitions between 12.8 and 18.7 GHz, based on the same laboratory work.

4.8.9. CH₂CHCH₃ (Propylene)

The detection of CH₂CHCH₃, also referred to as propene, was reported by Marcelino et al. (2007) in IRAM 30 m observations of TMC-1. A total of 13 rotational transitions between 84.2 and 103.7 GHz were identified and assigned based on the laboratory work of Wlodarczyk et al. (1994) and Pearson et al. (1994).

4.8.10. CH₃CH₂SH (Ethyl Mercaptan)

Kolesniková et al. (2014) reported the detection of CH₃CH₂SH in IRAM 30 m observations of Orion. A total of 77 unblended lines between 80 and 280 GHz were identified and assigned based on laboratory spectroscopy presented in the same manuscript. Subsequent attempts to identify the molecule in Sgr B2(N) by Müller et al. (2016) were unsuccessful. Rodríguez-Almeida et al. (2021) confirm the presence of CH₃CH₂SH in the ISM using IRAM 30 m and Yebes 40 m observations of G+0.693-0.027 based on the laboratory work of Schmidt & Quade (1975), Kolesniková et al. (2014), and Müller et al. (2016).

4.8.11. HC₇O (Hexadiynylformyl Radical)

McGuire et al. (2017a) reported the tentative detection of the HC₇O radical in GBT 100 m observations of TMC-1. Based on the laboratory work of Mohamed et al. (2005), a weak detection of the $J = 35/2 \rightarrow 33/2$ transition with partially resolved hyperfine structure was observed near 19.2 GHz. The detection was confirmed in Cordiner et al. (2017) by the observation of several additional weak features, without hyperfine structure, corresponding to the $33/2 \rightarrow 31/2$ transitions near 18.1 GHz. A composite average of these lines, plus the data from McGuire et al. (2017a), provided a 9.5σ detection.

4.8.12. CH₃NHCHO (n-methylformamide)

A tentative detection of CH₃NHCHO was reported in ALMA observations of Sgr B2(N2) by Belloche et al. (2017) and confirmed in Belloche et al. (2019). Numerous transitions in the range of 84–114 GHz were identified and assigned based on the laboratory rotational spectroscopy presented in Belloche et al. (2017).

4.8.13. $H_2CCCHCCH$ (Allenyl Acetylene)

The detection of $H_2CCCHCCH$ was reported in Yebes 40 m observations of TMC-1 by Cernicharo et al. (2021c). A total of 12 transitions between 34.4 and 49.2 GHz were identified and assigned based on the laboratory work of Lee & McCarthy (2019) and McCarthy et al. (2020).

4.8.14. $HCCCHCHCN$ (Cyanovinylacetylene)

Lee et al. (2021a) reported the detection of the *trans*-(E) conformer of $HCCCHCHCN$ in GBT 100 m observations of TMC-1. They identify and assign the $8_{0,8} - 7_{0,7}$, $9_{0,9} - 8_{0,8}$, and $9_{1,9} - 8_{1,8}$ transitions at 23.2, 26.1, and 25.9 GHz based on the laboratory work of Halter et al. (2001), Thorwirth et al. (2004a), and McCarthy et al. (2020). Using spectral line stacking and matched filtering techniques, a significance of 8.0σ was placed on the detection. Using these same techniques, tentative signal from the *trans*-(Z) conformer was identified at 2.8σ significance.

4.8.15. H_2CCHC_3N (Vinylcyanoacetylene)

Lee et al. (2021a) reported the detection of H_2CCHC_3N in GBT 100 m observations of TMC-1. Using spectral line stacking and matched filtering techniques, they reported a 5.5σ significance detection based on the laboratory work of Halter et al. (2001), Thorwirth et al. (2004a), and McCarthy et al. (2020).

4.9. Ten-Atom Molecules

4.9.1. $(CH_3)_2CO$ (Acetone)

Combes et al. (1987) reported the detection of $(CH_3)_2CO$ in IRAM 30 m, NRAO 140 ft, and NRAO 12 m observations of Sgr B2. A total of 11 transitions between 18.7 and 112.4 GHz were identified and assigned based on the laboratory work of Vacherand et al. (1986).

4.9.2. $HO(CH_2)_2OH$ (Ethylene Glycol)

The detection of the *g'*Ga conformer of $HO(CH_2)_2OH$ was reported by Hollis et al. (2002) in NRAO 12 m observations of Sgr B2. Four transitions between 75.1 and 93.0 GHz were identified and assigned based on the laboratory work of Christen et al. (1995). The higher-energy *aGg'* conformer was later detected by Rivilla et al. (2017) in GBT 100 m, IRAM 30 m, and SMA observations of G31.41+0.31.

4.9.3. CH_3CH_2CHO (Propanal)

Hollis et al. (2004b) reported the detection of CH_3CH_2CHO in GBT 100 m observations of Sgr B2. A total of five transitions between 19.2 and 22.2 GHz were identified and assigned based on the laboratory work of Butcher & Wilson (1964). CH_3CH_2CHO is also referred to as propionaldehyde.

4.9.4. CH_3C_5N (Methylcyanodiacetylene)

The detection of CH_3C_5N was reported by Snyder et al. (2006) in GBT 100 m telescope observations of TMC-1. Ten transitions between 18.7 and 24.9 GHz were identified and assigned to the $K = 0$ and $K = 1$ components of the $J_K = 12_* \rightarrow 11_*$ through $16_* \rightarrow 15_*$ transitions of CH_3C_5N based on the

laboratory work of Alexander et al. (1978) and Chen et al. (1998).

4.9.5. CH_3CHCH_2O (Propylene Oxide)

McGuire et al. (2016) reported the detection of CH_3CHCH_2O in GBT 100 m and Parkes 64 m observations of Sgr B2. The $J_{K_a, K_c} = 1_{1,0} \rightarrow 1_{0,1}$, $2_{1,1} \rightarrow 2_{0,2}$, and $3_{1,2} \rightarrow 3_{0,3}$ transitions at 12.1, 12.8, and 14.0 GHz, respectively, were identified and assigned based on laboratory spectroscopy presented in the same manuscript. CH_3CHCH_2O was the first chiral molecule detected in the ISM.

4.9.6. CH_3CH_2OH (Methoxymethanol)

The detection of CH_3CH_2OH was reported by McGuire et al. (2017b) in ALMA observations of NGC 6334I. More than two dozen largely unblended transitions between 239 and 349 GHz were identified and assigned based on the laboratory work of Motiyenko et al. (2018), which was in press at the time.

4.10. Eleven-Atom Molecules

4.10.1. HC_9N (Cyanotetraacetylene)

Broten et al. (1978) reported the detection of HC_9N in TMC-1 using the Algonquin Radio Observatory 46 m and NRAO 140 ft telescopes. The $J = 18 \rightarrow 17$ and $25 \rightarrow 24$ transitions at 10.5 and 14.5 GHz, respectively, were identified on the basis of theoretical calculations described in the same manuscript. The detection was later confirmed by the laboratory spectroscopy performed by Iida et al. (1991).

4.10.2. CH_3C_6H (Methyltriacetylene)

The detection of CH_3C_6H was reported by Remijan et al. (2006) in GBT 100 m observations of TMC-1. Ten spectral lines corresponding to the $K = 0$ and $K = 1$ components of the $J_K = 12_* \rightarrow 11_*$ through $16_* \rightarrow 15_*$ transitions between 18.7 and 24.9 GHz were identified and assigned based on the laboratory work of Alexander et al. (1978).

4.10.3. CH_3CH_2OCHO (Ethyl Formate)

Belloche et al. (2009) reported the detection of *trans*- CH_3CH_2OCHO in IRAM 30 m observations of Sgr B2. A total of 41 unblended transitions of *trans*- CH_3CH_2OCHO between 80 and 268 GHz were identified and assigned based on the laboratory data of Medvedev et al. (2009). The subsequent detection of the *gauche*-conformer was reported by Tercero et al. (2013) in IRAM 30 m observations of Orion. They identified and assigned 38 unblended transitions between 80 and 281 GHz based on the laboratory work of Demaison et al. (1984).

4.10.4. CH_3COOCH_3 (Methyl Acetate)

The detection of CH_3COOCH_3 was reported by Tercero et al. (2013) in IRAM 30 m observations of Orion. A total of 215 unblended transitions of CH_3COOCH_3 between 80 and 281 GHz were identified and assigned based on the laboratory work of Tudorie et al. (2011).

4.10.5. $\text{CH}_3\text{COCH}_2\text{OH}$ (Hydroxyacetone)

Zhou et al. (2020) reported the detection of $\text{CH}_3\text{COCH}_2\text{OH}$ in ALMA Science Verification observations of IRAS 16293. They report a number of largely unblended transitions between 145 and 159 GHz based on laboratory data from Kattija-Ari & Harmony (1980), Apponi et al. (2006), and Braakman et al. (2010).

4.10.6. C_5H_6 (Cyclopentadiene)

The detection of C_5H_6 in Yebes 40 m observations of TMC-1 was reported by Cernicharo et al. (2021a). Based on the laboratory work of Laurie (1956), Scharpen & Laurie (1965), Benson & Flygare (1970), and Bogey et al. (1988a), they identify and assign six largely unblended transitions of C_5H_6 between 37.5 and 46.8 GHz.

4.11. Twelve-Atom Molecules

4.11.1. C_6H_6 (Benzene)

Cernicharo et al. (2001) reported the detection of C_6H_6 in ISO observations of CRL 618. The ν_4 bending mode of C_6H_6 near $14.8 \mu\text{m}$ was identified and assigned based on the laboratory work of Lindenmayer et al. (1988).

4.11.2. $n\text{-C}_3\text{H}_7\text{CN}$ (*n*-propyl Cyanide)

The detection of $n\text{-C}_3\text{H}_7\text{CN}$, also referred to as *n*-butyronitrile, was reported by Belloche et al. (2009) in IRAM 30 m observations of Sgr B2. A total of 50 unblended transitions of the *anti*-conformer of $n\text{-C}_3\text{H}_7\text{CN}$ were identified and assigned based on an extensive reanalysis of the literature spectra presented in the same manuscript.

4.11.3. $i\text{-C}_3\text{H}_7\text{CN}$ (*iso*-propyl Cyanide)

Belloche et al. (2014) reported the detection of $i\text{-C}_3\text{H}_7\text{CN}$ in ALMA observations of Sgr B2 between 84 and 111 GHz, based on the laboratory work of Müller et al. (2011). This was the first branched carbon-chain molecule detected in the ISM.

4.11.4. $1\text{-C}_5\text{H}_5\text{CN}$ (*1*-cyano-1, 3-cyclopentadiene)

The detection of $1\text{-C}_5\text{H}_5\text{CN}$ was reported by McCarthy et al. (2021) using GBT 100 m observations of TMC-1. A 5.8σ detection was reported based on spectral line stacking and matched filtering using laboratory work reported in the same paper as well as that of Ford & Seitzman (1978) and Sakaizumi et al. (1987). Lee et al. (2021b) subsequently published the detections of the $7_{2,5} - 6_{2,4}$, $7_{1,6} - 6_{1,5}$, $8_{0,8} - 7_{0,7}$, and $9_{0,9} - 8_{0,8}$ transitions in the same source, citing an increased detection significance of 10.7σ . The molecule $1\text{-C}_5\text{H}_5\text{CN}$ is the first one to be reported in the ISM containing a five-membered ring.

4.11.5. $2\text{-C}_5\text{H}_5\text{CN}$ (*2*-cyano-1, 3-cyclopentadiene)

The detection of $2\text{-C}_5\text{H}_5\text{CN}$ was reported by Lee et al. (2021b) using GBT 100 m observations of TMC-1. Based on laboratory work presented in the same paper, as well as work from Ford & Seitzman (1978), Sakaizumi et al. (1987), and McCarthy et al. (2021), they report a 6.6σ detection based on spectral line stacking and matched filtering.

4.12. Thirteen-Atom Molecules

4.12.1. $\text{C}_6\text{H}_5\text{CN}$ (Benzonitrile)

McGuire et al. (2018) reported the detection of $\text{C}_6\text{H}_5\text{CN}$ in GBT 100 m observations of TMC-1. A total of nine transitions, some with resolved ^{14}N hyperfine structure, between 18.4 and 23.2 GHz were identified and assigned on the basis of laboratory work described in the same paper, as well as that of Wohlfart et al. (2008).

4.12.2. HC_{11}N (Cyanopentaacetylene)

Loomis et al. (2021) reported the detection of HC_{11}N at 5.0σ using spectral line stacking and matching filtering analyses of GBT 100 m observations of TMC-1. The detection was based on the laboratory work of Travers et al. (1996b).

The study of HC_{11}N in the ISM has a long history. Bell et al. (1997) reported a detection of HC_{11}N in NRAO 140 ft observations of TMC-1. They assigned two emission features at 12,848.728 MHz and 13,186.853 MHz to the $J = 38 \rightarrow 37$ and $39 \rightarrow 38$ transitions of HC_{11}N based on the laboratory work of Travers et al. (1996b). The detection was later disputed by Loomis et al. (2016), who reobserved TMC-1 using the 100 m GBT. They targeted six transitions of HC_{11}N , including those originally reported by Bell et al. (1997), and detected no signal at any of these frequencies. They suggest correlator artifacts may have been responsible for the signals seen in Bell et al. (1997). Subsequently, Cordiner et al. (2017) confirmed the findings of Loomis et al. (2016), setting a yet lower upper limit with more sensitive data.

4.13. PAH Molecules

4.13.1. $1\text{-C}_{10}\text{H}_7\text{CN}$ (*1*-cyanonaphthalene)

McGuire et al. (2021) reported the detection of *1*-cyanonaphthalene in GBT 100 m observations of TMC-1. The $20_{*,20} - 19_{*,19}$, $18_{*,16} - 17_{*,15}$, $21_{*,21} - 20_{*,20}$, $20_{*,19} - 19_{*,18}$, and $19_{*,17} - 18_{*,16}$ transitions were detected at $>5\sigma$ significance based on the laboratory work of McNaughton et al. (2018). A 13.5σ detection was claimed based on a spectral matched filtering analysis.

4.13.2. $2\text{-C}_{10}\text{H}_7\text{CN}$ (*2*-cyanonaphthalene)

McGuire et al. (2021) reported the detection of *2*-cyanonaphthalene in GBT 100 m observations of TMC-1. A 17.1σ detection was claimed based on a spectral matched filtering analysis, using the laboratory work of McNaughton et al. (2018). No individual rotational transitions were observed at $\geq 3\sigma$.

4.13.3. C_9H_8 (Indene)

The detection of C_9H_8 was reported nearly simultaneously by Burkhardt et al. (2021) in GBT 100 m observations of TMC-1 and Cernicharo et al. (2021a) in Yebes 40 m observations of TMC-1. Both detections relied on the laboratory work of Li et al. (1979), with Burkhardt et al. (2021) presenting new laboratory spectroscopy of C_9H_8 as well.

4.14. Fullerene Molecules

4.14.1. C_{60} (Buckminsterfullerene)

Cami et al. (2010) reported the detection of C_{60} in Spitzer observations of Tc 1. Strong emission features from C_{60} at 7.0,

85, 17.4, and 18.9 μm were identified and assigned based on the work of Martin et al. (1993) and Fabian (1996).

4.14.2. C_{60}^+ (Buckminsterfullerene Cation)

Berné et al. (2013) reported the detection of C_{60}^+ in Spitzer observations toward NGC 7023. Two emission features at 7.1 and 6.4 μm were assigned to C_{60}^+ based on the laboratory matrix-isolation work of Kern et al. (2013). A number of additional features were assigned based on theoretical calculations performed and described in Berné et al. (2013). Subsequent laboratory work by Campbell et al. (2015) confirmed the presence of C_{60}^+ in the ISM by measuring the gas-phase spectrum of C_{60}^+ . Based on those results, they determined that C_{60}^+ was the carrier of the 9632 and 9577 Å DIBs, the first definitive molecular assignment of a carrier of one of these bands. Follow-up observational and laboratory studies by Walker et al. (2015) and Campbell et al. (2016) solidified the identification.

4.14.3. C_{70} (Rugbyballene)

Cami et al. (2010) reported the detection of C_{70} in Spitzer observation, von Czarowski & Meiwes-Broer (1995), and Stratmann et al. (1998).

5. Tentative Detections

This section contains those molecules for which a detection has been classified by the authors as tentative. Those molecules once viewed as tentative that have since been confirmed are listed in Section 4.

5.1. $\text{C}_2\text{H}_5\text{N}$ (Aziridine)

Dickens et al. (2001) reported the tentative detection of the $J_{K_a, K_c} = 5_{5,0} \rightarrow 4_{4,1}$ transition of $\text{C}_2\text{H}_5\text{N}$, also known as ethylenimine, at 226 GHz toward Sgr B2, G34.3+2, G10.47+0.03, and G327.3-0.6 in observations made with the SEST 15 m, NRAO 12 m, and NASA Deep Space Network 70 m telescopes. The laboratory data were reported by Thorwirth et al. (2000).

5.2. SiH (Silicon Hydride)

Schilke et al. (2001) reported the tentative detection of two features in a CSO line survey of Orion that were coincident with transitions of SiH. Two groups of hyperfine transitions in the $^2\Pi_{1/2}$ state at 625 and 628 GHz fell within range of the observations. The lower set is significantly blended with other emitting species, whereas the higher-frequency set appears unblended and may show partially resolved hyperfine structure. The laboratory frequencies were from Brown et al. (1985a).

5.3. FeO (Iron Monoxide)

Walmsley et al. (2002) identified an absorption feature in IRAM 30 m observations of Sgr B2 at 153 GHz that they tentatively assign to the $J = 5 \rightarrow 4$, $\Omega = 4$ transition of FeO, based on the laboratory work of Allen et al. (1996). Later, Furuya et al. (2003) used the Nobeyama Millimeter Array to confirm the detection of this line, but no additional transitions were observed. Most recently, Decin et al. (2018) reported a tentative detection of the $11 \rightarrow 10$, $\Omega = 4$ transition in ALMA observations of R Dor at 337 GHz.

5.4. OCN^+ (Cyanate Anion)

There is a long history of attempts to identify the carrier of the “XCN” feature in astrophysical ice observations near 2167 cm^{-1} . On the basis of extensive laboratory work (see, e.g., Schutte & Greenberg 1997), van Broekhuizen et al. (2005) claim an identification of OCN^+ in ices along numerous sight lines to low-mass YSO’s using the Very Large Telescope. Only a single absorption feature could be ascribed to OCN^+ . As this is a single-feature detection, and no gas-phase detection has been claimed, OCN^+ has been listed as a tentative interstellar species in this census.

5.5. C_2H^- (Ethylylide Anion)

Cernicharo et al. (2008) suggest that an unidentified line at 83.278 GHz, classified as U83278, in IRAM 30 m observations of IRC+10216 may be due to the $J = 1 \rightarrow 0$ transition of C_2H^- . Although they list no source for their line frequency, it presumably is derived from the work of Brünken et al. (2007a) and Amano (2008a).

5.6. $\text{C}_6\text{H}_5\text{OH}$ (Phenol)

Kolesniková et al. (2013) reported the laboratory rotational spectroscopy of $\text{C}_6\text{H}_5\text{OH}$ and identified a number of coincidences between transitions of $\text{C}_6\text{H}_5\text{OH}$ and unassigned lines in IRAM 30 m observations of Orion between 80 and 280 GHz (Tercero et al. 2012).

5.7. NO^+ (Nitrosylium Cation)

Cernicharo et al. (2014) reported the tentative detection of a single line ($J = 2 \rightarrow 1$) of NO^+ at 238 GHz toward B1-b using the IRAM 30 m telescope. The assignment was made based on laboratory rotational spectroscopy described in the same paper.

5.8. NCCP (Cyanophosphaethyne)

Agúndez et al. (2014b) reported the tentative detection of NCCP in IRAM 30 m observations of IRC+10216. They identified and tentatively assigned three signals in their spectra to the $J = 15 \rightarrow 14$, $16 \rightarrow 15$, and $18 \rightarrow 17$ transitions of NCCP at 81, 87, and 97 GHz, respectively, based on the laboratory work of Bizzocchi et al. (2001).

5.9. $\text{C}_2\text{H}_5\text{OCH}_3$ (*t*-ethyl Methyl Ether)

Charnley et al. (2001) indicated a tentative detection of $\text{C}_2\text{H}_5\text{OCH}_3$ in NRAO 12 m and BIMA observations of Orion-KL and Sgr B2(N). A detection of $\text{C}_2\text{H}_5\text{OCH}_3$ was then later reported by Fuchs et al. (2005) in IRAM 30 m and SEST 15 m observations of W51e2. This detection was disputed by Carroll et al. (2015), who reobserved both W51e2 and Sgr B2(N) using the ARO 12 m and GBT 100 m telescopes and failed to detect $\text{C}_2\text{H}_5\text{OCH}_3$, setting an upper limit column density substantially lower than the reported value of Fuchs et al. (2005). Evidence supporting the tentative detection in Orion-KL was later reported by Tercero et al. (2015) using IRAM 30 m and ALMA observations of the region, although the authors claim the detection should still be viewed as tentative. The laboratory spectroscopy was performed by Hayashi & Kuwada (1975) and Fuchs et al. (2003).

Table 4
List of Molecules Detected in External Galaxies with References to the First Detections

2 Atoms		3 Atoms		4 Atoms		5 Atoms	
Species	Ref.	Species	Ref.	Species	Ref.	Species	Ref.
CH	1	H ₂ O	2	NH ₃	3	HC ₃ N	4, 5
CN	5	HCO ⁺	6	H ₂ CO	7	HCOOH	8
CH ⁺	9	HCN	10	HNCO	11	CH ₂ NH	12
OH	13	OCS	14	H ₂ CS	15	NH ₂ CN	15
CO	16	HNC	5	C ₂ H ₂	17	H ₂ CCO	12
H ₂	18	H ₂ S	19	C ₃ N	8	C ₄ H	12
SiO	20	N ₂ H ⁺	20	HOCO ⁺	21, 15	c-C ₃ H ₂	22
CS	23	C ₂ H	5	l-C ₃ H	12	CH ₂ CN	12
SO	24, 25	SO ₂	26	H ₃ O ⁺	27	H ₂ CCC	12
NS	26	HCO	28, 29	c-C ₃ H ^a	15		
C ₂	30	HCS ⁺	31	H ₂ CN	8		
NO	26	HOC ⁺	32	l-C ₃ H ⁺	8		
HCl	33	C ₂ S	15				
NH	34	C ₃	30				
SO ⁺	12	NH ₂	35				
CO ⁺	36	H ₃ ⁺	37				
HF	38, 39, 40	H ₂ O ⁺	41				
CF ⁺	42	H ₂ Cl ⁺	43				
O ₂	44						
OH ⁺	38, 39, 45						
SH ⁺	46						
ArH ⁺	47						

6 Atoms		7 Atoms		8 Atoms		9 Atoms		12 Atoms	
Species	Ref.	Species	Ref.	Species	Ref.	Species	Ref.	Species	Ref.
CH ₃ OH	48	CH ₃ CHO	12	HCOOCH ₃	49	CH ₃ OCH ₃	50, 49	C ₆ H ₆	51
CH ₃ CN	52	CH ₃ CCH	52	HC ₆ H	51				
NH ₂ CHO	31	CH ₃ NH ₂	12						
CH ₃ SH	8	CH ₂ CHCN	8						
HC ₄ H	51	HC ₅ N ^a	21						

References. Tentative detections are indicated, and some extra references are occasionally provided for context. (1) Whiteoak et al. 1980; (2) Churchwell et al. 1977; (3) Martin & Ho 1979; (4) Mauersberger et al. 1990; (5) Henkel et al. 1988; (6) Stark & Wolff 1979; (7) Gardner & Whiteoak 1974; (8) Tercero et al. 2020; (9) Magain & Gillet 1987; (10) Rickard et al. 1977; (11) Henkel et al. 1991; (12) Muller et al. 2011; (13) Weliachew 1971; (14) Mauersberger et al. 1995; (15) Martín et al. 2006; (16) Rickard et al. 1975; (17) Matsuura et al. 2002; (18) Thompson et al. 1978; (19) Heikkilä et al. 1999; (20) Mauersberger & Henkel 1991; (21) Aladro et al. 2015; (22) Seaquist & Bell 1986; (23) Henkel & Bally 1985; (24) Johansson 1991; (25) Petuchowski & Bennett 1992; (26) Martín et al. 2003; (27) van der Tak et al. 2008; (28) Sage & Ziurys 1995; (29) García-Burillo et al. 2002; (30) Welty et al. 2013; (31) Muller et al. 2013; (32) Usero et al. 2004; (33) Wallström et al. 2019; (34) González-Alfonso et al. 2004; (35) Müller et al. 2014; (36) Fuente et al. 2006; (37) Geballe et al. 2006; (38) van der Werf et al. 2010; (39) Rangwala et al. 2011; (40) Monje et al. 2011; (41) Weiß et al. 2010; (42) Muller et al. 2016; (43) Muller et al. 2014; (44) Wang et al. 2020; (45) González-Alfonso et al. 2013; (46) Muller et al. 2017; (47) Müller et al. 2015; (48) Henkel et al. 1987; (49) Sewilo et al. 2018; (50) Qiu et al. 2018; (51) Bernard-Salas et al. 2006; (52) Mauersberger et al. 1991.

^a Tentative detection.

Table 5
List of Molecules Detected in Interstellar Ices, with References to Representative Detections

Species	References
CO	1
H ₂ O	2
OCS	3, 4
CO ₂	5
OCN ⁺	6
NH ₃	7
H ₂ CO	8
HCOOH	9
CH ₄	10
CH ₃ OH	11

References. (1) Soifer et al. 1979; (2) Gillett & Forrest 1973; (3) Palumbo et al. 1995; (4) Palumbo et al. 1997; (5) D'Hendecourt & Jourdain de Muizon 1989; (6) van Broekhuizen et al. 2005; (7) Lacy et al. 1998; (8) Keane et al. 2001; (9) Schutte et al. 1999; (10) Lacy et al. 1991; (11) Grim et al. 1991.

5.10. HC₅NH⁺ (Protonated Cyanodiacetylene Cation)

Marcelino et al. (2020) report a tentative detection of HC₅NH⁺ in Yebes 40 m observations of TMC-1. They identify a series of eight harmonically spaced lines in the data corresponding to a rotational constant $B = 1295.8158$ MHz. Based on quantum chemical calculations, they suggest either HC₅NH⁺ or NC₄NH⁺ as the potential carrier, eventually proposing HC₅NH⁺ as the more likely. The lack of laboratory frequencies for confirmation is the remaining hinderance.

5.11. CH₃CH₂CCH (Ethyl Acetylene)

A tentative detection of CH₃CH₂CCH was reported by Cernicharo et al. (2021d) in Yebes 40 m observations of TMC-1. A number of transitions between 33.6 and 44.3 GHz are tentatively assigned based on the laboratory work of Landsberg & Suenram (1983), Demaison et al. (1983), Bestmann & Dreizler (1985), and Steber et al. (2012). A spectral stacking analysis was

Table 6
List of Molecules, Including Rare Isotopic Species, Detected in Protoplanetary Disks, with References to Representative Detections

2 Atoms		3 Atoms		4 Atoms		5 Atoms		6 Atoms	
Species	Ref.	Species	Ref.	Species	Ref.	Species	Ref.	Species	Ref.
CN	1, 2	H ₂ O	3, 4, 5	NH ₃	6	HC ₃ N	7	CH ₂ OH	8
C ¹⁵ N	9	HCO ⁺	1, 2	H ₂ CO	2	HCOOH	10	CH ₃ CN	11
CH ⁺	12	DCO ⁺	13	H ₂ CS	14, 15	c-C ₃ H ₂	16		
OH	17, 5	H ¹³ CO ⁺	18, 13	C ₂ H ₂	19	CH ₄	20		
CO	21	HCN	1, 2						
¹³ CO	22	DCN	23						
C ¹⁸ O	24	H ¹³ CN	25						
C ¹⁷ O	26, 27	H ¹⁵ CN	25						
¹³ C ¹⁸ O	39								
¹³ C ¹⁷ O	40								
H ₂	28	HNC	2						
HD	29	DNC	14						
CS	30, 31, 32	H ₂ S	33						
C ³⁴ S	14, 15	N ₂ H ⁺	34, 35						
¹³ CS	14, 15	N ₂ D ⁺	36						
SO	37	C ₂ H	2						
		C ₂ D	14						
		CO ₂	38						

References. The earliest reported detection of a species in the literature is provided on a best-effort basis. Tentative and disputed detections are not included (see text). (1) Kastner et al. 1997; (2) Dutrey et al. 1997; (3) Carr et al. 2004; (4) Hogerheijde et al. 2011; (5) Salyk et al. 2008; (6) Salinas et al. 2016; (7) Chapillon et al. 2012; (8) Walsh et al. 2016; (9) Hily-Blant et al. 2017; (10) Favre et al. 2018; (11) Öberg et al. 2015; (12) Thi et al. 2011; (13) van Dishoeck et al. 2003; (14) Loomis et al. 2020; (15) Le Gal et al. 2019; (16) Qi et al. 2013; (17) Mandell et al. 2008; (18) van Zadelhoff et al. 2001; (19) Lahuis et al. 2006; (20) Gibb & Home 2013; (21) Beckwith et al. 1986; (22) Sargent & Beckwith 1987; (23) Qi et al. 2008; (24) Dutrey et al. 1994; (25) Guzmán et al. 2015; (26) Smith et al. 2009; (27) Guilloteau et al. 2013; (28) Thi et al. 1999; (29) Bergin et al. 2013; (30) Ohashi et al. 1991; (31) Blake et al. 1992; (32) Guilloteau et al. 2012; (33) Phuong et al. 2018; (34) Qi et al. 2003; (35) Dutrey et al. 2007; (36) Huang & Öberg 2015; (37) Fuente et al. 2010; (38) Carr & Najita 2008; (39) Zhang et al. 2017; (40) Booth et al. 2019.

suggestive, but a few transitions predicted to be visible above the noise, but that were missing, concerned the authors.

6. Disputed Detections

This section contains those molecules for which a detection has been claimed and subsequently disputed in the literature. Those species that were disputed but later confirmed are listed in Section 4. Species for which a tentative detection has been claimed and also disputed are not listed.

6.1. NH₂CH₂COOH (Glycine)

Kuan et al. (2003) reported a detection of 27 lines of NH₂CH₂COOH in observations toward Orion, Sgr B2, and W51 using the NRAO 12 m telescope. Each source contained 13–16 of the 27 features; three features were seen in common between the sources. The frequencies were obtained from the rotational constants measured and reported in Suenram & Lovas (1980) and Lovas et al. (1995). The detection was later disputed by Snyder et al. (2005), who claimed to have identified a number of issues with the analysis. Notably, Snyder et al. (2005) argue that the frequency predictions used by Kuan et al. (2003) were extrapolated too far above the measured laboratory transitions. Snyder et al. (2005) used laboratory frequencies from Ilyushin et al. (2005) that covered the observed frequency range and examined archival NRAO 12 m and SEST 15 m observations of Orion, Sgr B2, and W51. They report a number of “missing” transitions of NH₂CH₂COOH that they predicted should have been strongly detected, if the detection of Kuan et al. (2003) held. Subsequent searches by Jones et al. (2007), Cunningham et al. (2007), and Belloche et al. (2008) using both interferometers and single-dish facilities failed to detect NH₂CH₂COOH and set upper

limits to the column density lower than that claimed in the detection of Kuan et al. (2003) (see Belloche et al. 2008 §4.4 for a detailed discussion).

7. Species Detected in External Galaxies

A remarkable fraction (73/241; ~30%) of known interstellar and circumstellar molecules has also been detected in observations of external galaxies. A list of these species is given in Table 4. For most species, the provided reference is to the earliest claim of a detection in the literature. In some cases, additional references are provided for context. Molecules for which a tentative detection in external galaxies have been claimed are indicated. In the case of fullerene molecules, there has been some debate in the literature over the claimed identification of these molecules (Duley & Hu 2012), and thus these are not included in this table at this time.

A few notable absences stand out. The detection of H₂Cl⁺ (Muller et al. 2014) hints that the detections of HCl and HCl⁺ may be achievable, assuming the extragalactic abundances follow those seen in our galaxy where these species are within factors of 1–3 of each other (Monje et al. 2013). Similarly, the presence of SH⁺ would indicate that SH is a likely candidate, given its marginally higher abundance in galactic sight lines (see, e.g., Neufeld et al. 2012). The detections of the much larger species HCOOCH₃ and CH₃OCH₃ (Qiu et al. 2018; Sewilo et al. 2018) suggest a reservoir of complex molecules may be also observable.

The complete list of external galaxies in which these detections were made are included in `astromol`. By far the largest contributors to these detections are the LOS to PKS 1830-211 (23 molecules), NGC 253 (22 molecules), and M82 (14 molecules).

Table 7

List of Molecules Detected in Exoplanetary Atmospheres, with References to Representative Detections.

Species	References
OH	1
CO	2, 3, 4, 5
TiO	6, 7, 8
H ₂ O	9, 10, 11, 12, 13
HCN	14
CO ₂	15, 2, 4
NH ₃	16
C ₂ H ₂	16
CH ₄	17, 3, 18, 5

Note. Tentative and disputed detections are not included. **References.** (1) Nugroho et al. 2021; (2) Madhusudhan et al. 2011; (3) Barman et al. 2011; (4) Lanotte et al. 2014; (5) Barman et al. 2015; (6) Haynes et al. 2015; (7) Sedaghati et al. 2017; (8) Nugroho et al. 2017; (9) Tinetti et al. 2007; (10) Deming et al. 2013; (11) Kreidberg et al. 2014; (12) Kreidberg et al. 2015; (13) Lockwood et al. 2014; (14) Hawker et al. 2018; (15) Stevenson et al. 2010; (16) Giacobbe et al. 2021; (17) Swain et al. 2008; (18) Stevenson et al. 2014.

8. Species Detected in Interstellar Ices

Molecules for which a relatively firm detection in interstellar ices has been reported in the literature are given in Table 5. Note that for some molecules, it is not clear whether a community consensus has been reached. Here, as for the ISM/CSM species, the default has been to list molecules as detected if a literature source claims such and no other study specifically disputes it. A review of the status of interstellar ices, which delves more deeply into the nuances of various claims, is given by Boogert et al. (2015). Observations of ices require a background-illuminating source for absorption, limiting the number of sight lines that are available for study. Further complications arise when comparing with laboratory spectra, as the peak positions, line widths, and intensities of molecular ice features are known to be sensitively dependent on temperature, crystal structure of the ice (or lack thereof), and mixing or layering with other species (see, e.g., Ehrenfreund et al. 1997; Schutte et al. 1999, and Cooke et al. 2016). As a result, only a handful of species (H₂O, CO, CO₂, CH₄, CH₃OH, and NH₃) have been definitively detected in interstellar ices.

The first molecular ice detection was reported by Gillett & Forrest (1973), who observed an absorption feature at 3.1 μm toward Orion-KL, which they attributed to H₂O based on comparison to the laboratory work of Irvine & Pollack (1968). Soifer et al. (1979) then reported the detection of CO at 4.61 μm in absorption toward W33A, based on the laboratory work of Mantz et al. (1975).

The laboratory work of D'Hendecourt & Allamandola (1986) was then used to detect a further four species. As mentioned in Section 4.2.17, CO₂ was detected by D'Hendecourt & Jourdain de Muizon (1989), based on their own laboratory work, in absorption at 15.2 μm toward several IRAS sources. Also discussed previously (Section 4.4.13), CH₄ was simultaneously detected in the gas and solid phases by Lacy et al. (1991) toward NGC 7538 IRS 9. A feature was attributed to CH₄ at 7.7 μm . That same year, Grim et al. (1991) identified and assigned an absorption feature at 3.53 μm in UKIRT observations toward W33A to CH₃OH. Finally, the detection of NH₃ was reported by Lacy et al. (1998), who assigned an absorption feature at 1110 cm^{-1} toward NGC 7538 IRS 9.

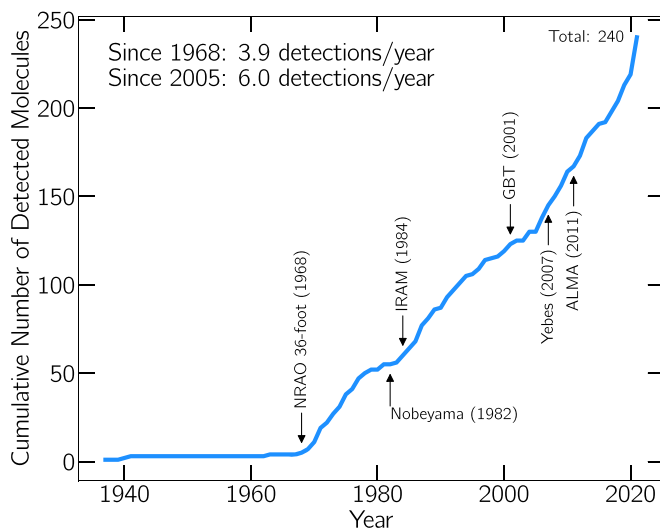


Figure 1. Cumulative number of known interstellar molecules over time. After the birth of molecular radio astronomy in the 1960s, there have been on average 3.9 new detections per year. The commissioning dates of several major contributing facilities are noted with arrows.

Several more species have been tentatively identified due to the coincidence of a spectral feature with laboratory data for a molecule under certain temperature or mixture conditions. Palumbo et al. (1995) and Palumbo et al. (1997) identified an absorption feature at 4.90 μm toward a number of sources that corresponded to OCS when mixed with CH₃OH, based on their own laboratory work. As discussed in Section 5.4, van Broekhuizen et al. (2005) claim an identification of OCN⁺ based on a lengthy history of laboratory work (e.g., Schutte & Greenberg 1997). Finally, detections of HCOOH and H₂CO are claimed by Schutte et al. (1999) and Keane et al. (2001), respectively.

Finally, a number of additional molecular carriers have been suggested or tentatively assigned but have not yet been definitively confirmed. These possible interstellar molecules are discussed in some detail in a review article by Boogert et al. (2015).

9. Species Detected in Protoplanetary Disks

To date, 25 unique molecules and 17 isotopologues have been detected in protoplanetary disks. Compared with the molecular clouds from which they form, the detected molecular inventory of protoplanetary disks is relatively sparse. A list of species detected in disks, including isotopologues, is given in Table 6, along with early and/or representative detection references. The detections of H₂D⁺ and HDO that were reported by Ceccarelli et al. (2004) and Ceccarelli et al. (2005), but were later disputed by Guilloteau et al. (2006), are not included. Only detections reported in sources identified by the authors or supporting literature as class II sources—those that are no longer embedded in their natal molecular cloud—are included. This distinction is made to avoid any possible ambiguity over whether a reported detection originates from the disk itself or the molecular cloud.

The (relatively) low number of gas-phase species so far detected in disks can likely be attributed to a combination of factors.

1. Often narrow ranges of physical environments conducive to a large gas-phase abundance. For example, many

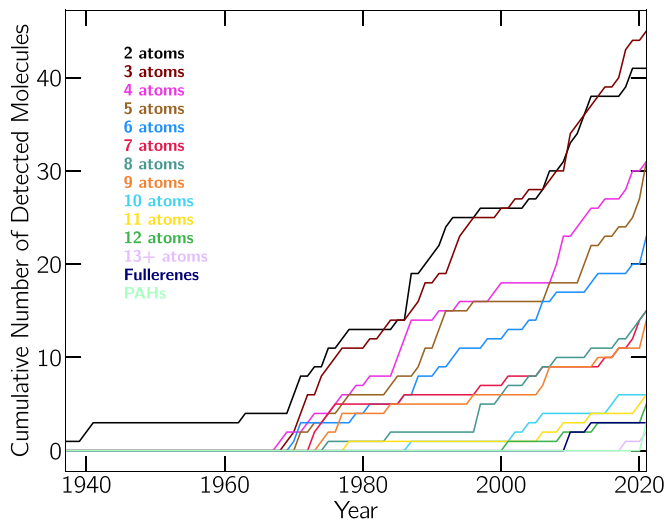


Figure 2. Cumulative number of known interstellar molecules with 2–13 atoms, as well as fullerene molecules, as a function of time. The traces are color coded by number of atoms and labeled on the right.

Table 8

Rates (m) of Detection of New Molecules per Year

# Atoms	m (yr^{-1})	R^2	Onset Year
2	0.68	0.99	1968
3	0.78	0.99	1968
4	0.53	0.99	1968
5	0.48	0.98	1971
6	0.40	0.99	1970
7	0.17	0.94	1973
8	0.31	0.96	1975
9	0.19	0.94	1974
10	0.21	0.93	2001
11	0.23	0.95	2004
12	0.16	0.92	2001
13	0.30	0.77	2018
Fullerenes	0.09	0.75	2010

Note. Sorted by number of atoms per molecule derived from linear fits to the data shown in Figure 2 as well as the R^2 values of the fits, for molecules with 2–12 atoms. The start year was chosen by the visual onset of a steady detection rate and is given for each fit. Rates and R^2 values were obtained using the `scipy.stats.linregress` module.

complex molecules are likely locked into ices in the cold, shielded midplane of the disk and are liberated into the gas phase for detection in only certain, narrow regions of the disk (Walsh et al. 2014).

- Conversely, gas-phase molecules that reach the upper layers of the disk are subject to the harsh, PDR-like radiation environment of the star and the resulting photodestructive processes (Henning et al. 2010).
- The angular extent of these sources on the sky is small (of order arcseconds; Brogan et al. 2015), largely degrading the utility of the most sensitive single-dish facilities due to beam dilution. As a result of the overall low abundance, the required surface brightness sensitivity likewise limits the effectiveness of many small and midscale interferometers. As a result, the most complex and low-abundance species are being detected exclusively with ALMA and are already pushing the limits of the instrument (Loomis et al. 2018).

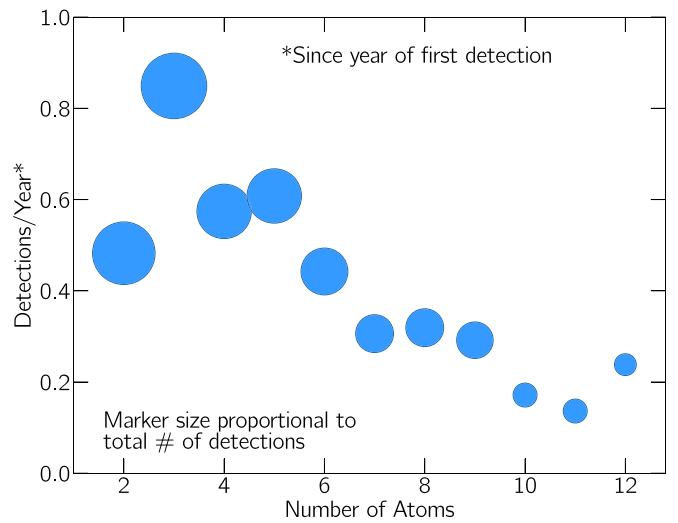


Figure 3. Number of detections per year for a molecule with a given number of atoms, beginning in the first year a molecule of that size was detected. The markers are sized proportionally to the bulk number of detections of molecules with those sizes. Diatomics are “penalized” due to their original detection in 1937, with a large gap until 1968.

Table 9

Total Number of Detections for Each Facility Listed in Section 4

Facility	#	Facility	#
IRAM 30 m	64	SMA	2
NRAO 36 ft	33	SEST	2
GBT 100 m	28	SOFIA	2
NRAO/ARO 12 m	27	Hat Creek 20 ft	2
Yebes 40 m	19	IRTF	2
Nobeyama 45 m	15	PdBI	2
NRAO 140 ft	13	OVRO	2
Bell 7 m	8	MWO 4.9 m	2
ALMA	8	Hubble	1
SMT	7	IRAS	1
Herschel	7	BIMA	1
Parkes	5	NRL 85 ft	1
FCRAO 14 m	5	ATCA	1
ISO	5	Mitaka 6 m	1
APEX	4	McMath Solar Telescope	1
Onsala 20 m	4	UKIRT	1
KPNO 4 m	4	Odin	1
Effelsberg 100 m	4	FUSE	1
Algonquin 46 m	3	KAO	1
Mt. Wilson	3	Mt. Hopkins 60-in	1
Spitzer	3	Aerobee-150 Rocket	1
Haystack	3	Millstone Hill 84 ft	1
CSO	2	Goldstone	1

Detection and analysis of the most complex molecules seen to date, CH_3OH and CH_3CN (Öberg et al. 2015; Walsh et al. 2016), have benefited from velocity stacking and newly developed matched-filtering techniques to extract useful signal-to-noise ratios (Loomis et al. 2018). While these techniques are likely to produce a number of new detections of lower-abundance molecules in the coming years, astrochemical models combined with sensitivity analyses suggest that the total number of molecules detectable with complexity greater than CH_3OH and CH_3CN may be small (Walsh et al. 2018).

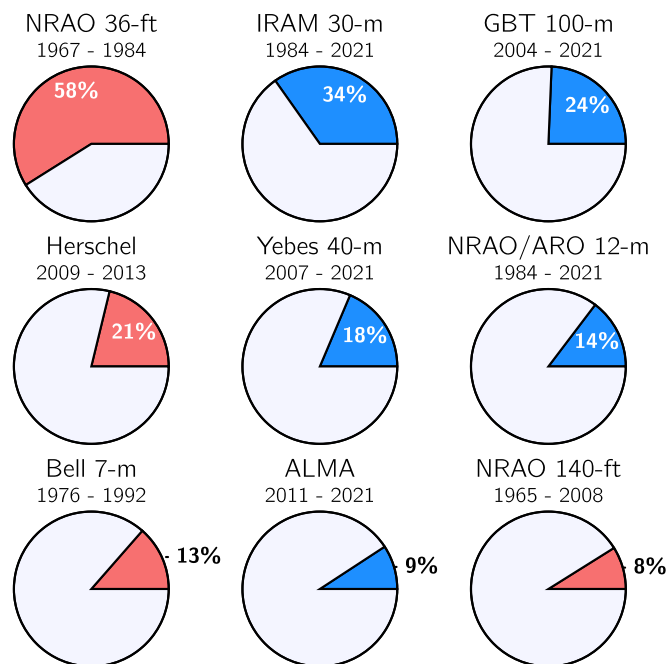


Figure 4. Percentage share of detections that a facility contributed (or is contributing) over its operational lifetime. For example, the NRAO 36 ft antenna accounted for 58% of all detections made during its operational lifetime. Facilities no longer in operation are colored red, and current facilities are in blue.

10. Species Detected in Exoplanetary Atmospheres

Although exoplanet atmospheres have now been observed for some time (Charbonneau et al. 2002), only a small handful of molecules have been detected in these environments. That number, and the ability to robustly measure molecules in exoplanetary atmospheres, is expected to increase somewhat with the launch of the James Webb Space Telescope (Schlawin et al. 2018). Table 7 lists those molecules for which a consensus seems to have been reached in the literature as being detected. There is extensive debate in the literature as to the robustness of many claimed detections (see Madhusudhan et al. 2016 for a thorough overview). Thus, references are provided both to some early detections, for historical context, and to some more recent literature. The reference list is intended to be representative, not exhaustive. Evidence for the presence of chromium hydride CrH in the atmosphere of WASP-31 b has been reported by Braam et al. (2020). Consensus has not been reached, however, on whether the evidence is robust enough to claim a detection.

11. Discussion

As of publication, a total of 241 individual molecules have been detected in the ISM. Here, several graphical representations of the census results presented above are shown and briefly discussed.

11.1. Cumulative Detection Rates

The cumulative number of known interstellar molecules with time is presented in Figure 1, as well as the commissioning dates of a number of key observational facilities. Although the first molecules were detected between 1937 and 1941 (see Sections 4.1.1, 4.1.2, and 4.1.3), and OH in 1963 (Section 4.1.4), it was not until the late 1960s with the development of

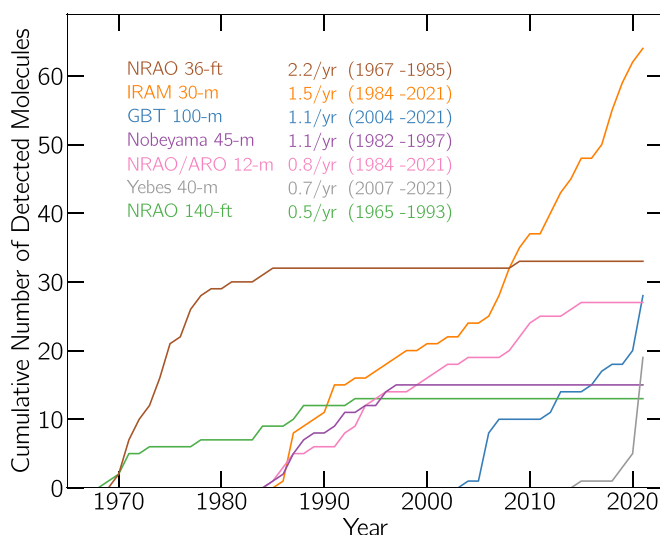


Figure 5. Cumulative number of detections per facility by year. For clarity, only those facilities with 10 or more total detections are shown. The detection rates for the facilities over selected time periods are highlighted.

high-resolution radio receivers optimized for line observations that detections began in earnest. The rate of detections had remained remarkably constant at ~ 3.9 new molecules per year. Notably, however, beginning in 2005 there is some evidence that this detection rate has increased. A fit of the data since 2005 yields a rate of ~ 6.0 molecules per year. This would appear to be consistent with the advent of the GBT as a molecule-detection telescope, a significant uptick in the rate of detections from IRAM, and the commissioning of the Yebes 40 m telescope.

Figure 2 displays the same data as Figure 1, broken down by the cumulative detections of molecules containing n atoms, while Table 8 and Figure 3 display the rates of new detections per year sorted by the number of atoms per molecule. These rates show a steady decrease with increasing size, as might be expected with generally decreasing trends in abundance and line intensities with size. Of note, molecules with 10 or more atoms did not begin to be routinely detected until the early 2000s.

11.2. Detecting Facilities

Table 9 lists the total number of detections by each facility listed in Section 4. When two or more telescopes were used for a detection, each was given full credit. In total, 46 different facilities have contributed to the detection of at least one new species. Acronym definitions for these are given in Table 1 or in text.

The Nobeyama 45 m, GBT, ARO/NRAO 12 m, NRAO 36 ft, IRAM 30 m, and Yebes 40 m telescopes have cumulatively contributed to more than half of the new molecular detections. It is worth examining the impact of a facility on the new detections over its operational lifetime. For instance, while the IRAM 30 m telescope clearly dominates in the total number of detections, the NRAO 36 ft telescope produced more detections per year of its operational life. Figure 4 shows this information graphically for the top six contributing facilities; in this case, the NRAO 12 m and ARO 12 m have been combined, despite being operated by different organizations over their lifetime. During its operation, the NRAO 36 ft contributed to more than half of all new molecular detections.

Figure 5 presents these data in another way, displaying the cumulative number of detections over time by each facility with

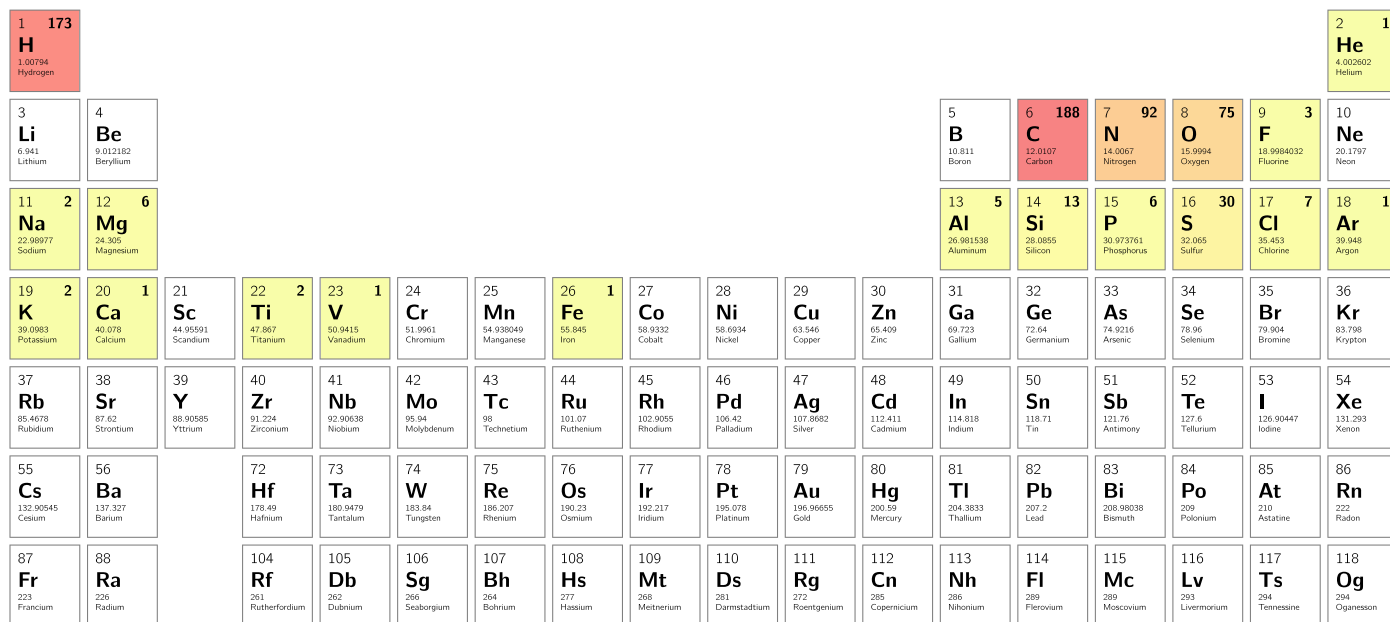


Figure 6. Periodic table of the elements, absent the lanthanide and actinide series, colored by number of detected species containing each element. For those elements with detected ISM molecules, that number is displayed in the upper right of each cell.

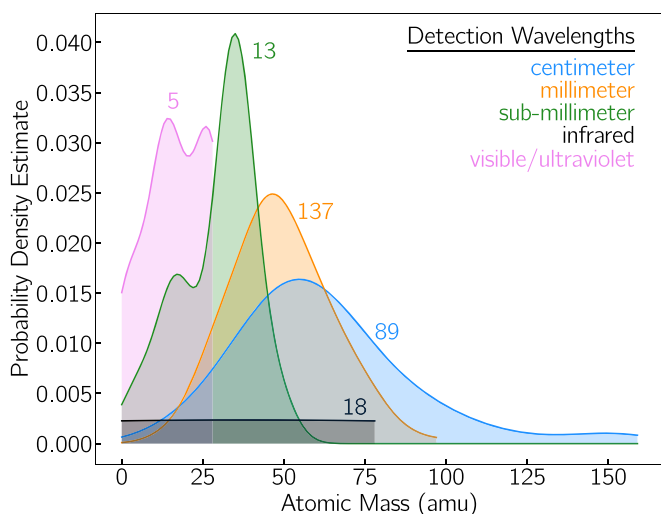


Figure 7. Kernel density estimate (KDE) analysis of molecules detected in each of the given wavelength ranges (excepting the fullerenes), generated with a bandwidth = 0.5. In some cases, the initial detection was reported in two or more wavelength ranges (see text), and credit was given to each for this analysis. The number of samples in each wavelength range is given next to the corresponding trace in the plot. The frequency ranges for centimeter, millimeter, and submillimeter used were 0–50, 50–300, and 300+ GHz, respectively.

more than 10 total detections. During its prime, the NRAO 36 ft telescope was producing an average of three new detections a year, a rate that has not been matched since, although the IRAM 30 m has shown a significant increase in its detection rate since 2006, more than tripling its yearly detections.

11.3. Molecular Composition

Carbon, hydrogen, nitrogen, and oxygen dominate the elemental composition of interstellar molecules, with sulfur and silicon in a distant second tier. Indeed, the entirety of the known molecular inventory is constructed out of a mere 19

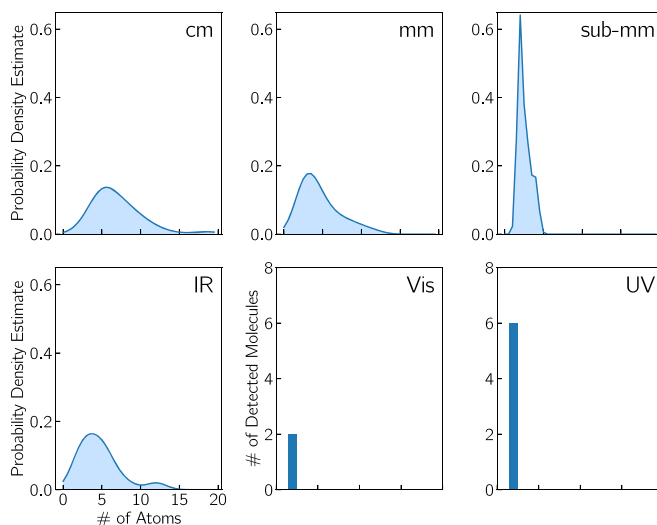


Figure 8. KDE analysis of the number of atoms in molecules detected in the centimeter, millimeter, submillimeter, and IR wavelength ranges, generated with a bandwidth = 0.5. For the visible and UV, only diatomic molecules have been detected. In some cases, the initial detection was reported in two or more wavelength ranges (see text), and credit was given to each for this analysis. The fullerene molecules are not included here.

elements. Figure 6 provides a visual representation of this composition.

Also of note is the relationship between the mass of the known molecules and the wavelength ranges that have contributed to their detection (Figure 7). As might be expected, there is little dependence on mass in the number of infrared detections, as the effects of increasing mass on vibrational frequencies are unlikely to shift these modes significantly enough to push them entirely out of the infrared region. Rotational transitions, however, are heavily dependent on mass. For a given rotational temperature, and to first order, the strongest rotational transitions of a molecule shift to lower frequencies with increasing mass (see Section 3.1 and Appendix A). This trend is reflected in the distribution of

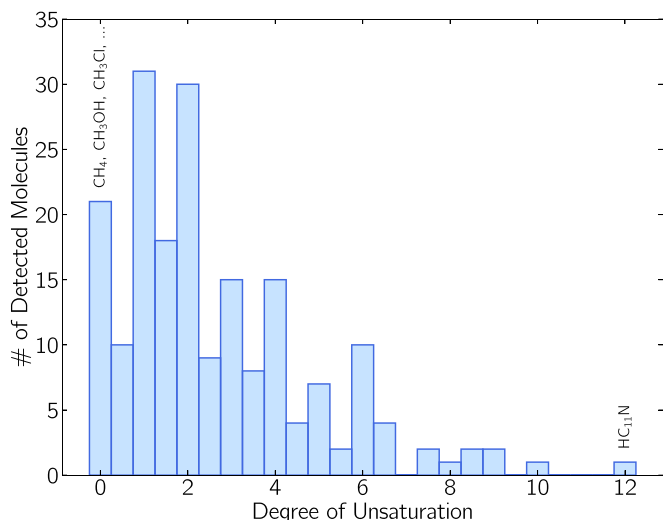


Figure 9. Histogram of the DU, or alternatively the number of rings and π bonds (see text), for hydrocarbon molecules containing only H, O, N, C, Cl, S, or F. Only 10 (7%) interstellar hydrocarbons are fully saturated with no rings or π bonds. Most molecules contain one or two rings or π bonds (a double bond is one π bond; a triple bond is two π bonds). The fullerene molecules are not shown.

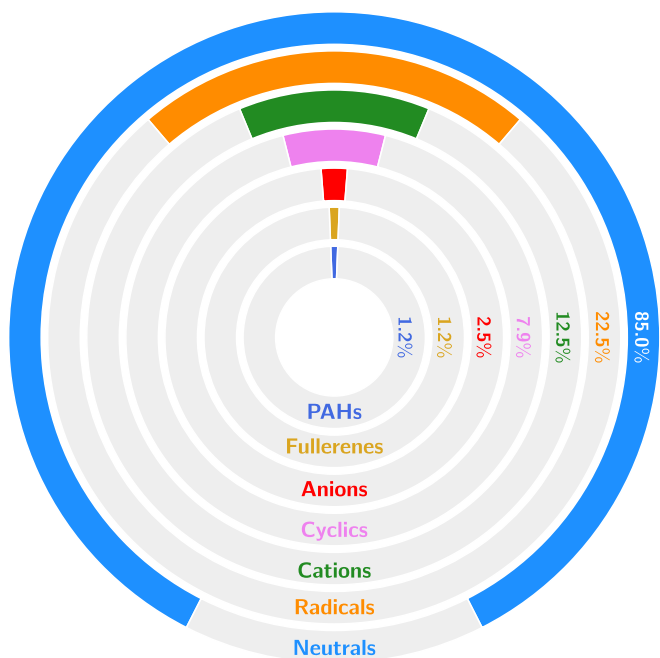


Figure 10. Percentage of known interstellar molecules that are neutral, cationic, anionic, radical species, or cyclic. Many molecules fall into more than one of these categories (e.g., most radical species have a net neutral charge).

atomic masses detected by centimeter, millimeter, and submillimeter instruments. There is a marked preference for low-mass species to be seen at high frequencies, and for high-mass species, especially those with mass >80 amu, to be detected at the lowest frequencies. For a more complete discussion of the effects of increased mass and complexity on the wavelength ranges where the strongest transitions occur, see Appendix A.

This trend is also borne out in the number of atoms in a molecule detected at each wavelength (Figure 8). The centimeter range has the peak of its distribution at five atoms but extends heavily to larger numbers. The millimeter range shows a lower

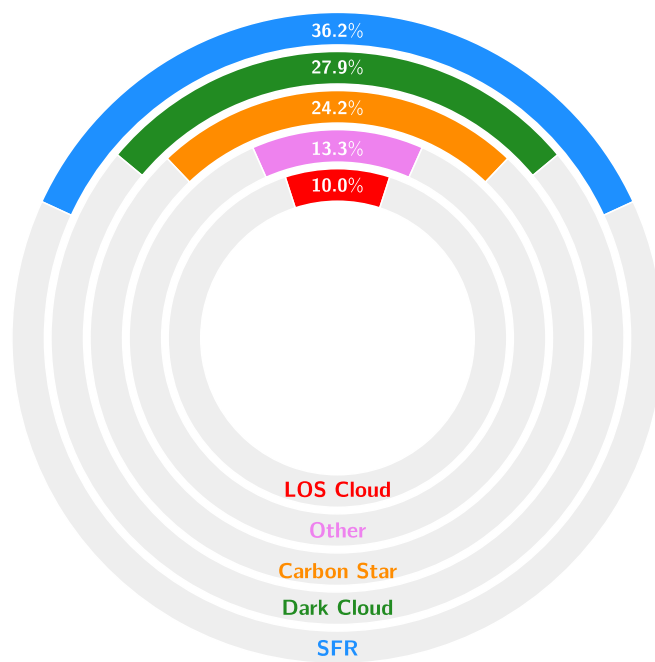


Figure 11. Percentage of known molecules that were detected for the first time in carbon stars, dark clouds, LOS clouds, and SFRs (see text). Some molecules were simultaneously detected in multiple source types (e.g., C_3H^- in TMC-1 and IRC+10216).

Table 10

Total Number of Detections That Each Source Contributed to for the Molecules Listed in Section 4

Source	#	Source	#
Sgr B2	69	L1527	2
TMC-1	57	L1544	2
IRC+10216	55	NGC 2024	2
LOS Cloud	42	NGC 7023	2
Orion	24	NGC 7027	2
L483	9	TC 1	2
W51	8	W49	2
VY Ca Maj	6	CRL 2688	1
B1-b	4	Crab Nebula	1
DR 21	4	DR 21(OH)	1
IRAS 16293	4	Galactic Center	1
NGC 6334	4	IC 443G	1
Sgr A	4	K3-50	1
CRL 618	3	L134	1
G+0.693-0.027	3	L183	1
NGC 2264	3	Lupus-1A	1
W3(OH)	3	M17SW	1
rho Oph A	3	NGC 7538	1
Horsehead PDR	2	Orion Bar	1

Note. Detections made in clouds along the LOS to a background source have been consolidated into LOS clouds, and detections in closely location regions have been grouped together as well (e.g., Sgr B2(OH), Sgr B2(N), Sgr B2(S), and Sgr B2(M) are all considered Sgr B2).

peak (three) atoms but also sees a distribution to larger numbers. As might be expected, the infrared shows a rather flat distribution, as the vibrational transitions of molecules probed here will all generally fall within the IR, regardless of mass or number of atoms. Interestingly, all molecules detected in the visible and UV are diatomics.

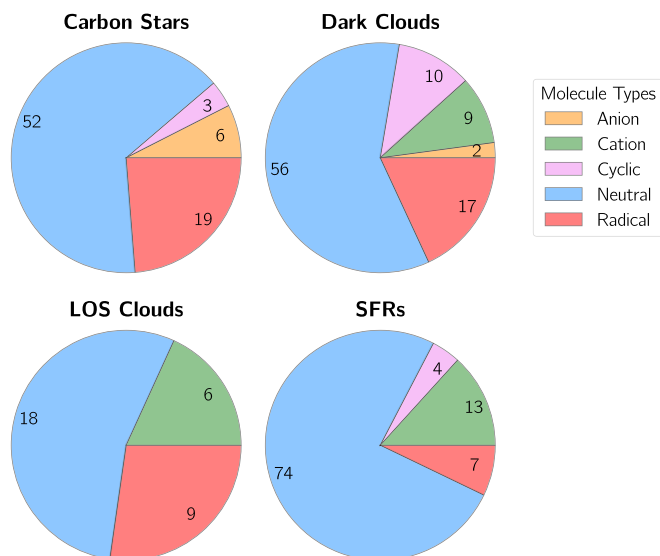


Figure 12. Number of known interstellar molecules that are neutral, cationic, anionic, radical species, or cyclic detected in four generalized source types. A small number of detections that did not fit easily into one of these categories are excluded. As with Figure 10, species falling into more than one molecule type are counted for each of that type.

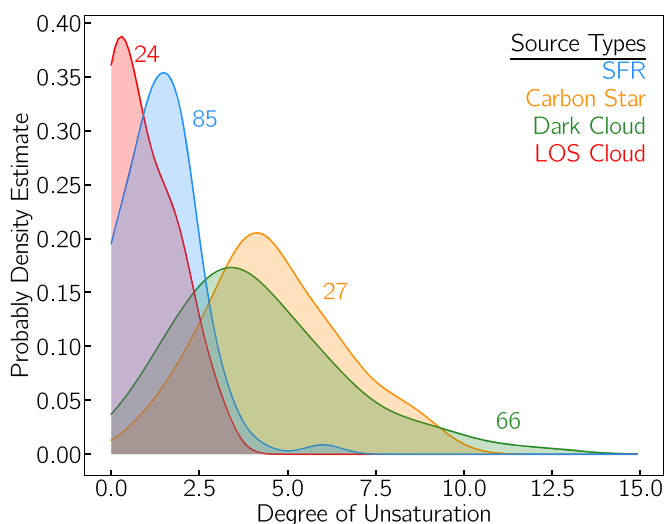


Figure 13. KDE analysis of the DU of detected nonfullerene molecules in each of the generalized source types, generated with a bandwidth = 0.5. The number of samples in each wavelength range is given next to the corresponding trace in the plot. Only molecules containing exclusively H, O, N, C, Cl, S, and/or F are considered.

Another interesting metric is the distribution of saturated and unsaturated hydrocarbon molecules detected. A fully saturated hydrocarbon is one where no π bonds (double or triple bonds) and no rings exist, with these electrons fully dedicated to bonding other elements (usually hydrogen). A simple formula for calculating the degree of unsaturation (DU) or equivalently the total number of rings and π bonds in a hydrocarbon molecule is given by Equation (4):

$$DU = 1 + n(C) + \frac{n(N)}{2} - \frac{n(H)}{2} - \frac{n(X)}{2}, \quad (4)$$

where n is the number of each element in the molecule and X is a halogen (F or Cl). Here, each atom contributes $x - 2$ to the

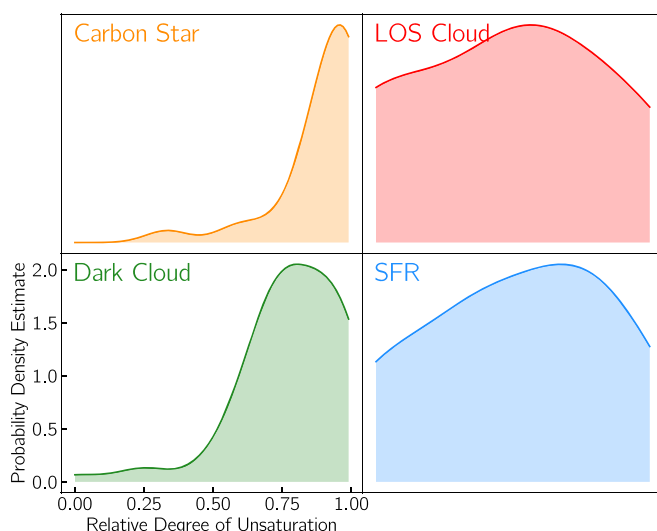


Figure 14. KDE analysis plots, generated with a bandwidth = 0.5, of the fraction of unsaturation of molecules across the generalized source types. A value of 0 is completely saturated, while a value of 1 is completely unsaturated.

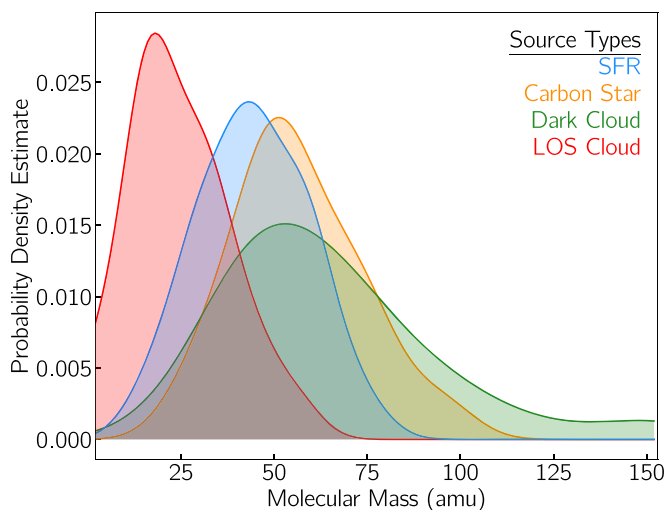


Figure 15. KDE analysis plot, generated with a bandwidth = 0.5, of the mass of nonfullerene molecules across the generalized source types. The KDE traces are truncated to run only between the limits of the masses detected.

DU, where x is its valence; thus, the divalent elements O and S do not contribute. A visual representation of this distribution for interstellar hydrocarbons is shown as a histogram in Figure 9. With the exception of the fullerenes (not shown), HC_9N is the most unsaturated interstellar molecule, while only 10 species are fully saturated: CH_4 , CH_3Cl , CH_3OH , CH_3SH , CH_3NH_2 , CH_3OCH_3 , $\text{CH}_3\text{CH}_2\text{OH}$, $\text{CH}_3\text{CH}_2\text{SH}$, $\text{HOCH}_2\text{CH}_2\text{OH}$, and $\text{CH}_3\text{CH}_2\text{OH}$. The most common DUs are 1.0 and 2.0, representing one or two rings and/or π bonds. In total, 93% of all interstellar hydrocarbons are unsaturated to some degree.

Figure 10 provides a visual breakdown of the number of known interstellar molecules that are neutral, cationic, anionic, radical species, or cyclic. Many molecules fall into more than one of these categories. An analysis of the rates of detection of these various types of molecules in differing types of interstellar sources is provided in Section 11.4.

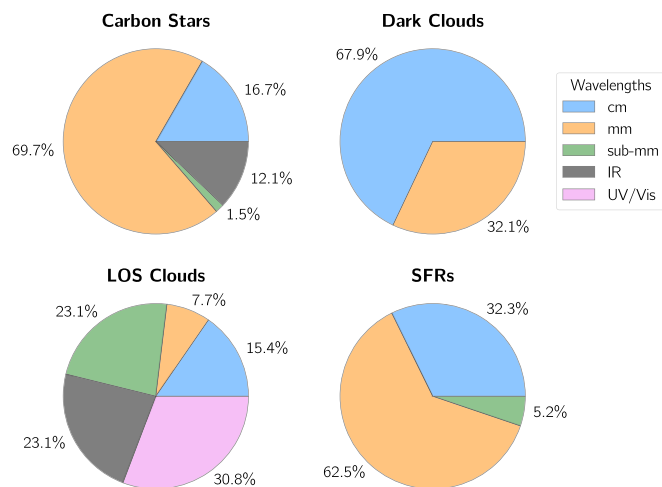


Figure 16. Percentage of first detections in each generalized source type that were made at centimeter, millimeter, submillimeter, infrared, visible, and UV wavelengths. Molecules detected at multiple wavelengths have been credited to all applicable wavelengths.

11.4. Detection Sources, Source Types, and Trends

More than 90% of the detections can be readily classified as being made in a source that falls into the generalized type of either a carbon star (e.g., IRC+10216), dark cloud (e.g., TMC-1), a diffuse/translucent/dense cloud along the LOS to a background source (hereafter “LOS cloud”), or a star-forming region (SFR; e.g., Sgr B2). Figure 11 displays the percentage of interstellar molecules that were detected in each source type. Note that because some molecules were simultaneously detected in more than one source type, these percentages add to >100%. The number of detections in each individual source is listed in Table 10.

The distribution of molecules, as categorized by their attributes in Figure 10, across the generalized source types is shown in Figure 12. Immediately obvious from this is that no molecular anions were first detected outside of carbon stars and dark clouds, a fact that remains the case even outside of first detections.

This may not be surprising when also considering the average DU across these generalized source types (Figure 13). The maximum DU of molecules is molecule dependent, meaning that the distribution of DU by source type is biased by the length/size of molecules seen there. This can be mitigated by examining the relative DU—meaning, how close to fully unsaturated the molecules in a source type are. This is shown in Figure 14, where the relative DU is the molecule’s DU divided by the DU for a fully unsaturated version of that species.

In both cases, and with very few exceptions, molecules detected in carbon stars and dark clouds are on average highly unsaturated compared with other sources, and the six known molecular anions, CN^- , C_3N^- , C_4H^- , C_5N^- , C_6H^- , and C_8H^- are no exception. As shown in Figure 15, the molecules detected in these sources also tend to be the most massive.

A possible explanation for this trend is the influence of grain-surface/ice-mantle chemistry in SFRs. One of the most efficient pathways for increasing the saturation of species in the ISM is through direct hydrogenation on grain surfaces. A substantial amount of laboratory (e.g., Linnartz et al. 2015 and Fedoseev et al. 2015), quantum chemical (e.g., Woon 2002), and chemical modeling (e.g., Garrod et al. 2008) work suggests

that these hydrogenation processes are efficient in the ISM, often even at low temperatures. In carbon stars, the bulk of the ice is thought to have been long since evaporated, with any hydrogenation occurring via catalysis on the (mostly) bare grain surfaces (Willacy 2003). In dark clouds, the temperatures are so low that although chemistry is likely occurring in ice mantles, there is no readily apparent mechanism for liberating these molecules into the gas phase for detection. Some recent work in this area has suggested that cosmic-ray impacts could nonthermally eject this material in these sources (Ribeiro et al. 2015), but this is certainly not as efficient a process as shock-induced (Requena-Torres et al. 2006) or thermal desorption, which play significant roles in SFRs.

Looking back at Figure 12, a few other trends are apparent. First, the fraction of species detected in SFRs that are radicals is substantially lower (8%) than seen in the other environments (25% in dark clouds). Radicals tend to be highly chemically reactive species and perhaps are being depleted as more reaction partners are being liberated from the surface of ice mantles in these regions. Second, it bears noting that the only source type in which all five types of species discussed here were first detected are dark clouds, perhaps suggesting that these regions are more chemically complex than they may appear at first glance, especially given the prominence of SFRs like Sgr B2 and Orion in the detection of new molecules.

It is also worth examining the wavelength ranges that contributed to first detections in each of these generalized source types (Figure 16). As discussed in Section 3.2 and Section 3.3, detections in the IR, visible, and UV portions of the spectrum are nearly always performed in absorption, necessitating both a background source and an optically thin absorbing medium. LOS clouds satisfy both of these requirements, and thus these regions show the greatest diversity in wavelengths used for detection, whereas SFR and dark clouds, which are often optically thick, have not yet seen a first detection at wavelengths shorter than the far-infrared.

12. Conclusions

In summary, 241 individual molecular species have been detected in the ISM. A further 11 molecules are considered to be tentatively detected, while two species have had their detections disputed. These detections have been dominated by radio astronomical observations, with the IRAM 30 m, GBT 100 m, Nobeyama 45 m, Yebes 40 m, and NRAO/ARO 12 m telescopes the most prolific extant facilities. Beginning in 1968, the rate of new detections per year can be well fit to a linear trend of 3.9 new molecules per year, although there is evidence for an increase in this rate in the last decade, due to the onset of GBT detections, a tripling of the rate of IRAM detections, and the advent of the Yebes 40 m. A substantial fraction (~30%) of known molecules has now been seen in external galaxies, while the numbers of molecules known in protoplanetary disks (25), interstellar ices (9), and exoplanet atmospheres (9) are much smaller due to observational challenges.

B.A.M. sincerely thanks the five anonymous referees (2018) and two anonymous referees (2021) for their careful reading and suggestions, which have substantially improved the quality of this census over the years. B.A.M. also thanks K. Kellerman, R. Wilson, and J. Mangum for discussions of the history of radio astronomical facilities, L. I. Cleeves for discussions of molecules in protoplanetary disks, A. Burkhardt and S. Ransom

for critical readings of the appendix, and K. L. K. Lee for helpful discussions regarding Python packages. The National Radio Astronomy Observatory is a facility of the National Science Foundation operated under cooperative agreement by Associated Universities, Inc. Support for B.A.M. during the initial portions of this work was provided by NASA through Hubble Fellowship grant #HST-HF2-51396 awarded by the Space Telescope Science Institute, which is operated by the Association of Universities for Research in Astronomy, Inc., for NASA, under contract NAS5-26555.

Appendix A Sources of Molecular Complexity and Their Impact on Detectability

The purpose of this appendix is to examine a number of the factors that affect the detectability of molecules in the ISM. When considering a molecule that has not yet been detected in the ISM (or in protoplanetary disks, etc.), examining each of the factors presented here should provide an informed first look at the reasons why detection may be challenging, beyond merely a potential low abundance. The list of factors outlined here is not exhaustive but instead focuses on those that commonly affect molecules observed in interstellar sources. Further, while some quantitative measures and analytical formulas will be presented, this discussion is intended to be primarily qualitative in nature. Some concepts will be presented as zeroth- or first-order approximations. The terminology may not always be quantum mechanically rigorous.

In the last decade, the common astrochemical parlance defining a complex organic molecule (COM) has been any molecule with six or more atoms, with methanol (CH_3OH) the prototypical simplest COM (Herbst & van Dishoeck 2009). This definition, while arbitrary, has proven a useful aid in the discussion of structural complexity. The detectability of molecules, however, is affected by much more than the number of atoms. Indeed, as will be shown later, a low-abundance linear molecule may be far easier to observe than a higher-abundance, asymmetric top containing far fewer atoms. Similarly, a low-abundance, structurally complex molecule may be more readily detected than a highly abundant, structurally simple molecule with very weak transitions.

As discussed in the main text, the bulk of new detections are made via observation of rotational transitions in the radio, and so that will be the focus of this discussion. Emission or absorption signals from molecules in the centimeter, millimeter, and submillimeter regimes almost always arise from rotational transitions as a molecule moves between two rotational energy levels. The intensity of any given signal is dependent on numerous factors, many of which will be discussed here, but these can largely be broken down into three primary components:

1. intrinsic, quantum-mechanical properties of the molecule
2. telescope and radioastronomical source properties
3. the absolute number of molecules undergoing that transition

The molecular, instrumental, and source properties (1 and 2) will vary from line to line, molecule to molecule, and source to source, but the effects of abundance (3), excluding a number of edge cases, are universal. There are only so many molecules available to undergo a transition, and produce an observable signal, in a source.

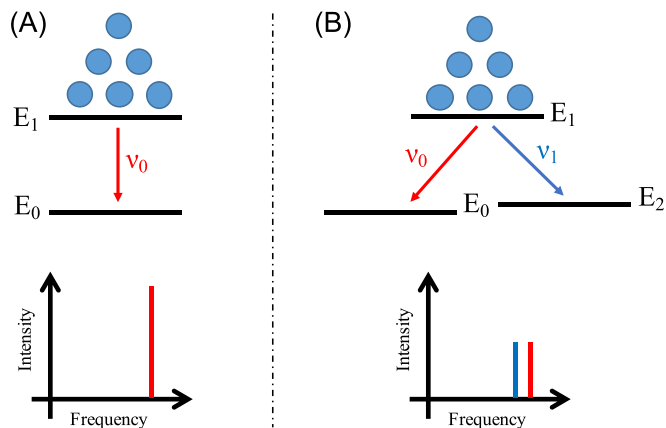


Figure A1. Idealized examples of the effects of having additional energy levels to undergo transitions. In case A, all six molecules can undergo transition ν_0 . In case B, about half the molecules will undergo transition ν_0 , but the other half will undergo transition ν_1 . In case B, the intensity of transition ν_0 is therefore half of what it is in case A.

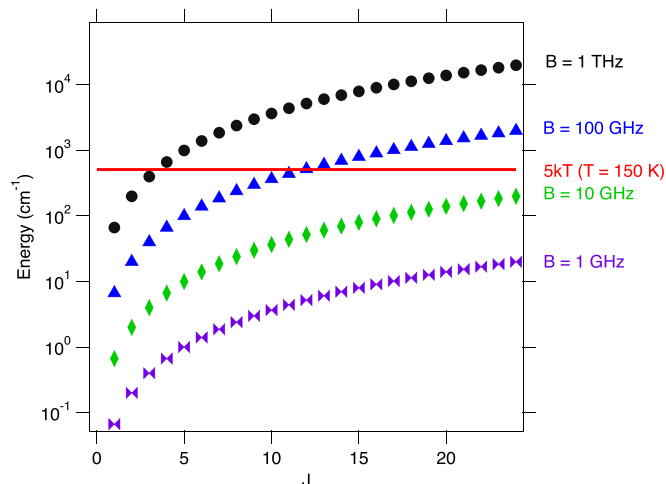


Figure A2. Rotational energy levels for molecules with rotational constants $B = 1000, 100, 10,$ and 1 GHz. The red line is drawn at 521 cm^{-1} , the value of $5kT$ at $T = 150 \text{ K}$; energy levels below this value are nontrivially populated.

Table A1

Rotational Constants and Number of Energy Levels below kT at 150 K for All HC_xN Species Detected in the ISM

Molecule	B (MHz)	# Levels ^a < kT @ 150 K	Lab Ref.
HCN	44316	18	1
HC ₂ N	10986	36	2
HC ₃ N	4549	58	3
HC ₄ N	2302	80	4
HC ₅ N	1331	107	5
HC ₇ N	564	166	6
HC ₉ N	290	231	7

References. (1) Ahrens et al. 2002; (2) Saito et al. 1984; (3) de Zafra 1971; (4) Tang et al. 1999; (5) Alexander et al. 1976; (6) Kirby et al. 1980; (7) McCarthy et al. 2000.

^a Hyperfine splitting not considered, for simplicity.

While this may seem a trivality, the effects are far-reaching. Figure A1 describes two cases for a molecule undergoing a transition and emitting light to be detected by a telescope

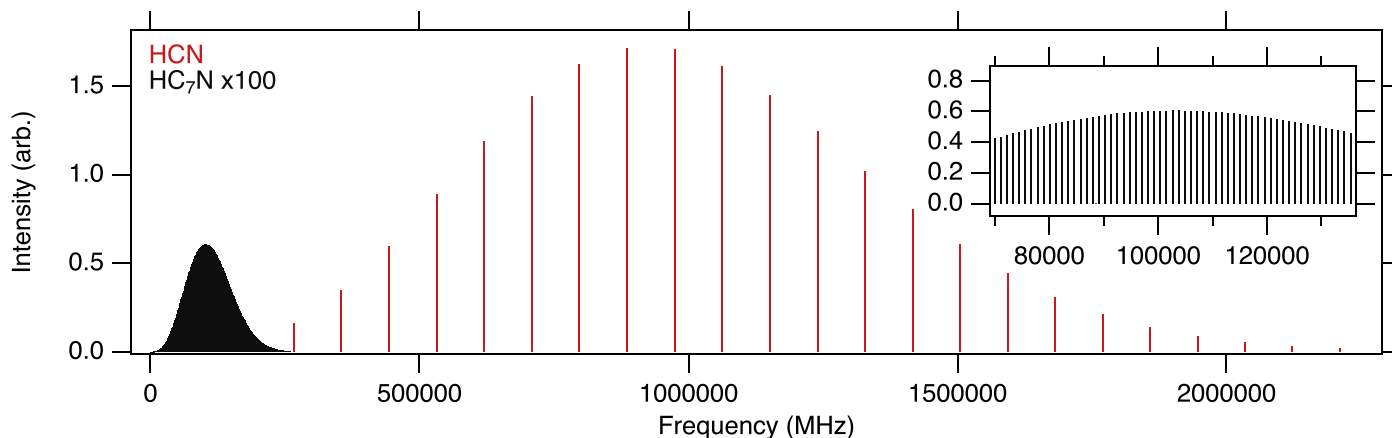


Figure A3. Rotational spectra of HCN (red) and HC₇N (black) at $T = 150$ K for the same number of molecules of each. Hyperfine has not been considered. The inset shows a magnified portion of the HC₇N to show detail as to the density of lines. In both the main plot and the inset, the intensities of the HC₇N lines are multiplied by a factor of 100.

looking for frequency ν_0 . In the first case, where all the population undergoes the transition, the light observed at frequency ν_0 is twice as great as that of the second case, where the molecule can now undergo a similar transition at a different frequency because of the presence of an additional energy level. As will become clear in the following sections, the true complexity of a species is largely measured in the number of rotational energy levels the population is distributed over and undergoing transitions between. The more levels, the fewer photons that are produced at any given transition frequency, and the more complex the spectrum becomes as additional transition frequencies appear. While a simple linear molecule like CO may have a few dozen energy levels populated at 300 K, a truly complex molecule may have hundreds of thousands.

Thus, a reasonable measure of the level of complexity is the number of rotational energy levels that can be expected to have a nontrivial fraction of the total number of that molecule in a source. Because these levels vary in energy, the fraction of the molecules in each state is dependent on the average energy of the population of molecules, which is described by an excitation temperature. In many cases, this distribution is governed by a Boltzmann distribution, where the fraction (F_n) of molecules in any given energy (E_n) state n is governed by Equation (A1) and the ratio of population between any two states (E_n, E_m) is governed by Equation (A2), at an excitation temperature T_{ex} :

$$F_n \propto e^{-\frac{E_n}{kT_{\text{ex}}}}, \quad (\text{A1})$$

$$\frac{F_n}{F_m} = e^{-\frac{E_m - E_n}{kT_{\text{ex}}}}. \quad (\text{A2})$$

The rigorous accounting of states with a significant F_n at a given temperature is expressed through the temperature-dependent partition function, which is discussed explicitly in Section A.6.6. While the partition function is often used as a practical proxy for the number of nontrivially populated energy levels, for the purposes of this initial discussion, a simpler approximation can be adopted. Drawing on Equations (A1) and (A2), the n th energy level of a molecule having energy $E_n = 5kT$ will have $F_n = e^{-5}$, or $\sim 1\%$ relative to the ground state ($E_0 = 0kT$) population. Thus, the number of states with energies $< 5kT$ is an excellent approximation for the number of

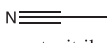
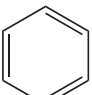
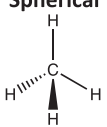
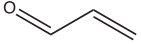
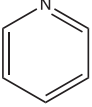
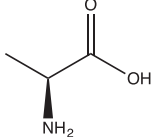
Prolate	Oblate	Spherical
		
acetonitrile	benzene	methane
A = 158099 MHz B = 9199 MHz C = 9199 MHz	A = 5687 MHz B = 5687 MHz C = 2843 MHz	A = 157122 MHz B = 157122 MHz C = 157122 MHz
$\kappa = -1$	$\kappa = 1$	$\kappa = N/A$
Near Prolate	Near Oblate	Asymmetric
		
propenal	pyridine	alanine
A = 47354 MHz B = 4660 MHz C = 4243 MHz	A = 6039 MHz B = 5805 MHz C = 2959 MHz	A = 5066 MHz B = 3100 MHz C = 2264 MHz
$\kappa = -0.98$	$\kappa = 0.85$	$\kappa = -0.40$

Figure A4. Examples of different molecular symmetries demonstrate equivalencies in rotational constants and the corresponding Ray's asymmetry parameters.

states that will have a nontrivial population at any given temperature.

As discussed above, the number of possible transitions increases with the number of states that have a nontrivial population: more states, more transitions, lower intensity for any given one. Thus, when examining the individual factors that affect the detectability of a molecule (i.e., the overall intensity of transitions and the number of those transitions), the number of states below $5kT$ can provide a gross approximation of the magnitude of an effect on detectability.

A.1. Number of Atoms

The number of atoms in a given molecule is a good first approximation of spectral complexity. The energy levels of a molecule are determined by the molecular structure and reflected in the moments of inertia. Consider a simple linear

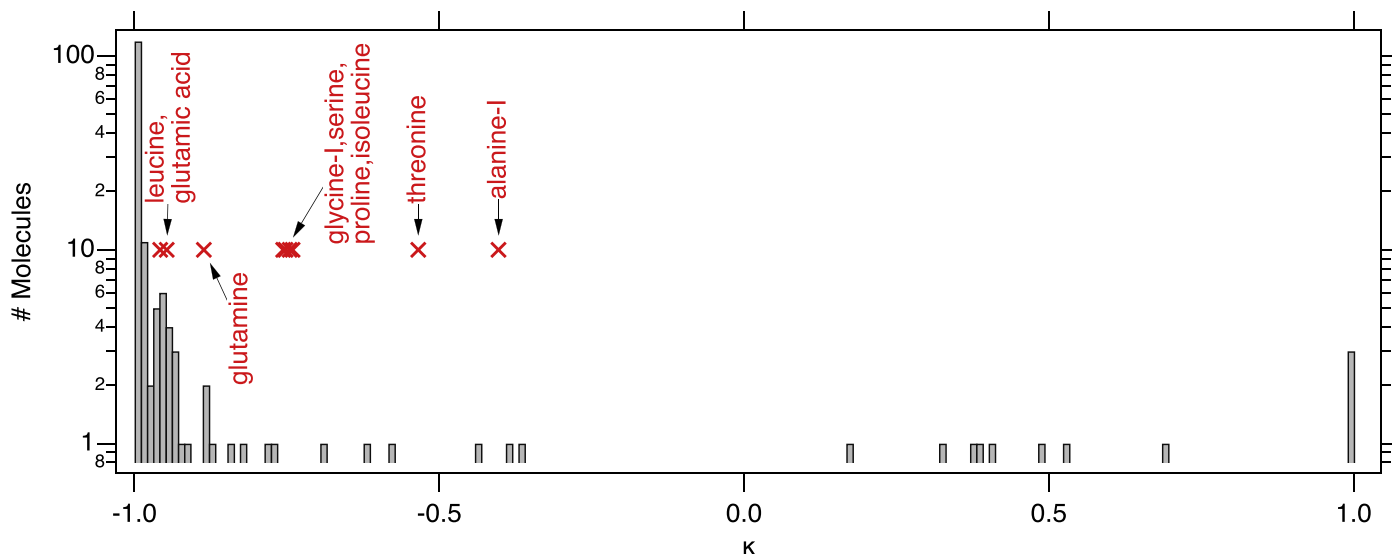


Figure A5. Histogram of all detected interstellar molecules by their Ray's asymmetry parameter, κ . Prolate rotors have $\kappa = -1$, while oblate rotors have $\kappa = 1$. A selection of amino acids is overlaid in red.

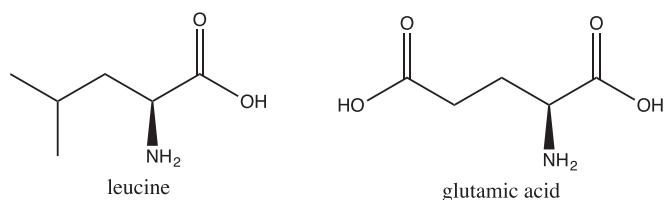


Figure A6. Structures of the amino acids leucine and glutamic acid.

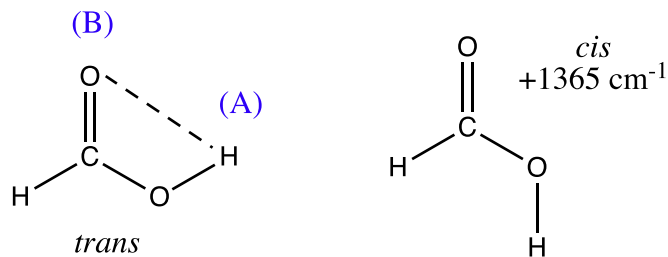


Figure A7. The *cis* and *trans* conformers of formic acid. The hydrogen-bonding interaction of the hydroxyl hydrogen (A) with the carbonyl oxygen (B) in the *trans* form substantially stabilizes (by 1365 cm^{-1} ; Hocking 1976) the conformer relative to the *cis* form.

molecule, whose energy levels are given, to zeroth order, by Equation (A3), where B is the rotational constant (often expressed in units of MHz or cm^{-1}) and J is a quantum number representing the total rotational angular momentum (Bernath 2005):

$$E_J = BJ(J + 1). \quad (\text{A3})$$

The rotational constant B is then related to the moment of inertia, I , along the molecular axis by Equation (A4) (Bernath 2005):

$$B = \frac{h^2}{8\pi^2 I}. \quad (\text{A4})$$

The moment of inertia is proportional to the amount of torque needed to rotate a molecule and is determined by the spatial distribution of mass from the axis of rotation, going as

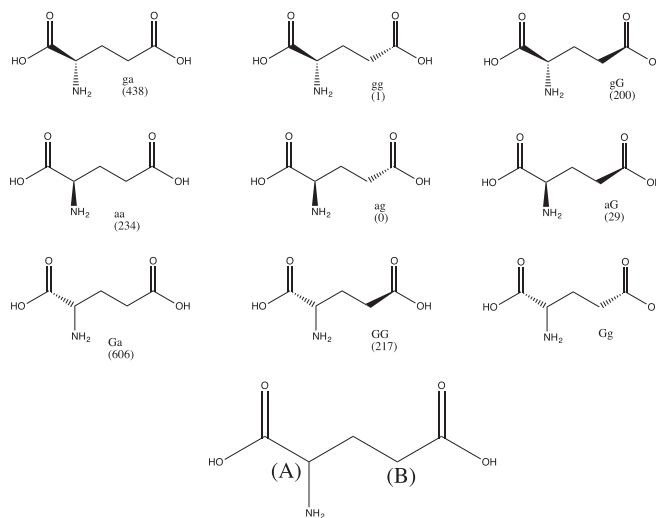


Figure A8. Nine lowest-energy conformers of glutamic acid. Bold angled lines indicate a bond that projects out of the plane of the page, while a dashed line indicates a bond into the plane. The conformers differ in the relative spatial location of the C(O)OH and NH_2 groups around the carbon atoms indicated by the (A) and (B) in the bottom (2D) structure. Where available, the zero-point corrected energies (in cm^{-1}) of the conformers are given, relative to the lowest energy (ag). Adapted from Figure 1 and Table S1 of Peña et al. (2012).

the square of the distance. A longer molecule will therefore, in general, have a larger I (and a correspondingly small B) than a shorter molecule with similar constituent atoms. This means for a given value of J , the energy of that level will be lower. In turn, there are more energy levels accessible $< 5kT$, and the total population will be spread more thinly among them. Figure A2 shows the number of levels that fall beneath $5kT$ for four hypothetical molecules with rotational constants spanning four orders of magnitude.

A more specific example is the HC_xN family of linear molecules, with astronomically observed constituents as large as HC_9N (Broten et al. 1978; Loomis et al. 2016). Table A1 gives the rotational constants and number of energy levels below kT for these molecules. It is clear that the number of populated energy levels increases with decreasing B , increasing

the spectral complexity by a density of lines argument alone. Additionally, however, consider that for an equivalent population of HCN and HC₇N, the HC₇N molecules are distributed over almost an order of magnitude more energy levels. As a result, the number of molecules undergoing a single rotational transition (and thus producing detectable signal) is overall lower for HC₇N, resulting in weaker signals.

This can be seen most easily by examining the rotational spectra of these molecules at $T = 150$ K. Figure A3 shows a comparison of the spectra of HCN and HC₇N at $T = 150$ K, assuming the same number of molecules for each. Not only is the HC₇N spectrum far more spectrally dense, but the intensities are so low that they must be scaled by a factor of 100 to be readily visible on the graph. The strongest transition of HCN at this temperature is the $J = 10 - 9$, while the strongest transition of HC₇N is the $J = 91 - 90$. The strongest HCN transition is nearly 300 times stronger than that of HC₇N. A further consequence is that the frequency of a given transition shifts to lower and lower frequency as the number of atoms increases, increasing the moment of inertia and decreasing the rotational constant. This is clearly seen in Figure A3, where the strongest HCN transitions are arising in the ~ 900 GHz region, while for HC₇N, these are at ~ 100 GHz.

In general, for families of molecules with similar elemental compositions, adding additional atoms will increase the spectral complexity (line density), decrease the overall intensity of these lines, and shift the lines to lower frequency.

A.2. Geometry and Symmetry

The previous discussion focused exclusively on linear molecules as the prime example, but few molecules commonly considered complex by interstellar standards are linear (although certainly this is a debatable position). When additional atoms are added off of the primary axis, additional complexity can be introduced, dependent on whether additional components to the dipole moment are manifest. One of the underlying causes of the relative simplicity of linear molecular rotational spectra is the inherent symmetry of a linear molecule. An allowed rotational transition can only occur when a permanent electric dipole moment is present. Due to symmetry, linear molecules can only ever possess at most a single component of the electric dipole moment, oriented along the linear axis. The addition of off-axis atoms introduces, in most cases, a degree of asymmetry.

A convenient measure for assessing the degree of asymmetry introduced is κ , the Ray's asymmetry parameter (Ray 1932), given in Equation (A5), where A , B , and C are the rotational constants of the molecule:

$$\kappa = \frac{2B - A - C}{A - C}. \quad (\text{A5})$$

A number of example molecules displaying symmetry, or near symmetry, are shown in Figure A4. A completely spherically symmetric molecule, such as methane (CH₄), will have $A = B = C$, and thus κ is undefined.

Among the known interstellar molecules, the most commonly occurring symmetric top species are prolate (commonly thought of as cigar shaped) with $\kappa = -1$ and $I_a < I_b = I_c$. Linear molecules are the most common prolate symmetric tops; however, any near-linear molecule in which the off-axis mass is symmetrically distributed such as methyl cyanide (acetonitrile, CH₃CN), resulting in $I_b = I_c$, is also prolate. As a consequence

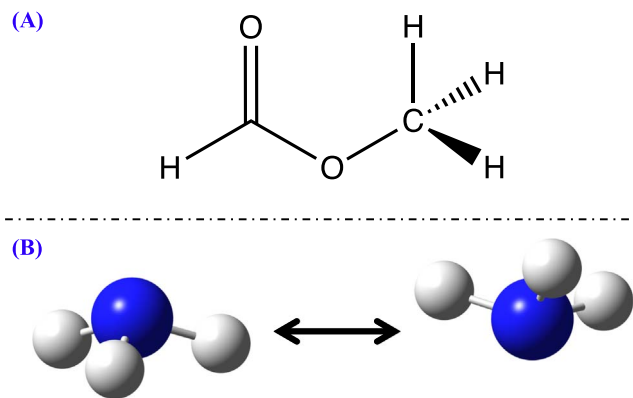


Figure A9. Examples of internal motions. (A) Structure of *cis*-methyl formate. As the methyl (-CH₃) group rotates about the C-O bond, the interaction potential between the hydrogen atoms and the oxygen atoms changes, affecting the coupling of the internal rotational angular momentum to that of the overall angular momentum of the system, perturbing energy levels, and increasing spectral complexity. (B) Representation of the umbrella-like inversion motion undergone by the NH₃ molecule, which perturbs the standard rotational energy levels and adds complexity to the rotational spectra.

of this symmetry, no additional permanent dipole components are introduced, and prolate symmetric tops behave largely like linear molecules as complexity increases.

Figure A5 displays the distribution of known interstellar molecules by their κ values. It is clear that the vast majority ($\sim 90\%$) of detected interstellar molecules are prolate or near prolate. Only 24 molecules have $\kappa > -0.9$. To first order, therefore, it is reasonable to claim that the more prolate a potential interstellar molecule is, the more likely it is to be detectable. For the sake of comparison, also plotted on Figure A5 are a number of amino acids, molecules not detected in space but highly sought and widely considered truly complex. In the case of glycine and alanine, the simplest amino acids by number of atoms, both are quite asymmetric ($\kappa_{\text{gly}} = -0.74$, $\kappa_{\text{ala}} = -0.4$), while the most nearly prolate amino acids, leucine and glutamic acid, contain many more atoms (Figure A6). Thus there is an offsetting balance to be considered in their detectability: the benefits of being (near) prolate versus the drawbacks of increasing number of atoms and structural size.

A.3. Structural Conformers

Without altering the overall bonding patterns (and thus changing the molecular makeup), there are often several ways for the atoms within a molecule to be arranged spatially. A single population of molecules can often be composed of one or more different arrangements, or *conformers*, of the species. Because these conformers have distinct moments of inertia, they therefore have distinct rotational spectra. As a result, the more conformers that a population of molecules can exist in at a given temperature, the fewer molecules are available to undergo any given rotational transition.

The simplest case of conformers is perhaps that between *cis* and *trans* arrangements for a small molecule. Often one conformer is substantially more stable with respect to the other, and there is little impact on the overall detectability of the species. A salient example is that of formic acid (HCOOH; Figure A7). Here, the *trans* conformer is greatly stabilized by a hydrogen-bonding interaction. As a result, while the lower-energy *trans* conformer was first detected in 1971 (Zuckerman

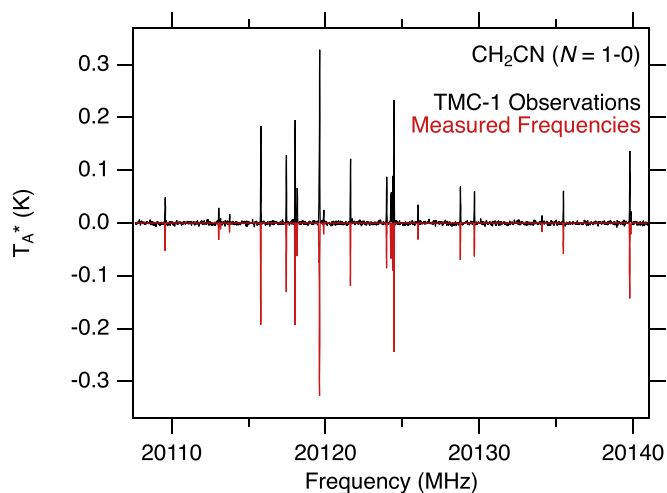


Figure A10. Observations of a single rotational transition ($N = 1-0$) of CH_2CN in TMC-1 from the Kaifu et al. (2004) survey in black, with the measured laboratory transitions overlaid in red. The split lines are the result of the coupling of both ^1H and ^{14}N hyperfine splitting of the transition.

et al. 1971), and is indeed quite common in regions with any degree of chemical complexity (Requena-Torres et al. 2006), the higher-energy *cis* conformer was only recently discovered and is only seen because of exceptional chemical and physical circumstances (Cuadrado et al. 2016).

For more complex molecules, such as amino acids, the number of conformers with similar energies is often greatly enhanced. The nine lowest-energy conformers of glutamic acid, for example, are shown in Figure A8 along with their relative energies; all are below 900 cm^{-1} . In this case, it is the spatial arrangement of the $\text{C}(\text{O})\text{OH}$ and NH_2 groups that differ between conformers. Indeed, dozens of additional higher-energy conformers, in which the relative arrangement changes around other central points, including the hydroxyl-carbonyl hydrogen bonds, also exist.

From a practical standpoint, the additional conformer of formic acid has no impact on the detectability of the lower-energy *trans* species. There simply is not enough *cis* to reduce the overall levels of *trans* in a population in a significant way. On the other hand, an attempt to detect glutamic acid would be severely hindered by the existence of a number of low-energy conformers. Of these conformers, the *ag*, *gg*, and *aG* are the lowest in energy. When Peña et al. (2012) measured the microwave spectrum of a sample of glutamic acid in the gas phase, they observed all three conformers simultaneously. Instead of (practically) the entire population existing as the lowest-energy conformer, as in the case of formic acid, here the overall intensity of any one conformer's spectral signature was diminished, making it harder to detect than if only a single conformer were energetically favored.

A.4. Internal Motion

Considering a single conformer of a molecule, the complexity of the rotational spectrum can be further increased due to the internal structure of that molecule. In the case of formic acid, the molecule can interconvert between the two conformers by rotation about the $\text{C}-\text{OH}$ bond. The barrier to this process is large (4827 cm^{-1} ; Hocking 1976), meaning that it is rare for a full rotation about this bond to occur, and this motion is unlikely to have a significant impact on the spectrum. For

Table A2

Definition of Parameters in the Single-excitation Model Calculation of Column Density

Parameter	Definition	Units
N_T	Column density	cm^{-2}
T_{ex}	Excitation temperature	K
T_{bg}	Background temperature	K
k	Boltzmann's constant	J K^{-1}
h	Planck's constant	J s
Q	Partition Function at T_{ex}	
E_u	Upper state energy of the transition	K
ΔT_A	Peak observed intensity of the transition	K
ΔV	FWHM of the transition	cm s^{-1}
B	Beam filling factor	
S	Line strength	
μ^2	Square of transition dipole moment	J cm^3
η_B	Beam efficiency	

functional groups that can undergo internal motion and have only a modest barrier to overcome, however, additional degrees of complexity arise.

A.4.1. Rotation

Perhaps the most common form of internal motion that increases spectral complexity is that of internal rotation, specifically that of methyl ($-\text{CH}_3$) functional groups. A detailed review of the effects of internal rotation on spectra is given by Lin & Swalen (1959). In short, the rotational angular momentum of the rotating (or pseudovibrating; i.e., torsion) subgroup within the molecule couples with the rotational angular momentum of the molecule as a whole, perturbing the energy levels and resulting in new possible transitions.

As a brief example, the lower-energy *cis* conformer of methyl formate (CH_3CHO) is shown in Figure A9(a). The methyl group is not locked into one orientation and instead rotates around the $\text{C}-\text{O}$ bond. As the hydrogen atoms move, their interaction with the carbonyl ($\text{C}=\text{O}$) and ester ($\text{C}-\text{O}-\text{C}$) oxygen atoms changes, hindering the rotation. As a result, every rotational energy level is split into three states: a pair of degenerate levels (denoted E) and a single nondegenerate state (denoted A).⁸ As a result, the spectrum becomes far more complex, and, because there are now many more states accessible at the same temperature, the overall intensity of any given transition is substantially decreased. To make matters worse (or better), the degree of this splitting changes with frequency/energy. Some transitions will suffer from this decrease in intensity, but for others, the splitting will be far less than the line width and will be unobservable.

A.4.2. Inversion

A second common type of motion is inversion. The underlying principle is the same as for internal rotation: the angular momentum of internal functional groups moving within the system couples to the overall angular momentum of the system and perturbs the energy levels. The most common example is seen in ammonia (NH_3), shown Figure A9(b). In the case of NH_3 , the entire molecule inverts in an umbrella motion. As with the internal rotation, this motion perturbs the standard

⁸ The energy ordering and degree of splitting changes as a function of energy, barrier heights, and other factors beyond the scope of this discussion. See Lin & Swalen (1959) for a detailed review.

rigid-rotor energy levels, increasing the number of states accessible, generating more transitions, and reducing individual spectral intensity. Townes (1946) and Townes & Schawlow (1975) provide excellent summaries of the laboratory and theoretical efforts to characterize this type of internal motion.

A.5. Nuclear Hyperfine

A final common type of perturbation is the coupling of nuclear angular momentum (from atoms with nonzero nuclear angular momentum) to the overall energy. This perturbation is often quite small; for example, the splitting from ^1H is rarely resolvable with even high-resolution instruments in the laboratory, much less in interstellar observations. ^{14}N hyperfine splitting, on the other hand, is routinely observed in the laboratory and is often seen in interstellar observations in sources with sufficiently narrow line widths. Figure A10 shows an example of resolved hyperfine transitions from a single rotational transition CH_2CN in TMC-1 observations showing both ^1H and ^{14}N splitting. The single rotational transition ($N = 1-0$) has been split into more than a dozen resolvable lines. The relative intensities of hyperfine-split transitions are well-known (Townes & Schawlow 1975) and, combined with the structure, can provide unique fingerprints for identification and as probes of temperature and optical depth.

A.6. Column Densities and Spectral Intensities

Given these sources of complexity in the spectrum, it is then useful to consider how the intensity of a spectral line actually changes as a result in a more quantitative way as well as the influence of some telescope-specific parameters on the line. Given a detection of a molecular line from observations, a column density can be determined, or, alternatively, given an expected column density, a predicted observational intensity can be derived. A detailed examination of the radiative transfer processes behind these calculations is beyond the scope of this work; the interested reader is referred to the recent work of Condon & Ransom (2016) and Mangum & Shirley (2015). Here, only the widely used single-excitation model is described in detail. A discussion of the effects on detectability when this model breaks down follows.

A.6.1. The Single-excitation Model

The most common approach used to analyze observational data is described in detail in Goldsmith & Langer (1999) and is often referred to as the “rotation diagram” method or an “LTE” analysis. Both terms omit the key assumption made in the analysis, which is that the number of molecules in each molecular energy level is assumed to be described exactly by a Boltzmann distribution at a single, uniform excitation temperature, T_{ex} .

Hollis et al. (2004a) formalized the calculations used to determine column densities and excitation temperatures, and that formalism is adopted here for the purposes of this discussion. Equation (A6) describes a calculation for molecules in emission or absorption, and the parameters used in this equation are given in Table A2. Detailed discussions of several of these parameters are given in Mangum & Shirley (2015).

$$N_T = \frac{1}{2} \frac{3k}{8\pi^3} \sqrt{\frac{\pi}{\ln 2}} \frac{Q e^{E_u/T_{\text{ex}}} \Delta T_A \Delta V}{B\nu S \mu^2 \eta_B} \frac{1}{1 - \frac{e^{h\nu/kT_{\text{ex}}} - 1}{e^{h\nu/kT_{\text{bg}}} - 1}} \quad (\text{A6})$$

Table A3

Approximate Line Density in Molecular Surveys of Sgr B2(N) at Different Frequencies

Source	Frequency	Line Density	
		Frequency Space	Velocity Space
PRIMOS	20 GHz	1 per 10 MHz	1 per 150 km s ⁻¹
IRAM	100 GHz	1 per 10 MHz	1 per 30 km s ⁻¹
NRAO 12 m	150 GHz	1 per 10 MHz	1 per 20 km s ⁻¹
CSO	275 GHz	1 per 10 MHz	1 per 10 km s ⁻¹

A key insight is provided by Equation (A6) upon inspection of the $\left(1 - \frac{e^{h\nu/kT_{\text{ex}}} - 1}{e^{h\nu/kT_{\text{bg}}} - 1}\right)$ term. In the case where $T_{\text{ex}} < T_{\text{bg}}$, this term becomes negative. As a negative value of N_T is unphysical, the value for ΔT_A must therefore be negative as well, indicating absorption.

A.6.2. Critical Density

When the number of molecules in each energy level is not well described by a Boltzmann distribution, one of the most common causes is that the density of the gas in which the molecule resides has fallen below the density required to thermalize the population. The distribution of a population of molecules across energy states is a balance between radiative (emission or absorption) processes and collisional (thermal) processes. Each transition of a given molecule has a characteristic rate (A_{ul}) that governs how quickly it undergoes spontaneous emission of photons, redistributing the population away from Boltzmann equilibrium. For a population of molecules to be in thermal equilibrium, collisions with other gas molecules must occur frequently enough to out-compete the radiative processes. In this case, T_{ex} becomes equal to the kinetic temperature (T_k) of the colliding gas, which is usually termed LTE conditions.

The density of gas required to ensure that these collisions dominate the distribution over radiative processes is the critical density (n_{cr}), given by Equation (A7) (Tielens 2005), where A_{ul} is the Einstein A coefficient (s⁻¹) and γ_{ul} is the collisional rate coefficient (cm³ s⁻¹) for the transition from upper state u to lower state l :

$$n_{\text{cr}} = \frac{A_{ul}}{\gamma_{ul}}. \quad (\text{A7})$$

A_{ul} is directly related to the rate at which a given molecule in state u will spontaneously decay to state l and emit a photon. Transitions with large A_{ul} undergo emission rapidly. To maintain a population distribution described by the thermal temperature, a correspondingly higher density—which results in more frequent collisions—is therefore required. A generalized approach for multilevel systems with many transitions into and out of a given level can be written as Equation (A8) (Tielens 2005):

$$n_{\text{cr}} = \frac{\sum_{l < u} A_{ul}}{\sum_{l \neq u} \gamma_{ul}}. \quad (\text{A8})$$

The rate at which these collisions occur is related to γ_{ul} , which is proportional to the average velocity of the molecules in the gas (v ; governed by T_k), a cross-sectional area (σ) related to the size of each collision partner, and their rotational and

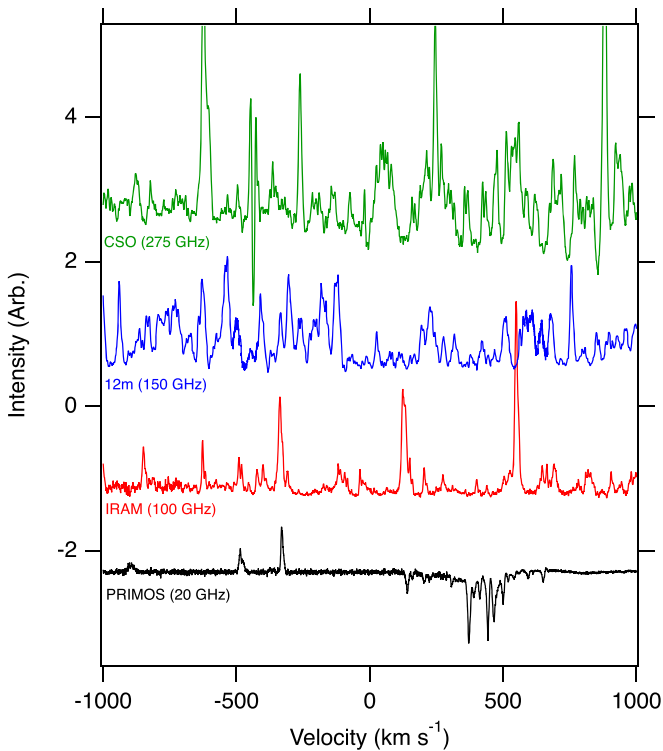


Figure A11. Comparison of observational data toward Sgr B2(N) at four different frequencies. The observations are plotted in velocity space, and the line widths are all quite similar ($\sim 8\text{--}10\text{ km s}^{-1}$).

vibrational excitation. These cross sections are almost universally calculated theoretically but are extraordinarily computationally expensive, especially with increasing molecular size (Faure et al. 2014).

In general, if the gas density exceeds n_{cr} , the relative populations of u and l will be described by a Boltzmann distribution at T_{ex} (which is nominally equal to T_k). Because n_{cr} is distinct for each transition, it is possible for only some of the energy levels of a molecule to be described by one T_{ex} , while the remaining energy levels are dominated by radiative processes and are not described by T_{ex} .

If all values of A_{ul} and γ_{ul} are known for a given molecule, then T_k and a column density can be modeled explicitly without the assumption of a single excitation temperature in what is known as a radiative transfer calculation. The approximations described in Section A.6.1 are accurate in the limit that the density is much larger than n_{cr} , and a full radiative transfer calculation in such situations will return an equivalent value to that determined by Equation (A6) and a single value for T_{ex} equal to T_k . A detailed review of radiative transfer calculations is given by van der Tak (2011).

A.6.3. Source and Beam Sizes

Often, the region of the sky from which molecular emission (or absorption) is seen is smaller than the telescope beam used for the observations. The result is a beam-diluted signal that reduces the intensity of the observed emission. Calculations that do not account for beam dilution would therefore underpredict the column density of a compact source. The beam-filling correction factor, B , is given by Equation (A9), where θ_s and θ_b are the circular Gaussian sizes of the source

and the half-power telescope beam, respectively:

$$B = \frac{\theta_s^2}{\theta_s^2 + \theta_b^2}. \quad (\text{A9})$$

By inspection, B approaches unity as the source size exceeds (fills) the beam size. Often, for single-dish observations where no reasonable a priori assumption can be made regarding the underlying source structure, the emission is assumed to “fill the beam,” and no correction for beam dilution is performed.

A related issue, not explicitly accounted for in these calculations, is the loss of sensitivity in interferometric observations to extended emission as a function of increasing spatial resolution. The magnitude of this effect is often determined by comparing the total flux observed with a single-dish telescope beam that is assumed or known to contain all of the emission to that recovered by the interferometer. If the interferometric observations display significantly lower flux, meaning that it has been resolved out, a correction can be made to any column density calculations if the total column (and not just that of the compact sources resolved by the array) is desired.

A.6.4. Background Continuum

The background continuum, T_{bg} , against which molecules absorb plays a crucial role in the overall intensity of the detected molecular signal. While the fractional absorption seen for a molecular transition is constant with column density, the absolute observed signal is of course dependent on the magnitude of the background being absorbed against. Thus, even a large population will present a small signal against a weak background, while, conversely, a very small population can be detected if T_{bg} is large. The background temperature also affects the intensity of emission lines, with the effect of reducing the overall ΔT_A that is observed.

A.6.5. Frequency-dependent Line Shapes

In interstellar observations, the width of a spectral line is defined, in the nonrelativistic limit, in Equation (A10), where ΔV is the velocity line width (km s^{-1}), $\Delta\nu$ is the width of the line in frequency space (MHz), ν_0 is the reference frequency (typically the central line frequency; MHz), and c is the speed of light (km s^{-1}):

$$\Delta V = \frac{\Delta\nu}{\nu_0} c. \quad (\text{A10})$$

The velocity width of a line is frequency independent; it is a physical effect of the source.⁹ Because ΔV is therefore constant, $\Delta\nu$ must increase with increasing ν_0 . Thus, at higher frequencies, the lines are far broader in frequency space.

This has a somewhat subtle but profound effect on the ability to detect weak signals in sources with large degrees of molecular complexity. As a concrete example, we can consider the density of lines in observations of Sgr B2(N) taken at different frequencies from the centimeter through the sub-millimeter. These are tabulated in Table A3 and shown visually in Figure A11.¹⁰

⁹ The uncertainty principle also dictates a quantum-mechanical width to every line, but in radioastronomical observations this is an immeasurably small contribution in almost all circumstances.

¹⁰ References—PRIMOS: Neill et al. (2012); IRAM: Belloche et al. (2013), NRAO 12 m: Remijan et al. (2008b), CSO: McGuire et al. (2013b).

Upon visual inspection, it is clear that in velocity space, the spectra are increasingly crowded at higher frequencies, even though the line density in frequency space remains the same. Indeed, at the highest frequencies, the spectra are nearly line confusion limited, a condition in which there is spectral line emission in every channel of the data. This issue sets in when the line density in velocity space becomes equal to the line width. Once a spectrum is line confusion limited, there is, to a large extent, no additional information to be gained by deeper integration. All weaker lines from undetected molecules will be buried beneath the lines already visible, thus making it impractical to identify new, rare molecules.

It is important to note that the observations used here are just illustrative. They were taken with different facilities, having different beam sizes, and to different sensitivities. Still, the general trend does hold that lower-frequency observations, while no less rich in molecular signals, have far more velocity space available to be filled with spectral lines. Indeed, of the observations shown here, those from PRIMOS at 20 GHz are the deepest and most sensitive (~ 3 mK) but still have the lowest line density. Thus, even once line confusion is reached in a source at millimeter and submillimeter frequencies, substantial discovery space often remains at centimeter wavelengths.

A.6.6. Partition Functions

The temperature-dependent partition function, $Q(T)$, for a molecule is a representation of the number of energy levels a population is spread out over. For astronomical purposes, $Q(T)$ is often composed almost entirely of a rotational component, with small additional contributions from vibrational components (Equation (A11)):

$$Q = Q_v \times Q_r. \quad (\text{A11})$$

The rotational partition function, Q_r , is often calculated according to a high-temperature approximation, given by Equation (A12) where σ is a symmetry parameter, T_{ex} is the excitation temperature (K), and A , B , and C , the rotational constants of the molecule (MHz), also as discussed earlier (c.f. Gordy & Cook 1984):

$$Q_r = \left(\frac{5.34 \times 10^6}{\sigma} \right) \left(\frac{T_{\text{ex}}^3}{ABC} \right)^{1/2}. \quad (\text{A12})$$

This approximation offers excellent values down to modestly low temperatures. Indeed, for most molecules, deviations from the explicitly calculated value do not reach 1% until ≤ 5 K. In cases where the temperature is low enough for this deviation to be significant, a direct summation of energy levels is required; this process is outlined in Gordy & Cook (1984). From inspection, it is also clear that larger, more complex molecules, with smaller rotational constants, will have a larger value of Q_r . This is the same trend discussed earlier in a qualitative fashion. Finally, it is necessary to note that this approximation does not take into account many of the additional sources of complexity discussed earlier such as internal rotation and nuclear hyperfine splitting, which are not represented in the rotational constants A , B , and C . This can be addressed either through the addition of degeneracy terms, through explicit state counting, or through a combination of both, as described in Gordy & Cook (1984).

The vibrational contribution, Q_v , is given by Equation (A13):

$$Q_v = \prod_{i=1}^{3N-6} \frac{1}{1 - e^{-E_i/kT_{\text{ex}}}}. \quad (\text{A13})$$

Here, the energies of each vibrational energy level E_i are considered. Only when T_{ex} is sufficiently high, and there are sufficiently low-lying vibrational states, does Q_v make any significant contribution. This correction factor accounts for the fact that the rotational energy level structure in an excited vibrational state is practically identical to that in the ground state. Thus, if some nontrivial population of molecules exists in a vibrationally excited state, those levels become accessible as well, spreading out intensity. Thus, the contribution to the total partition function Q from Q_v is multiplicative. Often the vibrational contribution is $< 1\%$ up to at least 30–40 K, although it can be significant (≥ 2) at warmer temperatures for some species. Strictly speaking, an electronic contribution Q_e may also be considered but is almost never a factor in interstellar detections, at least with radio telescopes.

A.7. Generalized Source Types

Section 11 presented four generalized source types—SFRs, dark clouds, carbon stars, and LOS clouds—in which most detections have been made. The analysis there showed that the types of molecules that are detected for the first time in each of these environments tend to have distinct properties. Thus, the environment in which a molecular search is conducted can have a significant impact on the detectability from several standpoints. These include total abundance (related to chemistry and density), excitation temperature (density and kinetic temperature), line width and spectral crowding (turbulent vs. quiescent regions), and source size (beam dilution). Five of the common types of environments for these searches are described below. While this is by no means an exhaustive list, it covers a large range in physical and chemical conditions and provides a grounding in the factors that must be considered and can be applied to other situations.

A.7.1. Diffuse (LOS) Clouds

The first detections of interstellar molecules (CH, CH⁺, and CN) were made in the LOS diffuse clouds that pervade the Galaxy (Swings & Rosenfeld 1937; McKellar 1940; Douglas & Herzberg 1941). While much of the molecular discovery quickly shifted to SFRs, dark clouds, and carbon stars, new detections in diffuse environments do still occur (see, e.g., the detection of SH by Neufeld et al. 2012).

These environments are characterized by low total number densities ($n_{\text{H}} \sim 10$ to $< 10^4$ cm⁻³), cool, but not cold kinetic temperatures ($T_k < 100$ K), and enhanced radiation environments over those seen in “standard” dense molecular clouds (for a detailed review, see Snow & McCall 2006). The excitation temperature of most molecules observed in these clouds is extremely subthermal at $T_{\text{ex}} \sim 3$ K, with the population largely distributed over only the few lowest rotational energy levels. Most sources show moderately to extremely broad spectral absorption features (3–20 km s⁻¹; Corby et al. 2018). The width of the features tends to correspond to the density and compactness of the absorbing gas, with narrow features arising from denser, more compact sources.

Table A4
Attributes of HC₅S and Their Effects on Detectability

HC ₅ S ...	Effects
... is prolate	Most ISM molecules are prolate or near prolate—high symmetry reduces Q , generally increasing line intensity
... is highly unsaturated	Highly unsaturated molecules tend to be first detected in carbon stars and dark clouds
... has two added sources of spectral complexity (Λ doubling and resolvable ¹ H splitting)	Q will be increased and the line intensities decreased if the splitting is resolved in observations
... has a rotational constant of ~ 876 MHz	The primary rotational transitions will occur at low frequency (centimeter wavelengths)
... has no low-lying structural conformers	Nearly all the population will be in the ground-state conformer—no decrease in its line intensities

The overall angular size of a distinct cloud can vary significantly with distance but is typically assumed to be larger than the continuum against which it is observed and is thus at least modestly extended ($>10''$). While the general assumption is that the gas is homogeneously distributed across the cloud, there is growing evidence that there may be significant substructure within each complex (Corby et al. 2018). This can lead to regions of increased density and decreased temperature and radiation effects.

These physical conditions put constraints on the type and extent of complex chemistry that can occur in these regions. The harsh radiation environment largely prevents a buildup of the icy dust grain layers thought to be needed to make many complex species, although there is some recent evidence showing surprising chemical complexity (Thiel et al. 2017), and the overall low number density results in difficulties achieving detectable abundances of molecules. Many of the new species detected in these environments are small, simpler precursor molecules that have often reacted away to form more complex molecules in other more evolved sources.

A.7.2. Dark Clouds

The prototypical dark cloud is TMC-1, a largely homogeneous, extended ($>60''$), cold ($T_{\text{kin}} \sim 10\text{--}20$ K), and modestly dense ($n_{\text{H}} \sim 10^4 \text{ cm}^{-3}$) source (Bell et al. 1998; Hincelin et al. 2011; Liszt & Ziurys 2012) with extremely narrow line widths ($\sim 0.3 \text{ km s}^{-1}$; McGuire et al. 2017a). The higher density compared with diffuse clouds (with correspondingly high extinction) shields the source and allows the formation of ice on the surfaces of dust grains. While saturated COMs may evolve on these surfaces, the cold kinetic temperatures and quiescent environment tend to force these species to remain on the surface. As a result, the (detectable) gas-phase inventory tends to be dominated by complex, unsaturated organic molecules formed by gas-phase reactions, typically long-chain carbon molecules like the cyanopolyynes (HC_{*n*}N; $n = 3, 5, 7, 9$). As discussed in Section A.1, these larger molecules will tend to have more transitions at lower frequencies. At the temperatures in these sources, the Boltzmann peak will tend to fall at low frequencies as well and has a favorable effect on the otherwise very large partition function (Section A.6.6). Thus, these regions tend to see a particularly pronounced number of detections of large, unsaturated molecules at frequencies below ~ 100 GHz. Because of the narrow velocity widths, line blending is rarely an issue.

A.7.3. Star-forming Regions

Upon gravitational collapse, dense molecular clouds begin to form molecular cores, compact, warm ($T_{\text{kin}} > 100$ K), and dense ($n_{\text{H}} \sim 10^5\text{--}10^8 \text{ cm}^{-3}$) sources, often associated with a

nascent star. In these regions, as the icy surfaces of the dust grains are heated, or are subjected to shocks, the complex molecular inventories are liberated into the gas phase and become detectable with radio astronomy. As was shown in Section 11, these molecules tend to be more saturated than those seen in dark clouds. Further, the molecules formed on these surfaces tend to be highly reactive and can then interact with the previously (largely) isolated gas-phase inventory from the dense cloud stage, depleting those abundances. The more complex physical environment, including transient events such as shocks and longer-term interactions from protostellar outflows, injects additional energy into the system, driving chemistry not otherwise possible under cooler, more quiescent conditions (Burkhardt et al. 2016).

The higher densities tend to thermalize the excitation temperatures, pushing the distributions toward LTE. Single-dish observations of these cores typically fail to resolve a single subsource, resulting in modestly broad line widths ($5\text{--}15 \text{ km s}^{-1}$; see, e.g., Widicus Weaver et al. 2017). Interferometric observations in these regions, however, can often isolate individual cores, significantly narrowing the line widths to a few km s^{-1} (Belloche et al. 2016). The large abundances and warm temperatures often result in spectra rapidly approaching (or having reached) line confusion in the millimeter and submillimeter regimes with modern facilities, both single dish and interferometric.

A.7.4. Evolved (Carbon) Stars

While complex chemistry in the ISM is dominated by carbon, a number of exotic—by interstellar standards—species are also seen in evolved star sources, the definition of which is expanded here to include oxygen-rich stars. Indeed, every detected molecule with six or more atoms contains a carbon atom; the largest molecule detected without a carbon atom is SiH₄, which was first detected (perhaps ironically) in the evolved carbon-rich star IRC+10216 (Goldhaber & Betz 1984). The intense physical environments of sources like IRC+10216 and the hypergiant VY Canis Majoris inject heavier atoms like Si, as well as Mg, Fe, Ti, and Al, into the gas phase, where they can be detected as components of molecules such as SiH₄, MgCN, FeCN, TiO₂, and AlOH (Ziurys et al. 1995; Tenenbaum & Ziurys 2010; Zack et al. 2011; Kamiński et al. 2013). While the circumstellar envelope around the stars themselves is compact, molecular emission is often seen in an extended distribution around the star itself (Cernicharo et al. 2013a). The physical conditions change as a function of distance from the star, often in a measurable manner, providing the opportunity to study, for example, dust evolutionary

Table A5
Attributes of CH₃CH₂CH₂OH and Their Effects on Detectability

CH ₃ CH ₂ CH ₂ OH ...	Effects
... is nearly prolate ($\kappa = -0.84$)	Most ISM molecules are prolate or near prolate —high symmetry reduces Q , generally increasing line intensity
... is fully saturated	Fully saturated molecules are most commonly observed in SFRs and LOS clouds
... is large (12 atoms, 60 amu)	Large molecules are rarely found in LOS clouds and have large partition functions
... has an internal methyl rotor	Q will be increased and the line intensities decreased if the splitting is resolved in observations
... has modest rotational constants (5–10 GHz)	The primary rotational transitions will occur in the millimeter and lower submillimeter wavelength ranges
... has five structural conformers	Some population may be spread out into these other conformers, reducing the overall intensity of the main conformer's lines
... has low-lying vibrational states	The contribution of these states to Q is likely to be nontrivial

processes within the ISM using a single source (Cernicharo et al. 2011). Line confusion is rarely an issue in these sources.

A.8. Bringing It All Together

With these tools in hand, and the trends and statistics discussed in Section 11, it is possible to make some informed guesses about the likely environments, facilities, and frequency ranges needed to detect a potential interstellar molecule. The thought process for two such example cases, HC₅S and *n*-propanol (CH₃CH₂CH₂OH), is outlined below. These discussions presume that the chemistry and elemental abundances in the ISM are favorable enough to produce at least some abundance of a species.

A.8.1. Searching for HC₅S

HC₅O (Section 4.6.11) was recently detected in the ISM in observations of TMC-1 at centimeter wavelengths with the GBT. Because they often have similar bonding characteristics with oxygen and are isovalent, it is logical to assume the S-substituted versions of O-containing compounds may be good interstellar candidates (e.g., CH₃OH/CH₃SH, C₃O/C₃S, SiO/SiS). The rotational spectrum of HC₅S is known (Gordon et al. 2002). Table A4 lists a few key considerations for the molecule and the corresponding effects on its likely detectability.

Given the highly unsaturated and C-rich nature of HC₅S, it is reasonable to expect that a carbon star or dark cloud is the most likely place for a detection (Section 11.4). The molecule is to zeroth order a linear rotor and so will have a relatively simple spectrum. The Λ -doubling splitting is a few MHz, and the ¹H splitting is ~ 0.5 MHz for the lowest of its centimeter wave transitions. The ¹H splitting quickly collapses, while the Λ -doubling splitting remains. These splittings translate to as little as 1 km s⁻¹ (¹H) to as much as 250 km s⁻¹ (Λ doubling) across the centimeter wave region (where the small B constant dictates most transitions will fall). In a carbon star source such as IRC +10216, line widths >10 km s⁻¹ are routine, and thus only the Λ doubling is likely to be resolved; the ¹H contribution (and reduction in line intensity) could be ignored. In a dark cloud,

where line widths can be as little as 0.1 km s⁻¹, both splittings are in play. Molecules detected in carbon stars tend to be modestly warm (>50 K), increasing Q and decreasing line intensities by a factor of ~ 6 over molecules at the temperatures typical of dark clouds (5–15 K).

Carbon Star Search. For a detection experiment toward a carbon star, the broader line widths, and accompanying unresolved hyperfine structure, may slightly offset the increased value of Q . The small B value likely necessitates a centimeter wave observation. Molecules in these sources are seen both in extended emission in the expanding envelope and surrounding gas and in compact emission nearer the star (Cernicharo et al. 2013a); thus a combined search with both an interferometer and a single-dish facility may be required.

Dark Cloud Search. For a detection experiment toward a dark cloud, the very narrow line widths will likely resolve much of the hyperfine structure, reducing the overall intensity. The decreased value of Q at low temperatures may help offset this, but nevertheless a high sensitivity will likely be required in narrow spectral channels and high resolution, indicating long integration times. At these even lower temperatures, observations in the centimeter wave are more or less mandatory. Molecules in these sources tend to be quite extended, and thus interferometers will resolve out most signal, requiring a single-dish facility to observe.

Verdict? A search in either a carbon star or a dark cloud would seem logical, given the unsaturated nature of the molecule. Insight from a chemical model as to an approximate abundance may help to break the tie. Any search will need to be done at centimeter wavelengths, and given that both source types likely require a single-dish measurement, that would seem a logical place to start.

A.8.2. Searching for CH₃CH₂CH₂OH

The detections of methanol (CH₃OH; Section 4.5.1) and ethanol (CH₃CH₂OH; Section 4.8.2), along with their large abundances, make the next largest fully saturated alcohol, propanol (CH₃CH₂CH₂OH), a logical target, and it has indeed been recently searched for without success (Müller et al. 2016). The rotational spectrum of CH₃CH₂CH₂OH is known (Kisiel et al. 2010). Table A5 below lists a few key considerations for the molecule and the corresponding effects on its likely detectability.

The fully saturated nature of the molecule suggests SFRs and LOS clouds are the most likely sources for detection, but the size of the molecule strongly favors SFRs (Section 11.4). The line widths in these sources are modest depending on whether single-dish or array observations are used (~ 1 –5 km s⁻¹), but these are far broader than the expected internal rotor splitting, so this should not greatly affect the observations. The temperature in these sources, however, is often quite warm (80–300 K). This can nontrivially populate both the low-lying vibrational states of the lowest-energy conformer but also populate the other conformers of the molecule as well, all with cumulative decreases in the population of the lowest conformer in its ground vibrational state. At these temperatures, the strongest transitions will fall around 200 GHz and will extend into the submillimeter.

Verdict? Given the expected low line intensity due to the large partition function and the existence of multiple low-lying vibrational states and conformers, individual lines are expected to be quite weak. At (sub)millimeter wavelengths, single-dish

spectra of SFRs are often line confusion limited, making the identification of weak features challenging. The compact nature of these sources also causes single-dish observations to suffer from beam dilution effects. Interferometric observations are likely better suited to these observations, as they generally result in narrower line widths that permit the observation of weaker lines before line confusion sets in. Choosing a target SFR that is on the cooler side would help push the population toward the ground vibrational state and lowest-energy conformer.

Appendix B astromol

New to the 2021 census update, the database of information is now available as a downloadable Python 3 package, `astromol` (McGuire 2021), accessible at <https://github.com/bmcguir2/astromol>. The package is version controlled on GitHub, and releases are documented and assigned DOI numbers through the Zenodo platform.

This object-oriented package comes preloaded with all of the relevant information on the molecules presented in this work, as well as the sources in which they are detected and the facilities used to detect them. All figures in the main text are generated using this package, and prewritten functions exist within the package that will regenerate any figures desired for the interested reader. Some limited customizability has been included with these functions that allows the user to, for example, replicate Figure 1, but plotting only the cumulative number of detections of ionic species with time. Users are also able to write their own custom plotting functions using the underlying database structure.

A value-added benefit of the package that may be of particular interest to readers is the inclusion of a function to automatically generate a PowerPoint slide of detected molecules in the ISM/CSM. The `make_mols_slide()` function will generate a slide containing a formatted display of all detected ISM/CSM molecules to date, in widescreen PowerPoint format, sorted by the number of atoms. It will display as well the total number of species, the date of the most recent update, the version of `astromol` used to generate the slide, and the appropriate reference to this manuscript. This, too, can take a modified list of species.

Finally, this package is intended to be updated substantially more often than this manuscript. This was also the hope for the prior set of scripts released with the original 2018 census; however the architecture of that code made regular updates far more challenging than anticipated. The `astromol` package was redesigned from the ground up with extensibility in mind. Indeed, a “Day 0” update is planned at release to include any molecules detected since this document’s contents were locked for publication.

ORCID iDs

Brett A. McGuire  <https://orcid.org/0000-0003-1254-4817>

References

- Adam, A. G., Barnes, M., Berno, B., Bower, R. D., & Merer, A. J. 1995, *JMoSp*, 170, 94
- Adams, W. S. 1941, *ApJ*, 93, 11
- Agúndez, M., Cabezas, C., Tercero, B., et al. 2021, *A&A*, 647, L10
- Agúndez, M., Cernicharo, J., Decin, L., Encrenaz, P., & Teyssier, D. 2014a, *ApJL*, 790, L27
- Agúndez, M., Cernicharo, J., & Guélin, M. 2007, *ApJL*, 662, L91
- Agúndez, M., Cernicharo, J., & Guélin, M. 2014b, *A&A*, 570, A45
- Agúndez, M., Cernicharo, J., & Guélin, M. 2015a, *A&A*, 577, L5
- Agúndez, M., Cernicharo, J., Pardo, J. R., Guélin, M., & Phillips, T. G. 2008, *A&A*, 485, L33
- Agúndez, M., Marcelino, N., & Cernicharo, J. 2018a, *ApJL*, 861, L22
- Agúndez, M., Marcelino, N., Cernicharo, J., & Tafalla, M. 2018b, *A&A*, 611, L1
- Agúndez, M., Cernicharo, J., Guélin, M., et al. 2010, *A&A*, 517, L2
- Agúndez, M., Cernicharo, J., De Vicente, P., et al. 2015b, *A&A*, 579, L10
- Ahrens, V., Lewen, F., & Takano, S. 2002, *ZNatA*, 57, 669
- Aladro, R., Martín, S., Riquelme, D., et al. 2015, *A&A*, 579, A101
- Alexander, A. J., Kroto, H. W., Maier, M., & Walton, D. R. M. 1978, *JMoSp*, 70, 84
- Alexander, A. J., Kroto, H. W., & Walton, D. R. M. 1976, *JMoSp*, 62, 175
- Allen, M. D., Ziurys, L. M., & Brown, J. M. 1996, *CPL*, 257, 130
- Aller, L. H. 1966, *PNAS*, 55, 671
- Altman, R. S., Crofton, M. W., & Oka, T. 1984, *JChPh*, 80, 3911
- Amano, T. 2008a, *JChPh*, 129, 244305
- Amano, T. 2008b, *JChPh*, 129, 244305
- Amano, T., & Amano, T. 1991, *JChPh*, 95, 2275
- Amano, T., Amano, T., & Warner, H. E. 1991, *JMoSp*, 146, 519
- Amano, T., Saito, S., Hirota, E., & Morino, Y. 1969, *JMoSp*, 32, 97
- Amano, T., & Scappini, F. 1991, *JChPh*, 95, 2280
- Anderson, J. K., Halfen, D. T., & Ziurys, L. M. 2015, *JMoSp*, 307, 1
- Anderson, J. K., & Ziurys, L. M. 2014, *ApJL*, 795, L1
- Anderson, M. A., Steimle, T. C., & Ziurys, L. M. 1994, *ApJL*, 429, L41
- Apponi, A. J., Barclay, W. L. J., & Ziurys, L. M. 1993, *ApJL*, 414, L129
- Apponi, A. J., Hoy, J. J., Halfen, D. T., Ziurys, L. M., & Brewster, M. A. 2006, *ApJ*, 652, 1787
- Apponi, A. J., McCarthy, M. C., Gottlieb, C. A., & Thaddeus, P. 1999a, *ApJL*, 516, L103
- Apponi, A. J., McCarthy, M. C., Gottlieb, C. A., & Thaddeus, P. 1999b, *JChPh*, 111, 3911
- Apponi, A. J., McCarthy, M. C., Gottlieb, C. A., & Thaddeus, P. 2000, *ApJL*, 536, L55
- Araiki, M., Furuya, T., & Saito, S. 2001, *JMoSp*, 210, 132
- Arié, E., & Johns, J. W. C. 1992, *JMoSp*, 155, 195
- Avery, L. W., Broten, N. W., MacLeod, J. M., Oka, T., & Kroto, H. W. 1976, *ApJL*, 205, L173
- Bailleux, S., Bogey, M., Demuynck, C., Liu, Y., & Walters, A. 2002, *JMoSp*, 216, 465
- Baird, K. M., & Bredohl, H. 1971, *ApJL*, 169, L83
- Baldacci, A., Ghersetti, S., & Rao, K. N. 1973, *JMoSp*, 48, 600
- Ball, J. A., Gottlieb, C. A., Lilley, A. E., & Radford, H. E. 1970, *ApJL*, 162, L203
- Barlow, M. J., Swinyard, B. M., Owen, P. J., et al. 2013, *Sci*, 342, 1343
- Barman, T. S., Konopacky, Q. M., Macintosh, B., & Marois, C. 2015, *ApJ*, 804, 61
- Barman, T. S., Macintosh, B., Konopacky, Q. M., & Marois, C. 2011, *ApJ*, 733, 65
- Beckwith, S., Sargent, A. I., Scoville, N. Z., et al. 1986, *ApJ*, 309, 755
- Beers, Y., & Howard, C. J. 1975, *JChPh*, 63, 4212
- Bekooy, J. P., Verhoeve, P., Meerts, W. L., & Dymanus, A. 1985, *JChPh*, 82, 3868
- Bell, M. B., Avery, L. W., & Feldman, P. A. 1993, *ApJL*, 417, L37
- Bell, M. B., Feldman, P. A., Travers, M. J., et al. 1997, *ApJL*, 483, L61
- Bell, M. B., Watson, J. K. G., Feldman, P. A., & Travers, M. J. 1998, *ApJ*, 508, 286
- Bellet, J., Deldalle, A., Samson, C., Stenbeckeliers, G., & Wertheimer, R. 1971a, *JMoSt*, 9, 65
- Bellet, J., Samson, C., Stenbeckeliers, G., & Wertheimer, R. 1971b, *JMoSt*, 9, 49
- Belloche, A., Garrod, R. T., Müller, H. S. P., & Menten, K. M. 2014, *Sci*, 345, 1584
- Belloche, A., Garrod, R. T., Müller, H. S. P., et al. 2009, *A&A*, 499, 215
- Belloche, A., Garrod, R. T., Müller, H. S. P., et al. 2019, *A&A*, 628, A10
- Belloche, A., Menten, K. M., Comito, C., et al. 2008, *A&A*, 482, 179
- Belloche, A., Müller, H. S. P., Garrod, R. T., & Menten, K. M. 2016, *A&A*, 587, A91
- Belloche, A., Müller, H. S. P., Menten, K. M., Schilke, P., & Comito, C. 2013, *A&A*, 559, A47
- Belloche, A., Meshcheryakov, A. A., Garrod, R. T., et al. 2017, *A&A*, 601, A49
- Benson, R. C., & Flygare, W. H. 1970, *JChS*, 92, 7523
- Benson, R. C., Flygare, W. H., Oda, M., & Breslow, R. 1973, *JChS*, 95, 2772
- Benz, A. O., Bruderer, S., van Dishoeck, E. F., et al. 2010, *A&A*, 521, L35

- Bergin, E. A., Cleves, L. I., Gorti, U., et al. 2013, *Natur*, 493, 644
- Bergman, P., Parise, B., Liseau, R., et al. 2011, *A&A*, 531, L8
- Bernard-Salas, J., Peeters, E., Sloan, G. C., et al. 2006, *ApJL*, 652, L29
- Bernath, P. F. 2005, *Spectra of Atoms and Molecules* (2nd ed.; New York: Oxford Univ. Press)
- Bernath, P. F., Hinkle, K. H., & Keady, J. J. 1989, *Sci*, 244, 562
- Berné, O., Mulas, G., & Joblin, C. 2013, *A&A*, 550, L4
- Bestmann, G., & Dreizler, H. 1985, *ZNatA*, 40, 263
- Betz, A. L. 1981, *ApJL*, 244, L103
- Birk, M., Winnewisser, M., & Cohen, E. A. 1989, *JMoSp*, 136, 402
- Bizzocchi, L., Thorwirth, S., Müller, H. S. P., Lewen, F., & Winnewisser, G. 2001, *JMoSp*, 205, 110
- Bizzocchi, L., Prudeniano, D., Rivilla, V. M., et al. 2020, *A&A*, 640, A98
- Blackman, G. L., Brown, R. D., Godfrey, P. D., & Gunn, H. I. 1976, *Natur*, 261, 395
- Blake, G. A., Keene, J., & Phillips, T. G. 1985, *ApJ*, 295, 501
- Blake, G. A., Sutton, E. C., Masson, C. R., et al. 1984, *ApJ*, 286, 586
- Blake, G. A., van Dishoeck, E. F., & Sargent, A. I. 1992, *ApJL*, 391, L99
- Blom, C. E., Grassi, G., & Bauder, A. 1984, *JChS*, 106, 7427
- Blukis, U., Kasai, P. H., & Myers, R. J. 1963, *JChPh*, 38, 2753
- Bogey, M., Demuyneck, C., Denis, M., & Destombes, J. L. 1985a, *A&A*, 148, L11
- Bogey, M., Demuyneck, C., & Destombes, J. L. 1984, *A&A*, 138, L11
- Bogey, M., Demuyneck, C., & Destombes, J. L. 1985b, *JChPh*, 83, 3703
- Bogey, M., Demuyneck, C., & Destombes, J. L. 1988a, *JMoSp*, 132, 277
- Bogey, M., Demuyneck, C., Destombes, J. L., & Vallee, Y. 1995, *JMoSp*, 172, 344
- Bogey, M., Destombes, J. L., Vallee, Y., & Ripoll, J. L. 1988b, *CPL*, 146, 227
- Bogey, M., Dubus, H., & Guillemin, J. C. 1990, *JMoSp*, 143, 180
- Boogert, A. C. A., Gerakines, P. A., & Whittet, D. C. B. 2015, *ARA&A*, 53, 541
- Booth, A. S., Walsh, C., Ilee, J. D., et al. 2019, *ApJL*, 882, L31
- Botschwina, P., Heyl, A., Chen, W., et al. 1998, *JChPh*, 109, 3108
- Botschwina, P., & Oswald, R. 2008, *JChPh*, 129, 044305
- Bouchy, A., Demaison, J., Roussy, G., & Barriol, J. 1973, *JMoSt*, 18, 211
- Braakman, R., Drouin, B. J., Weaver, S. L. W., & Blake, G. A. 2010, *JMoSp*, 264, 43
- Braam, M., van der Tak, F. F. S., Chubb, K. L., & Min, M. 2020, *A&A*, 646, A17
- Brazier, C. R., & Brown, J. M. 1983, *JChPh*, 78, 1608
- Brewster, M. A., Apponi, A. J., Xin, J., & Ziurys, L. M. 1999, *CPL*, 310, 411
- Brogan, C. L., Pérez, L. M., Hunter, T. R., et al. 2015, *ApJL*, 808, L3
- Brotten, N. W., MacLeod, J. M., Avery, L. W., et al. 1984, *ApJL*, 276, L25
- Brotten, N. W., MacLeod, J. M., Oka, T., et al. 1976, *ApJL*, 209, L143
- Brotten, N. W., Oka, T., Avery, L. W., MacLeod, J. M., & Kroto, H. W. 1978, *ApJL*, 223, L105
- Brown, F. X., Saito, S., & Yamamoto, S. 1990, *JMoSp*, 143, 203
- Brown, J. M., Curl, R. F., & Evenson, K. M. 1985a, *ApJ*, 292, 188
- Brown, J. M., & Müller, H. S. P. 2009, *JMoSp*, 255, 68
- Brown, R. D., Crofts, J. G., Gardner, F. F., et al. 1975a, *ApJL*, 197, L29
- Brown, R. D., Dyal, K. G., Elmes, P. S., Godfrey, P. D., & McNaughton, D. 1988, *JChS*, 110, 789
- Brown, R. D., Eastwood, F. W., Elmes, P. S., & Godfrey, P. D. 1983, *JChS*, 105, 6496
- Brown, R. D., Godfrey, P. D., & Storey, J. 1975b, *JMoSp*, 58, 445
- Brown, R. D., Godfrey, P. D., Cragg, D. M., et al. 1985b, *ApJ*, 297, 302
- Brünken, S., Belloche, A., Martín, S., Verheyen, L., & Menten, K. M. 2010, *A&A*, 516, A109
- Brünken, S., Gottlieb, C. A., Gupta, H., McCarthy, M. C., & Thaddeus, P. 2007a, *A&A*, 464, L33
- Brünken, S., Gottlieb, C. A., McCarthy, M. C., & Thaddeus, P. 2009a, *ApJ*, 697, 880
- Brünken, S., Gupta, H., & Gottlieb, C. A. 2007b, *ApJL*, 664, L43
- Brünken, S., Kluge, L., Stoffels, A., Asvany, O., & Schlemmer, S. 2014, *ApJ*, 783, L4
- Brünken, S., Müller, H. S. P., Menten, K. M., McCarthy, M. C., & Thaddeus, P. 2008, *ApJ*, 676, 1367
- Brünken, S., Yu, Z., Gottlieb, C. A., McCarthy, M. C., & Thaddeus, P. 2009b, *ApJ*, 706, 1588
- Buhl, D., & Snyder, L. E. 1970, *Natur*, 228, 267
- Buhl, D., & Snyder, L. E. 1973, in *Molecules in the Galactic Environment*, ed. M. A. Gordon & L. E. Snyder (New York: Wiley), 187
- Buhl, D., Snyder, L. E., & Edrich, J. 1972, *ApJ*, 177, 625
- Burkhardt, A. M., Dollhopf, N. M., Corby, J. F., et al. 2016, *ApJ*, 827, 21
- Burkhardt, A. M., Lee, K. L. K., Changala, P. B., et al. 2021, *ApJL*, 913, L18
- Burkholder, J. B., Howard, C. J., & McKellar, A. R. W. 1988, *JMoSp*, 127, 415
- Butcher, S. S., & Wilson, E. B. 1964, *JChPh*, 40, 1671
- Cabezas, C., Cernicharo, J., Alonso, J. L., et al. 2013, *ApJ*, 775, 133
- Cameron, A. G. W. 1973, *SSRv*, 15, 121
- Cami, J., Bernard-Salas, J., Peeters, E., & Malek, S. E. 2010, *Sci*, 329, 1180
- Campbell, E. K., Holz, M., Gerlich, D., & Maier, J. P. 2015, *Natur*, 523, 322
- Campbell, E. K., Holz, M., Maier, J. P., et al. 2016, *ApJ*, 822, 17
- Carr, J. S., & Najita, J. R. 2008, *Sci*, 319, 1504
- Carr, J. S., Tokunaga, A. T., & Najita, J. 2004, *ApJ*, 603, 213
- Carrington, A., & Ramsay, D. A. 1982, *PhysS*, 25, 272
- Carroll, P. B., McGuire, B. A., Blake, G. A., et al. 2015, *ApJ*, 799, 15
- Carruthers, G. R., & Carruthers, G. R. 1970, *ApJL*, 161, L81
- Cazzoli, G., & Pazzarini, C. 2006, *JMoSp*, 239, 64
- Ceccarelli, C., Dominik, C., Caux, E., Lefloch, B., & Caselli, P. 2005, *ApJL*, 631, L81
- Ceccarelli, C., Dominik, C., Lefloch, B., Caselli, P., & Caux, E. 2004, *ApJL*, 607, L51
- Cernicharo, J., Agúndez, M., Cabezas, C., et al. 2021a, *A&A*, 649, L15
- Cernicharo, J., Agúndez, M., Kahane, C., et al. 2011, *A&A*, 529, L3
- Cernicharo, J., Cabezas, C., Endo, Y., et al. 2021b, *A&A*, 646, L3
- Cernicharo, J., Cernicharo, J., Guélin, M., & Guélin, M. 1987a, *A&A*, 183, L10
- Cernicharo, J., Daniel, F., Castro-Carrizo, A., et al. 2013a, *ApJL*, 778, L25
- Cernicharo, J., Goicoechea, J. R., & Caux, E. 2000, *ApJL*, 534, L199
- Cernicharo, J., Gottlieb, C. A., Guélin, M., et al. 1991a, *ApJL*, 368, L39
- Cernicharo, J., Gottlieb, C. A., Guélin, M., et al. 1991b, *ApJL*, 368, L43
- Cernicharo, J., Gottlieb, C. A., Guélin, M., Thaddeus, P., & Vrtilek, J. M. 1989, *ApJL*, 341, L25
- Cernicharo, J., & Guélin, M. 1996, *A&A*, 309, L27
- Cernicharo, J., Guélin, M., Agúndez, M., et al. 2007, *A&A*, 467, L37
- Cernicharo, J., Guélin, M., Agúndez, M., McCarthy, M. C., & Thaddeus, P. 2008, *ApJL*, 688, L83
- Cernicharo, J., Guélin, M., Menten, K. M., & Walmsley, C. M. 1987b, *A&A*, 181, L1
- Cernicharo, J., Guélin, M., & Pardo, J. R. 2004, *ApJL*, 615, L145
- Cernicharo, J., Guélin, M., & Walmsley, C. M. 1987c, *A&A*, 172, L5
- Cernicharo, J., Heras, A. M., Tielens, A. G. G. M., et al. 2001, *ApJL*, 546, L123
- Cernicharo, J., Kahane, C., Gomez-Gonzales, J., & Guélin, M. 1986a, *A&A*, 167, L5
- Cernicharo, J., Kahane, C., Gómez-González, J., & Guélin, M. 1986b, *A&A*, 164, L1
- Cernicharo, J., Kahane, C., Guélin, M., & Gómez-González, J. 1988, *A&A*, 189, L1
- Cernicharo, J., Kahane, C., Guélin, M., & Hein, H. 1987d, *A&A*, 181, L9
- Cernicharo, J., Liu, X. W., González-Alfonso, E., et al. 1997, *ApJL*, 483, L65
- Cernicharo, J., Marcelino, N., Agúndez, M., et al. 2020a, *A&A*, 642, L8
- Cernicharo, J., Marcelino, N., Agúndez, M., et al. 2020b, *A&A*, 642, L17
- Cernicharo, J., Marcelino, N., Roueff, E., et al. 2012, *ApJL*, 759, L43
- Cernicharo, J., Tercero, B., Fuente, A., et al. 2013b, *ApJL*, 771, L10
- Cernicharo, J., Bailleux, S., Alekseev, E., et al. 2014, *ApJ*, 795, 40
- Cernicharo, J., McCarthy, M. C., Gottlieb, C. A., et al. 2015, *ApJ*, 806, 1
- Cernicharo, J., Kisiel, Z., Tercero, B., et al. 2016, *A&A*, 587, L4
- Cernicharo, J., Agúndez, M., Velilla Prieto, L., et al. 2017, *A&A*, 606, L5
- Cernicharo, J., Lefloch, B., Agúndez, M., et al. 2018, *ApJL*, 853, L22
- Cernicharo, J., Velilla Prieto, L., Agúndez, M., et al. 2019a, *A&A*, 627, L4
- Cernicharo, J., Cabezas, C., Pardo, J. R., et al. 2019b, *A&A*, 630, L2
- Cernicharo, J., Cabezas, C., Agúndez, M., et al. 2021c, *A&A*, 647, L3
- Cernicharo, J., Agúndez, M., Cabezas, C., et al. 2021d, *A&A*, 647, L2
- Cernicharo, J., Cabezas, C., Bailleux, S., et al. 2021e, *A&A*, 646, L7
- Cernicharo, J., Cabezas, C., Agúndez, M., et al. 2021f, *A&A*, 648, L3
- Champion, J. P., Hilico, J. C., Wenger, C., & Brown, L. R. 1989, *JMoSp*, 133, 256
- Chapillon, E., Dutrey, A., Guilloteau, S., et al. 2012, *ApJ*, 756, 58
- Charbonneau, D., Brown, T. M., Noyes, R. W., & Gilliland, R. L. 2002, *ApJ*, 568, 377
- Charnley, S. B., Ehrenfreund, P., & Kuan, Y.-J. 2001, *AcSpA*, 57, 685
- Charo, A., & De Lucia, F. C. 1982, *JMoSp*, 94, 426
- Charo, A., Herbst, E., de Lucia, F. C., & Sastry, K. V. L. N. 1981, *ApJL*, 244, L111
- Chen, W., Grabow, J. U., Travers, M. J., et al. 1998, *JMoSp*, 192, 1
- Cheung, A., Hajigeorgiou, P. G., Huang, G., Huang, S.-Z., & Merer, A. J. 1994, *JMoSp*, 163, 443

- Cheung, A. C., Rank, D. M., Townes, C. H., Thornton, D. D., & Welch, W. J. 1968, *PhRvL*, **21**, 1701
- Cheung, A. C., Rank, D. M., Townes, C. H., Thornton, D. D., & Welch, W. J. 1969, *Natur*, **221**, 626
- Chomiak, D., Taleb-Bendiab, A., Civis, S., & Amano, T. 1994, *CaJPh*, **72**, 1078
- Christen, D., Coudert, L. H., Suenram, R. D., & Lovas, F. J. 1995, *JMoSp*, **172**, 57
- Churchwell, E., & Winnewisser, G. 1975, *A&A*, **45**, 229
- Churchwell, E., Witzel, A., Huchtmeier, W., et al. 1977, *A&A*, **54**, 969
- Cleeton, C. E., & Williams, N. H. 1934, *PhRv*, **45**, 234
- Cochran, E. L., Adrian, F. J., & Bowers, V. A. 1964, *JChPh*, **40**, 213
- Combes, F., Gerin, M., Wootten, A., et al. 1987, *A&A*, **180**, L13
- Condon, J. J., & Ransom, S. J. 2016, *Essential Radio Astronomy*, Princeton Series in Modern Observational Astronomy (Princeton: Princeton Univ. Press)
- Cooke, I. R., Fayolle, E. C., & Öberg, K. I. 2016, *ApJ*, **832**, 5
- Corby, J. F., McGuire, B. A., Herbst, E., & Remijan, A. J. 2018, *A&A*, **610**, A10
- Cord, M. S., Lojko, M. S., & Petersen, J. D. 1968, *Microwave Spectral Tables* (Washington, DC: Superintendent of Documents), 5
- Cordiner, M. A., Charnley, S. B., Kisiel, Z., McGuire, B. A., & Kuan, Y.-J. 2017, *ApJ*, **850**, 187
- Coutans, A., Ligterink, N. F. W., Loison, J. C., et al. 2019, *A&A*, **623**, L13
- Cuadrado, S., Goicoechea, J. R., Roncero, O., et al. 2016, *A&A*, **596**, L1
- Cummins, S. E., Linke, R. A., & Thaddeus, P. 1986, *ApJS*, **60**, 819
- Cunningham, M. R., Jones, P. A., Godfrey, P. D., et al. 2007, *MNRAS*, **376**, 1201
- Cupp, R. E., Kempf, R. A., & Gallagher, J. J. 1968, *PhRv*, **171**, 60
- De Luca, M., Gupta, H., Neufeld, D., et al. 2012, *ApJL*, **751**, L37
- De Lucia, F. C., Helminger, P., & Gordy, W. 1971, *PhRvA*, **3**, 1849
- de Zafra, R. L. 1971, *ApJ*, **170**, 165
- Decin, L., Danilovich, T., Gobrecht, D., et al. 2018, *ApJ*, **855**, 113
- Dehayem-Kamadjeu, A., Pirali, O., Orphal, J., Kleiner, I., & Flaud, P. M. 2005, *JMoSp*, **234**, 182
- Delucia, F., & Gordy, W. 1969, *PhRv*, **187**, 58
- Demaison, J., Boucher, D., Burie, J., & Dubrulle, A. 1983, *ZNatA*, **38**, 447
- Demaison, J., Boucher, D., Burie, J., & Dubrulle, A. 1984, *ZNatA*, **39**, 560
- Demaison, J., Pohl, I., & Rudolph, H. D. 1985, *JMoSp*, **114**, 210
- Deming, D., Wilkins, A., McCullough, P., et al. 2013, *ApJ*, **774**, 95
- D'Hendecourt, L. B., & Allamandola, L. J. 1986, *A&AS*, **64**, 453
- D'Hendecourt, L. B., & Jourdain de Muizon, M. 1989, *A&A*, **223**, L5
- Dickens, J. E., Irvine, W. M., Nummelin, A., et al. 2001, *AcSpA*, **57**, 643
- Dickens, J. E., Irvine, W. M., Ohishi, M., et al. 1997, *ApJ*, **489**, 753
- Dickinson, D. F. 1972, *ApL*, **12**, 235
- Dixon, R. N. 1959, *CaJPh*, **37**, 1171
- Dixon, T. A., & Woods, R. C. 1975, *PhRvL*, **34**, 61
- Dixon, T. A., & Woods, R. C. 1977, *JChPh*, **67**, 3956
- Domenech, J. L., Cueto, M., Herrero, V. J., et al. 2013, *ApJL*, **771**, L11
- Douglas, A. E., & Herzberg, G. 1941, *ApJ*, **94**, 381
- Drouin, B. J., Yu, S., Miller, C. E., et al. 2010, *JQSRT*, **111**, 1167
- Duley, W. W., & Hu, A. 2012, *ApJL*, **745**, L11
- Dunham, T. J. 1937, *PASP*, **49**, 26
- Dutrey, A., Guilloteau, S., & Guélin, M. 1997, *A&A*, **317**, L55
- Dutrey, A., Guilloteau, S., & Simon, M. 1994, *A&A*, **286**, 149
- Dutrey, A., Henning, T., Guilloteau, S., et al. 2007, *A&A*, **464**, 615
- Ehrenfreund, P., Boogert, A. C. A., Gerakines, P. A., Tielens, A. G. G. M., & van Dishoeck, E. F. 1997, *A&A*, **328**, 649
- Ehrenstein, G., Townes, C. H., & Stevenson, M. J. 1959, *PhRvL*, **3**, 40
- Endo, Y., & Hirota, E. 1987, *JChPh*, **86**, 4319
- Endo, Y., & Mizushima, M. 1982, *JaJAP*, **21**, L379
- Endo, Y., Saito, S., & Hirota, E. 1984, *JChPh*, **81**, 122
- Erickson, N. R., Snell, R. L., Loren, R. B., Mundy, L., & Plambeck, R. L. 1981, *ApJL*, **245**, L83
- Fabian, J. 1996, *PhRvB*, **53**, 13864
- Faure, A., Remijan, A. J., Szalewicz, K., & Wiesenfeld, L. 2014, *ApJ*, **783**, 72
- Favre, C., Fedele, D., Semenov, D., et al. 2018, *ApJL*, **862**, L2
- Fayolle, E. C., Öberg, K. I., Jørgensen, J. K., et al. 2017, *NatAs*, **1**, 703
- Fedoseev, G., Cuppen, H. M., Ioppolo, S., Lamberts, T., & Linnartz, H. 2015, *MNRAS*, **448**, 1288
- Feuchtgruber, H., Helmich, F. P., van Dishoeck, E. F., & Wright, C. M. 2000, *ApJL*, **535**, L111
- Flory, M. A., & Ziurys, L. M. 2011, *JChPh*, **135**, 184303
- Ford, R. G., & Seitzman, H. A. 1978, *JMoSp*, **69**, 326
- Fortenberry, R. C., Huang, X., Crawford, T. D., & Lee, T. J. 2013, *ApJ*, **772**, 39
- Forthomme, D., Linton, C., Tokaryk, D. W., Adam, A. G., & Granger, A. D. 2010, *CPL*, **488**, 116
- Fortman, S. M., McMillan, J. P., Neese, C. F., et al. 2012, *JMoSp*, **280**, 11
- Fourikis, N., Sinclair, M. W., Robinson, B. J., Godfrey, P. D., & Brown, R. D. 1974a, *AuJPh*, **27**, 425
- Fourikis, N., Takagi, K., & Morimoto, M. 1974b, *ApJL*, **191**, L139
- Frerking, M. A., Linke, R. A., & Thaddeus, P. 1979, *ApJL*, **234**, L143
- Friberg, P., Hjalmarsen, Å., Guélin, M., & Irvine, W. M. 1980, *ApJL*, **241**, L99
- Friesen, R. K., Medeiros, L., Schnee, S., et al. 2013, *MNRAS*, **436**, 1513
- Fuchs, G. W., Fuchs, U., Giesen, T. F., & Wyrowski, F. 2005, *A&A*, **444**, 521
- Fuchs, U., Winnewisser, G., Groner, P., De Lucia, F. C., & Herbst, E. 2003, *ApJS*, **144**, 277
- Fuente, A., Cernicharo, J., Agúndez, M., et al. 2010, *A&A*, **524**, A19
- Fuente, A., García-Burillo, S., Gerin, M., et al. 2006, *ApJL*, **641**, L105
- Fuente, A., Goicoechea, J. R., Pety, J., et al. 2017, *ApJL*, **851**, L49
- Furuya, R. S., Walmsley, C. M., Nakanishi, K., Schilke, P., & Bachiller, R. 2003, *A&A*, **409**, L21
- Gallagher, J. J., & Johnson, C. M. 1956, *PhRv*, **103**, 1727
- García-Burillo, S., Martín-Pintado, J., Fuente, A., Usero, A., & Neri, R. 2002, *ApJL*, **575**, L55
- Gardner, F. F., & Whiteoak, J. B. 1974, *Natur*, **247**, 526
- Gardner, F. F., & Winnewisser, G. 1975, *ApJL*, **195**, L127
- Garrod, R. T., Weaver, S. L. W., & Herbst, E. 2008, *ApJ*, **682**, 283
- Gausset, L., Herzberg, G., Lagerqvist, A., & Rosen, B. 1965, *ApJ*, **142**, 45
- Geballe, T. R., Goto, M., Usuda, T., Oka, T., & McCall, B. J. 2006, *ApJ*, **644**, 907
- Geballe, T. R., & Oka, T. 1996, *Natur*, **384**, 334
- Georgiou, K., Kroto, H. W., & Landsberg, B. M. 1979, *JMoSp*, **77**, 365
- Gerin, M., De Luca, M., Black, J., et al. 2010, *A&A*, **518**, L110
- Gerry, M. C. L., Stroh, F., & Winnewisser, M. 1990, *JMoSp*, **140**, 147
- Gerry, M. C. L., & Winnewisser, G. 1973, *JMoSp*, **48**, 1
- Giacobbe, P., Brogi, M., Gandhi, S., et al. 2021, *Natur*, **592**, 205
- Gibb, E. L., & Horne, D. 2013, *ApJL*, **776**, L28
- Gillett, F. C., & Forrest, W. J. 1973, *ApJ*, **179**, 483
- Godfrey, P. D., Brown, R. D., & Hunter, A. N. 1997, *JMoSt*, **413-414**, 405
- Godfrey, P. D., Brown, R. D., Robinson, B. J., & Sinclair, M. W. 1973, *ApL*, **13**, 119
- Golden, S., Wentink, T., Hillger, R., & Strandberg, M. W. 1948, *PhRv*, **73**, 92
- Goldhaber, D. M., & Betz, A. L. 1984, *ApJL*, **279**, L55
- Goldsmith, P. F., Krotkov, R., Snell, R. L., Brown, R. D., & Godfrey, P. 1983, *ApJ*, **274**, 184
- Goldsmith, P. F., & Langer, W. D. 1999, *ApJ*, **517**, 209
- Goldsmith, P. F., Li, D., Bergin, E. A., et al. 2002, *ApJ*, **576**, 814
- Goldsmith, P. F., Liseau, R., Bell, T. A., et al. 2011, *ApJ*, **737**, 96
- González-Alfonso, E., Smith, H. A., Fischer, J., & Cernicharo, J. 2004, *ApJ*, **613**, 247
- González-Alfonso, E., Fischer, J., Bruderer, S., et al. 2013, *A&A*, **550**, A25
- Gordon, V. D., McCarthy, M. C., Apponi, A. J., & Thaddeus, P. 2001, *ApJS*, **134**, 311
- Gordon, V. D., McCarthy, M. C., Apponi, A. J., & Thaddeus, P. 2002, *ApJS*, **138**, 297
- Gordy, W., & Cook, R. L. 1984, *Microwave Molecular Spectra* (3rd ed.; New York: Wiley)
- Goss, W. M. 1966, *ApJ*, **145**, 707
- Gottlieb, C. A. 1973, in *Molecules in the Galactic Environment*, ed. M. A. Gordon & L. E. Snyder (New York: Wiley), 181
- Gottlieb, C. A., Apponi, A. J., McCarthy, M. C., Thaddeus, P., & Linnartz, H. 2000, *JChPh*, **113**, 1910
- Gottlieb, C. A., & Ball, J. A. 1973, *ApJL*, **184**, L59
- Gottlieb, C. A., Ball, J. A., Gottlieb, E. W., Lada, C. J., & Penfield, H. 1975, *ApJL*, **200**, L147
- Gottlieb, C. A., Gottlieb, E. W., & Thaddeus, P. 1986, *A&A*, **164**, L5
- Gottlieb, C. A., Gottlieb, E. W., Thaddeus, P., & Kawamura, H. 1983, *ApJ*, **275**, 916
- Gottlieb, C. A., Vrtilik, J. M., Gottlieb, E. W., Thaddeus, P., & Hjalmarsen, Å. 1985, *ApJL*, **294**, L55
- Gottlieb, C. A., Vrtilik, J. M., & Thaddeus, P. 1989, *ApJL*, **343**, L29
- Graham, W. R. M., Dismuke, K. I., & Weltner Jr., W. 1974, *JChPh*, **60**, 3817
- Gratier, P., Pety, J., Guzmán, V., et al. 2013, *A&A*, **557**, A101
- Green, S., A. J., Montgomery, J., & Thaddeus, P. 1974, *ApJL*, **193**, L89
- Green, S., Schor, H., Siegbahn, P., & Thaddeus, P. 1976, *CP*, **17**, 479
- Grim, R. J. A., Baas, F., Geballe, T. R., Greenberg, J. M., & Schutte, W. A. 1991, *A&A*, **243**, 473
- Gudeman, C. S., Haese, N. N., Piltch, N. D., & Woods, R. C. 1981, *ApJL*, **246**, L47
- Gudeman, C. S., & Woods, R. C. 1982, *PhRvL*, **48**, 1344

- Guélin, M., & Cernicharo, J. 1991, *A&A*, **244**, L21
- Guélin, M., Cernicharo, J., Kahane, C., & Gomez-Gonzales, J. 1986, *A&A*, **157**, L17
- Guélin, M., Cernicharo, J., Paubert, G., & Turner, B. E. 1990, *A&A*, **230**, L9
- Guélin, M., Green, S., & Thaddeus, P. 1978, *ApJL*, **224**, L27
- Guélin, M., Muller, S., Cernicharo, J., et al. 2000, *A&A*, **363**, L9
- Guélin, M., Muller, S., Cernicharo, J., McCarthy, M. C., & Thaddeus, P. 2004, *A&A*, **426**, L49
- Guélin, M., Neininger, N., & Cernicharo, J. 1998, *A&A*, **335**, L1
- Guélin, M., & Thaddeus, P. 1977, *ApJL*, **212**, L81
- Guélin, M., Cernicharo, J., Travers, M. J., et al. 1997, *A&A*, **317**, L1
- Guillemin, J. C., Wlodarczak, G., López, J. C., & Demaison, J. 1990, *JMoSp*, **140**, 190
- Guilloteau, S., Di Folco, E., Dutrey, A., et al. 2013, *A&A*, **549**, A92
- Guilloteau, S., Dutrey, A., Wakelam, V., et al. 2012, *A&A*, **548**, A70
- Guilloteau, S., Piétu, V., Dutrey, A., & Guélin, M. 2006, *A&A*, **448**, L5
- Guilmo, J. M., Godefroid, M., & Herman, M. 1993a, *JMoSp*, **160**, 387
- Guilmo, J. M., Melen, F., & Herman, M. 1993b, *JMoSp*, **160**, 401
- Gunther-Mohr, G. R., White, R. L., Schawlow, A. L., Good, W. E., & Coles, D. K. 1954, *PhRv*, **94**, 1184
- Gupta, H., Brünken, S., Tamassia, F., et al. 2007, *ApJL*, **655**, L57
- Gupta, H., Drouin, B. J., & Pearson, J. C. 2012, *ApJL*, **751**, L38
- Gupta, H., Gottlieb, C. A., Lattanzi, V., Pearson, J. C., & McCarthy, M. C. 2013, *ApJL*, **778**, L1
- Güsten, R., Wiesemeyer, H., Neufeld, D., et al. 2019, *Natur*, **568**, 357
- Guzmán, V. V., Öberg, K. I., Loomis, R., & Qi, C. 2015, *ApJ*, **814**, 53
- Haas, S., Winnewisser, G., Yamada, K. M. T., Matsumura, K., & Kawaguchi, K. 1994, *JMoSp*, **167**, 176
- Habara, H., & Yamamoto, S. 2000, *JChPh*, **112**, 10905
- Habara, H., Yamamoto, S., & Amano, T. 2002, *JChPh*, **116**, 9232
- Halfen, D. T., Clouthier, D. J., & Ziurys, L. M. 2008, *ApJL*, **677**, L101
- Halfen, D. T., Ilyushin, V. V., & Ziurys, L. M. 2015, *ApJ*, **812**, 1
- Halfen, D. T., Ziurys, L. M., Brünken, S., et al. 2009, *ApJL*, **702**, L124
- Halter, R. J., Fimmen, R. L., McMahon, R. J., et al. 2001, *JChS*, **123**, 12353
- Hawker, G. A., Madhusudhan, N., Cabot, S. H. C., & Gandhi, S. 2018, *ApJL*, **863**, L11
- Hayashi, M., & Kuwada, K. 1975, *JMoSt*, **28**, 147
- Haynes, K., Mandell, A. M., Madhusudhan, N., Deming, D., & Knutson, H. 2015, *ApJ*, **806**, 146
- Heath, G. A., Thomas, L. F., Sherrard, E. I., & Sheridan, J. 1955, *Discuss. Faraday Soc.*, **19**, 38
- Heikkilä, A., Johansson, L. E. B., & Olofsson, H. 1999, *A&A*, **344**, 817
- Heise, H. M., Lutz, H., & Dreizler, H. 1974, *ZNatA*, **29**, 1345
- Helminger, P., Bowman, W. C., & De Lucia, F. C. 1981, *JMoSp*, **85**, 120
- Henkel, C., & Bally, J. 1985, *A&A*, **150**, L25
- Henkel, C., Jacq, T., Mauersberger, R., Menten, K. M., & Steppe, H. 1987, *A&A*, **188**, L1
- Henkel, C., Mauersberger, R., & Schilke, P. 1988, *A&A*, **201**, L23
- Henning, T., Semenov, D., Guilloteau, S., et al. 2010, *ApJ*, **714**, 1511
- Herbst, E., & van Dishoeck, E. F. 2009, *ARA&A*, **47**, 427
- Hily-Blant, P., Magalhaes, V., Kastner, J., et al. 2017, *A&A*, **603**, L6
- Hincelin, U., Wakelam, V., Hersant, F., et al. 2011, *A&A*, **530**, A61
- Hinkle, K. W., Keady, J. J., & Bernath, P. F. 1988, *Sci*, **241**, 1319
- Hirahara, Y., Ohshima, Y., & Endo, Y. 1993, *ApJL*, **408**, L113
- Hirose, C. 1974, *ApJL*, **189**, L145
- Hocking, W. H. 1976, *ZNatA*, **31**, 1113
- Hocking, W. H., & Winnewisser, G. 1976, *ZNatA*, **31**, 995
- Hoefl, J. 1965, *ZNatA*, **A20**, 1327
- Hogerheijde, M. R., Bergin, E. A., Brinch, C., et al. 2011, *Sci*, **334**, 338
- Hollis, J. M., Churchwell, E. B., Herbst, E., & de Lucia, F. C. 1986, *Natur*, **322**, 524
- Hollis, J. M., Jewell, P. R., & Lovas, F. J. 1989, *ApJ*, **346**, 794
- Hollis, J. M., Jewell, P. R., & Lovas, F. J. 1995, *ApJ*, **438**, 259
- Hollis, J. M., Snyder, P. R., Lovas, F. J., & Remijan, A. 2004a, *ApJL*, **613**, L45
- Hollis, J. M., Jewell, P. R., Lovas, F. J., Remijan, A., & Møllendal, H. 2004b, *ApJL*, **610**, L21
- Hollis, J. M., Lovas, F. J., & Jewell, P. R. 2000, *ApJL*, **540**, L107
- Hollis, J. M., Lovas, F. J., Jewell, P. R., & Coudert, L. H. 2002, *ApJL*, **571**, L59
- Hollis, J. M., Lovas, F. J., Remijan, A. J., et al. 2006a, *ApJL*, **643**, L25
- Hollis, J. M., Remijan, A. J., Jewell, P. R., & Lovas, F. J. 2006b, *ApJ*, **642**, 933
- Hollis, J. M., Snyder, L. E., Blake, D. H., et al. 1981, *ApJ*, **251**, 541
- Hollis, J. M., Snyder, L. E., Ziurys, L. M., & McGonagle, D. 1991, ASP Conf. Ser. 16, *Atoms, Ions and Molecules: New Results in Spectral Line Astrophysics* (San Francisco, CA: ASP), 407
- Hovde, D. C., & Saykally, R. J. 1987, *JChPh*, **87**, 4332
- Huang, J., & Öberg, K. I. 2015, *ApJ*, **809**, L26
- Huang, X., Fortenberry, R. C., & Lee, T. J. 2013, *ApJL*, **768**, L25
- Humphreys, R. M., Ziurys, L. M., Bernal, J. J., et al. 2019, *ApJL*, **874**, L26
- Iida, M., Ohshima, Y., & Endo, Y. 1991, *ApJL*, **371**, L45
- Ikuta, S. 1997, *JChPh*, **106**, 4536
- Ilyushin, V. V., Alekseev, E. A., Dyubko, S. F., Kleiner, I., & Hougen, J. T. 2004, *JMoSp*, **227**, 115
- Ilyushin, V. V., Alekseev, E. A., Dyubko, S. F., Motiyenko, R. A., & Lovas, F. J. 2005, *JMoSp*, **231**, 15
- Irvine, W. M., & Pollack, J. B. 1968, *Icar*, **8**, 324
- Irvine, W. M., Brown, R. D., Cragg, D. M., et al. 1988a, *ApJL*, **335**, L89
- Irvine, W. M., Friberg, P., Hjalmarsen, Å., et al. 1988b, *ApJL*, **334**, L107
- Jabs, W., Winnewisser, M., Belov, S., Klaus, T., & Winnewisser, G. 1997, *CP*, **225**, 77
- Jager, W., Krause, H., Mäder, H., & Gerry, M. 1990, *JMoSp*, **143**, 50
- Jefferts, K. B., Penzias, A. A., & Wilson, R. W. 1970, *ApJL*, **161**, L87
- Jefferts, K. B., Penzias, A. A., Wilson, R. W., & Solomon, P. M. 1971, *ApJL*, **168**, L111
- Jenkins, F. A., & Wooldridge, D. E. 1938, *PhRv*, **53**, 137
- Jevons, W. 1932, Report on Band-spectra of Diatomic Molecules (London: Physical Society)
- Johansson, L. E. B. 1991, IAU Symp. 146, *Dynamics of Galaxies and Their Molecular Cloud Distributions*, ed. F. Combes & F. Casoli, (Dordrecht: Kluwer), 1
- Johns, J. W. C., Stone, J. M. R., & Winnewisser, G. 1972, *JMoSp*, **42**, 523
- Johnson, D. R., & Lovas, F. J. 1972, *CPL*, **15**, 65
- Johnson, D. R., Lovas, F. J., Gottlieb, C. A., et al. 1977, *ApJ*, **218**, 370
- Johnson, D. R., & Powell, F. X. 1970, *Sci*, **169**, 679
- Johnson, D. R., Suenram, R. D., & Lafferty, W. J. 1976, *ApJ*, **208**, 245
- Johnson, H. R., & Strandberg, M. W. P. 1952, *JChPh*, **20**, 687
- Jones, H., & Sheridan, J. 1982, *JMoSt*, **78**, 303
- Jones, P. A., Cunningham, M. R., Godfrey, P. D., & Cragg, D. M. 2007, *MNRAS*, **374**, 579
- Kaifu, N., Morimoto, M., Nagane, K., et al. 1974, *ApJL*, **191**, L135
- Kaifu, N., Suzuki, H., Ohishi, M., et al. 1987, *ApJL*, **317**, L111
- Kaifu, N., Ohishi, M., Kawaguchi, K., et al. 2004, *PASJ*, **56**, 69
- Kamiński, T., Gottlieb, C. A., Menten, K. M., et al. 2013, *A&A*, **551**, A113
- Kania, P., Hermanns, M., Brünken, S., Müller, H. S. P., & Giesen, T. F. 2011, *JMoSp*, **268**, 173
- Kasai, P. H., & Myers, R. J. 1959, *JChPh*, **30**, 1096
- Kasai, Y., Obi, K., Ohshima, Y., et al. 1993, *ApJL*, **410**, L45
- Kasai, Y., Sumiyoshi, Y., Endo, Y., & Kawaguchi, K. 1997, *ApJL*, **477**, L65
- Kasten, W., & Dreizler, H. 1986, *ZNatA*, **41**, 1173
- Kastner, J. H., Zuckerman, B., Weintraub, D. A., & Forveille, T. 1997, *Sci*, **277**, 67
- Kattija-Ari, M., & Harmony, M. D. 1980, *IJCQ*, **18**, 443
- Kaushik, V. K. 1977, *CPL*, **49**, 89
- Kawaguchi, K., Kagi, E., Hirano, T., Takano, S., & Saito, S. 1993, *ApJL*, **406**, L39
- Kawaguchi, K., Kasai, Y., & Ishikawa, S. I. 1995, *PASJ*, **47**, 853
- Kawaguchi, K., Kasai, Y., Ishikawa, S.-I., et al. 1994, *ApJL*, **420**, L95
- Kawaguchi, K., Ohishi, M., Ishikawa, S.-I., & Kaifu, N. 1992a, *ApJL*, **386**, L51
- Kawaguchi, K., Saito, S., & Hirota, E. 1983, *JChPh*, **79**, 629
- Kawaguchi, K., Saito, S., & Hirota, E. 1985, *MolPh*, **55**, 341
- Kawaguchi, K., Takano, S., Ohishi, M., et al. 1992b, *ApJL*, **396**, L49
- Keane, J. V., Tielens, A. G. G. M., Boogert, A. C. A., Schutte, W. A., & Whittet, D. C. B. 2001, *A&A*, **376**, 254
- Kern, B., Strelnikov, D., Weis, P., Böttcher, A., & Kappes, M. M. 2013, *JPCA*, **117**, 8251
- Kessler, M., Ring, H., Trambarulo, R., & Gordy, W. 1950, *PhRv*, **79**, 54
- Kewley, R., Sastry, K. V. L. N., & Winnewisser, M. 1963, *JMoSp*, **10**, 418
- Kilb, R. W. 1955, *JChPh*, **23**, 1736
- Kilb, R. W., Lin, C. C., & Wilson Jr., E. B. 1957, *JChPh*, **26**, 1695
- Killian, T. C., Gottlieb, C. A., Gottlieb, E. W., Vrtilek, J. M., & Thaddeus, P. 1990, *ApJL*, **365**, L89
- Kim, E., Habara, H., & Yamamoto, S. 2002, *JMoSp*, **212**, 83
- King, W. C., & Gordy, W. 1954, *PhRv*, **93**, 407
- Kirby, C., Kroto, H. W., & Walton, D. R. M. 1980, *JMoSp*, **83**, 261
- Kirchhoff, W. H. 1972, *JMoSp*, **41**, 333
- Kisiel, Z., Dorosh, O., Maeda, A., et al. 2010, *PCCP*, **12**, 8329
- Klaus, T., Takano, S., & Winnewisser, G. 1997, *A&A*, **322**, L1
- Klemperer, W. 1970, *Natur*, **227**, 1230
- Klisch, E., Klaus, T., Belov, S. P., et al. 1996, *ApJ*, **473**, 1118

- Knauth, D. C., Andersson, B. G., McCandliss, S. R., & Moos, H. W. 2004, *Natur*, **429**, 636
- Knez, C., Lacy, J. H., Evans, N. J., van Dishoeck, E. F., & Richter, M. J. 2009, *ApJ*, **696**, 471
- Kolesniková, L., Daly, A. M., Alonso, J. L., Tercero, B., & Cernicharo, J. 2013, *JMoSp*, **289**, 13
- Kolesniková, L., Tercero, B., Cernicharo, J., et al. 2014, *ApJL*, **784**, L7
- Kreidberg, L., Bean, J. L., Désert, J.-M., et al. 2014, *ApJL*, **793**, L27
- Kreidberg, L., Line, M. R., Bean, J. L., et al. 2015, *ApJ*, **814**, 66
- Kretschmer, U., Consalvo, D., Knaack, A., et al. 1996, *MolPh*, **87**, 1159
- Kroto, H. W., Kirby, C., Walton, D. R. M., et al. 1977, *BAAS*, **9**, 303
- Kroto, H. W., Kirby, C., Walton, D. R. M., et al. 1978, *ApJL*, **219**, L133
- Kroto, H. W., McNaughton, D., & Osman, O. I. 1984, *ChCom*, 993
- Krueger, M., Dreizler, H., Preugschat, D., & Lentz, D. 2010, *ChemInform*, **23**, 1644
- Kuan, Y.-J., Charnley, S. B., Huang, H.-C., Tseng, W.-L., & Kisiel, Z. 2003, *ApJ*, **593**, 848
- Kuiper, T. B. H., Kuiper, E. N. R., Dickinson, D. F., Turner, B. E., & Zuckerman, B. 1984, *ApJ*, **276**, 211
- Kuiper, T. B. H., Zuckerman, B., Kakar, R. K., & Kuiper, E. N. R. 1975, *ApJL*, **200**, L151
- Kukulich, S. G. 1965, *PhRv*, **138**, A1322
- Kukulich, S. G. 1967, *PhRv*, **156**, 83
- Kukulich, S. G. 1972, *JChPh*, **57**, 869
- Kwok, S., & Zhang, Y. 2013, *ApJ*, **771**, 5
- Lacy, J. H., Carr, J. S., Evans, N. J. I., et al. 1991, *ApJ*, **376**, 556
- Lacy, J. H., Carr, J. S., J. N., et al. 1991, *ApJ*, **376**, 556
- Lacy, J. H., Faraji, H., Sandford, S. A., & Allamandola, L. J. 1998, *ApJL*, **501**, L105
- Lahuis, F., van Dishoeck, E. F., Boogert, A. C. A., et al. 2006, *ApJL*, **636**, L145
- Lambeau, C., Fayt, A., Duncan, J. L., & Nakagawa, T. 1980, *JMoSp*, **81**, 227
- Landsberg, B. M., & Suenram, R. D. 1983, *JMoSp*, **98**, 210
- Langer, W. D., Velusamy, T., Kuiper, T. B. H., et al. 1997, *ApJL*, **480**, L63
- Lanotte, A. A., Gillon, M., Demory, B. O., et al. 2014, *A&A*, **572**, A73
- Larsson, B., Liseau, R., Pagani, L., et al. 2007, *A&A*, **466**, 999
- Latter, W. B., Walker, C. K., & Maloney, P. R. 1993, *ApJL*, **419**, L97
- Laurie, V. W. 1956, *JChPh*, **24**, 635
- Laurie, V. W. 1959, *JChPh*, **31**, 1500
- Le Gal, R., Öberg, K. I., Loomis, R. A., Pegues, J., & Bergner, J. B. 2019, *ApJ*, **876**, 72
- Lee, J.-Y., Marti, K., Severinghaus, J. P., et al. 2006, *GeCoA*, **70**, 4507
- Lee, K. L. K., & McCarthy, M. 2019, *J. Phys. Chem. Lett.*, **10**, 2408
- Lee, K. L. K., Loomis, R. A., Burkhardt, A. M., et al. 2021a, *ApJL*, **908**, L11
- Lee, K. L. K., Changala, P. B., Loomis, R. A., et al. 2021b, *ApJL*, **910**, L2
- Lee, S. 1997, *CPL*, **268**, 69
- Lee, S. K., & Amano, T. 1987, *ApJL*, **323**, L145
- Lees, R. M., & Mohammadi, M. A. 1980, *CajPh*, **58**, 1640
- Li, Y. S., Jalilian, M. R., & Durig, J. R. 1979, *JMoSt*, **51**, 171
- Lide, D. R. 1962, *JMoSp*, **8**, 142
- Lin, C. C., & Swalen, J. D. 1959, *RvMP*, **31**, 841
- Lindenmayer, J., Magg, U., & Jones, H. 1988, *JMoSp*, **128**, 172
- Linke, R. A., Frerking, M. A., & Thaddeus, P. 1979, *ApJL*, **234**, L139
- Linnartz, H., Ioppolo, S., & Fedoseev, G. 2015, *IRPC*, **34**, 205
- Lis, D. C., Pearson, J. C., Neufeld, D. A., et al. 2010, *A&A*, **521**, L9
- Liszt, H. S. 1978, *ApJ*, **219**, 454
- Liszt, H. S., & Turner, B. E. 1978, *ApJL*, **224**, L73
- Liszt, H. S., & Ziurys, L. M. 2012, *ApJ*, **747**, 55
- Little, L. T., Macdonald, G. H., Riley, P. W., & Matheson, D. N. 1978, *MNRAS*, **183**, 45P
- Liu, D.-J., & Oka, T. 1985, *PhRvL*, **54**, 1787
- Lockwood, A. C., Johnson, J. A., Bender, C. F., et al. 2014, *ApJL*, **783**, L29
- Lofthud, A., & Krupenie, P. H. 1977, *JPCRD*, **6**, 113
- Loomis, R. A., Öberg, K. I., Andrews, S. M., et al. 2018, *AJ*, **155**, 182
- Loomis, R. A., Zaleski, D. P., Steber, A. L., et al. 2013, *ApJL*, **765**, L9
- Loomis, R. A., Shingledecker, C. N., Langston, G., et al. 2016, *MNRAS*, **463**, A175
- Loomis, R. A., Öberg, K. I., Andrews, S. M., et al. 2020, *ApJ*, **893**, 101
- Loomis, R. A., Burkhardt, A. M., Shingledecker, C. N., et al. 2021, *NatAs*, **5**, 188
- Loren, R. B., Mundy, L. G., & Wootten, A. 1984, *ApJL*, **286**, L23
- Lovas, F. J. 1978, *JPCRD*, **7**, 1445
- Lovas, F. J., Hollis, J. M., Remijan, A. J., & Jewell, P. R. 2006a, *ApJL*, **645**, L137
- Lovas, F. J., Kawashima, Y., Grabow, J. U., et al. 1995, *ApJL*, **455**, L201
- Lovas, F. J., Remijan, A. J., Hollis, J. M., Jewell, P. R., & Snyder, L. E. 2006b, *ApJL*, **637**, L37
- Lovas, F. J., Suenram, R. D., & Evenson, K. M. 1983, *ApJL*, **267**, L131
- Lovas, F. J., & Tiemann, E. 1974, *JPCRD*, **3**, 609
- MacLeod, J. M., Avery, L. W., & Broten, N. W. 1984, *ApJL*, **282**, L89
- Mäder, H., Heise, H. M., & Dreizler, H. 1974, *ZNatA*, **29**, 164
- Madhusudhan, N., Agúndez, M., Moses, J. I., & Hu, Y. 2016, *SSRv*, **205**, 285
- Madhusudhan, N., Harrington, J., Stevenson, K. B., et al. 2011, *Natur*, **469**, 64
- Maeda, A., Habara, H., & Amano, T. 2007, *MolPh*, **105**, 477
- Magain, P., & Gillet, D. 1987, *A&A*, **184**, L5
- Mandell, A. M., Mumma, M. J., Blake, G. A., et al. 2008, *ApJL*, **681**, L25
- Mangum, J. G., & Shirley, Y. L. 2015, *PASP*, **127**, 266
- Mantz, A. W., Maillard, J. P., Roh, W. B., & Narahari Rao, K. 1975, *JMoSp*, **57**, 155
- Marcelino, N., Agúndez, M., Cernicharo, J., Roueff, E., & Tafalla, M. 2018, *A&A*, **612**, L10
- Marcelino, N., Agúndez, M., Tercero, B., et al. 2020, *A&A*, **643**, L6
- Marcelino, N., Cernicharo, J., Agúndez, M., et al. 2007, *ApJL*, **665**, L127
- Marcelino, N., Cernicharo, J., Tercero, B., & Roueff, E. 2009, *ApJL*, **690**, L27
- Margulès, L., McGuire, B. A., Senent, M. L., et al. 2017, *A&A*, **601**, A50
- Marstokk, K. M., & Møllendal, H. 1973, *JMoSt*, **16**, 259
- Martin, D. W., McDaniel, E. W., & Meeks, M. L. 1961, *ApJ*, **134**, 1012
- Martin, M. C., Koller, D., & Mihaly, L. 1993, *PhRvB*, **47**, 14607
- Martin, R. N., & Ho, P. T. P. 1979, *A&A*, **74**, L7
- Martín, S., Mauersberger, R., Martín-Pintado, J., García-Burillo, S., & Henkel, C. 2003, *A&A*, **411**, L465
- Martín, S., Mauersberger, R., Martín-Pintado, J., Henkel, C., & García-Burillo, S. 2006, *ApJS*, **164**, 450
- Matsuura, M., Zijlstra, A. A., van Loon, J. T., et al. 2002, *ApJL*, **580**, L133
- Mathews, H. E., Irvine, W. M., Friberg, P., Brown, R. D., & Godfrey, P. D. 1984, *Natur*, **310**, 125
- Mathews, H. E., & Sears, T. J. 1983, *ApJ*, **272**, 149
- Mauersberger, R., & Henkel, C. 1991, *A&A*, **245**, 457
- Mauersberger, R., Henkel, C., & Chin, Y. N. 1995, *A&A*, **294**, 23
- Mauersberger, R., Henkel, C., & Sage, L. J. 1990, *A&A*, **236**, 63
- Mauersberger, R., Henkel, C., Walmsley, C. M., Sage, L. J., & Wiklind, T. 1991, *A&A*, **247**, 307
- McCall, B. J., & Griffin, R. E. 2013, *RSPSA*, **469**, 20120604
- McCarthy, M. C. 1997, *Sci*, **275**, 518
- McCarthy, M. C., Apponi, A. J., & Thaddeus, P. 1999, *JChPh*, **110**, 10645
- McCarthy, M. C., Baraban, J. H., Changala, P. B., et al. 2015, *J. Phys. Chem. Lett.*, **6**, 2107
- McCarthy, M. C., Cooksy, A. L., Mohamed, S., Gordon, V. D., & Thaddeus, P. 2003, *ApJS*, **144**, 287
- McCarthy, M. C., Gottlieb, C. A., Gupta, H., & Thaddeus, P. 2006, *ApJL*, **652**, L141
- McCarthy, M. C., Lee, K. L. K., Carroll, P. B., et al. 2020, *JPCA*, **124**, 5170
- McCarthy, M. C., Levine, E. S., Apponi, A. J., & Thaddeus, P. 2000, *JMoSp*, **203**, 75
- McCarthy, M. C., Travers, M. J., Kovacs, A., Gottlieb, C. A., & Thaddeus, P. 1996, *A&A*, **309**, L31
- McCarthy, M. C., Lee, K. L. K., Loomis, R. A., et al. 2021, *NatAs*, **5**, 176
- McGuire, B. A. 2018, *ApJS*, **239**, 17
- McGuire, B. A. 2021, astromol, Zenodo, doi:10.5281/zenodo.5046939
- McGuire, B. A., Burkhardt, A. M., Kalenskii, S. V., et al. 2018, *Sci*, **359**, 202
- McGuire, B. A., Burkhardt, A. M., Shingledecker, C. N., et al. 2017a, *ApJL*, **843**, L28
- McGuire, B. A., Carroll, P. B., Loomis, R. A., et al. 2013a, *ApJ*, **774**, 56
- McGuire, B. A., Carroll, P. B., Loomis, R. A., et al. 2016, *Sci*, **352**, 1449
- McGuire, B. A., Carroll, P. B., & Remijan, A. J. 2013b, arXiv:1306.0927
- McGuire, B. A., Loomis, R. A., Charness, C. M., et al. 2012, *ApJL*, **758**, L33
- McGuire, B. A., Carroll, P. B., Gratier, P., et al. 2014, *ApJ*, **783**, 36
- McGuire, B. A., Shingledecker, C. N., Willis, E. R., et al. 2017b, *ApJL*, **851**, L46
- McGuire, B. A., Burkhardt, A. M., Loomis, R. A., et al. 2020, *ApJL*, **900**, L10
- McGuire, B. A., Loomis, R. A., Burkhardt, A. M., et al. 2021, *Sci*, **371**, 1265
- McKellar, A. 1940, *PASP*, **52**, 187
- McNaughton, D., Jahn, M. K., Travers, M. J., et al. 2018, *MNRAS*, **476**, 5268
- McNaughton, D., Osman, O. I., & Kroto, H. W. 1988a, *JMoSt*, **190**, 195
- McNaughton, D., Robertson, E. G., & Hatherley, L. D. 1996, *JMoSp*, **175**, 377
- McNaughton, D., Romeril, N. G., Lappert, M. F., & Kroto, H. W. 1988b, *JMoSp*, **132**, 407
- Medvedev, I. R., De Lucia, F. C., & Herbst, E. 2009, *ApJS*, **181**, 433
- Meerts, W. L., & Ozier, I. 1982, *JMoSp*, **94**, 38
- Mehring, D. M., Snyder, L. E., Míao, Y., & Lovas, F. J. 1997, *ApJL*, **480**, L71

- Menten, K. M., Wyrowski, F., Belloche, A., et al. 2011, *A&A*, **525**, A77
- Meyer, D. M., & Roth, K. C. 1991, *ApJL*, **376**, L49
- Michalopoulos, D. L., Geusic, M. E., Langridge Smith, P. R. R., & Smalley, R. E. 1984, *JChPh*, **80**, 3556
- Millen, D. J., Topping, G., & Lide, D. R. 1962, *JMoSp*, **8**, 153
- Mockler, R. C., & Bird, G. R. 1955, *PhRv*, **98**, 1837
- Mohamed, S., McCarthy, M. C., Cooksy, A. L., Hinton, C., & Thaddeus, P. 2005, *JChPh*, **123**, 234301
- Moises, A., Boucher, D., Burie, J., Demaison, J., & Dubrulle, A. 1982, *JMoSp*, **92**, 497
- Momose, T., Endo, Y., Hirota, E., & Shida, T. 1988, *JChPh*, **88**, 5338
- Monje, R. R., Lis, D. C., Roueff, E., et al. 2013, *ApJ*, **767**, 81
- Monje, R. R., Phillips, T. G., Peng, R., et al. 2011, *ApJL*, **742**, L21
- Morino, I., & Kawaguchi, K. 1995, *JMoSp*, **170**, 172
- Morino, I., Yamada, K. M. T., Klein, H., et al. 2000, *JMoSt*, **517**, 367
- Morris, M., Gilmore, W., Palmer, P., Turner, B. E., & Zuckerman, B. 1975, *ApJL*, **199**, L47
- Motiyenko, R., Margules, L., Despois, D., & Guillemin, J.-C. 2018, *PCCP*, **20**, 5509
- Müller, H. S. P. 2013, *JQSRT*, **130**, 335
- Müller, H. S. P., Coutens, A., Walters, A., Grabow, J.-U., & Schlemmer, S. 2011, *JMoSp*, **267**, 100
- Müller, H. S. P., Müller, S., Schilke, P., et al. 2015, *A&A*, **582**, L4
- Müller, H. S. P., Belloche, A., Xu, L.-H., et al. 2016, *A&A*, **587**, A92
- Muller, S., Kawaguchi, K., Black, J. H., & Amano, T. 2016, *A&A*, **589**, L5
- Muller, S., Beelen, A., Guélin, M., et al. 2011, *A&A*, **535**, A103
- Muller, S., Beelen, A., Black, J. H., et al. 2013, *A&A*, **551**, A109
- Muller, S., Combes, F., Guélin, M., et al. 2014, *A&A*, **566**, A112
- Muller, S., Black, J. H., Guélin, M., et al. 2014, *A&A*, **566**, L6
- Muller, S., Müller, H. S. P., Black, J. H., et al. 2017, *A&A*, **606**, A109
- Murakami, A., Kawaguchi, K., & Saito, S. 1987, *PASJ*, **39**, 189
- Mürtz, P., Zink, L. R., Evenson, K. M., & Brown, J. M. 1998, *JChPh*, **109**, 9744
- Namiki, K.-i., Saito, S., Robinson, J. S., & Steimle, T. C. 1998, *JMoSp*, **191**, 176
- Neill, J. L., Muckle, M. T., Zaleski, D. P., et al. 2012, *ApJ*, **755**, 153
- Neill, J. L., Bergin, E. A., Lis, D. C., et al. 2014, *ApJ*, **789**, 8
- Nemes, L., Ram, R. S., Bernath, P. F., et al. 1994, *CPL*, **218**, 295
- Neufeld, D. A., Zmuidzinas, J., Schilke, P., & Phillips, T. G. 1997, *ApJL*, **488**, L141
- Neufeld, D. A., Schilke, P., Menten, K. M., et al. 2006, *A&A*, **454**, L37
- Neufeld, D. A., Falgarone, E., Gerin, M., et al. 2012, *A&A*, **542**, L6
- Nguyen-Q-Rieu, Henkel, C., Jackson, J. M., & Mauersberger, R. 1991, *A&A*, **241**, L33
- Nolt, I. G., Radostitz, J. V., Dilonardo, G., et al. 1987, *JMoSp*, **125**, 274
- Nugroho, S. K., Kawahara, H., Masuda, K., et al. 2017, *AJ*, **154**, 221
- Nugroho, S. K., Kawahara, H., Gibson, N. P., et al. 2021, *ApJL*, **910**, L9
- Öberg, K. I., Guzmán, V. V., Furuya, K., et al. 2015, *Natur*, **520**, 198
- Öberg, K. I., Guzmán, V. V., Furuya, K., et al. 2015, *Natur*, **520**, 198
- Öberg, K. I., Murray-Clay, R., & Bergin, E. A. 2011, *ApJL*, **743**, L16
- Ohashi, N., Kawabe, R., Hayashi, M., & Ishiguro, M. 1991, *AJ*, **102**, 2054
- Ohishi, M., Ishikawa, S.-I., Amano, T., et al. 1996, *ApJL*, **471**, L61
- Ohishi, M., McGonagle, D., Irvine, W. M., Yamamoto, S., & Saito, S. 1994, *ApJL*, **427**, L51
- Ohishi, M., Yamamoto, S., Saito, S., et al. 1988, *ApJ*, **329**, 511
- Ohishi, M., Kaifu, N., Kawaguchi, K., et al. 1989, *ApJL*, **345**, L83
- Ohishi, M., Suzuki, H., Ishikawa, S.-I., et al. 1991, *ApJL*, **380**, L39
- Ohshima, Y., & Endo, Y. 1993, *JMoSp*, **159**, 458
- Oka, T. 1980, *PhRvL*, **45**, 531
- Ossenkopf, V., Müller, H. S. P., Müller, H., et al. 2010, *A&A*, **518**, L111
- Pagani, L., Olofsson, A. O. H., Bergman, P., et al. 2003, *A&A*, **402**, L77
- Palumbo, M. E., Geballe, T. R., & Tielens, A. G. G. M. 1997, *ApJ*, **479**, 839
- Palumbo, M. E., Tielens, A. G. G. M., & Tokunaga, A. T. 1995, *ApJ*, **449**, 674
- Parise, B., Bergman, P., & Du, F. 2012, *A&A*, **541**, L11
- Paso, R., Kauppinen, J., & Anttila, R. 1980, *JMoSp*, **79**, 236
- Pauzat, F., Ellinger, Y., & McLean, A. D. 1991, *ApJL*, **369**, L13
- Pearson, J. C., Gottlieb, C. A., Woodward, D. R., & Thaddeus, P. 1988, *A&A*, **189**, L13
- Pearson, J. C., Sastry, K. V. L. N., Herbst, E., & De Lucia, F. C. 1997, *ApJ*, **480**, 420
- Pearson, J. C., Sastry, K. V. L. N., Herbst, E., & Delucia, F. C. 1994, *JMoSp*, **166**, 120
- Peña, I., Sanz, M. E., López, J. C., & Alonso, J. L. 2012, *JChS*, **134**, 2305
- Penzias, A. A., Solomon, P. M., Wilson, R. W., & Jefferts, K. B. 1971, *ApJL*, **168**, L53
- Perry, A. J., Hodges, J. N., Markus, C. R., Kocheril, G. S., & McCall, B. J. 2014, *JChPh*, **141**, 101101
- Petkie, D. T., Goyette, T. M., Holton, J. J., Delucia, F. C., & Helminger, P. 1995, *JMoSp*, **171**, 145
- Petuchowski, S. J., & Bennett, C. L. 1992, *ApJ*, **391**, 137
- Pety, J., Gratier, P., Guzmán, V., et al. 2012, *A&A*, **548**, A68
- Phillips, J. G. 1948, *ApJ*, **107**, 389
- Phuong, N. T., Chapillon, E., Majumdar, L., et al. 2018, *A&A*, **616**, L5
- Plummer, G. M., Anderson, T., Herbst, E., & De Lucia, F. C. 1986, *JChPh*, **84**, 2427
- Plummer, G. M., Herbst, E., & De Lucia, F. C. 1985, *JChPh*, **83**, 1428
- Prieto, G., & Rigutti, M. 1965, *NCims*, **39**, 519
- Priem, D., Cosléou, J., Demaison, J., et al. 1998, *JMoSp*, **191**, 183
- Pulliam, R. L., Savage, C., Agúndez, M., et al. 2010, *ApJL*, **725**, L181
- Qi, C., Kessler, J. E., Koerner, D. W., Sargent, A. I., & Blake, G. A. 2003, *ApJ*, **597**, 986
- Qi, C., Öberg, K. I., Wilner, D. J., & Rosenfeld, K. A. 2013, *ApJL*, **765**, L14
- Qi, C., Wilner, D. J., Aikawa, Y., Blake, G. A., & Hogerheijde, M. R. 2008, *ApJ*, **681**, 1396
- Qiu, J., Wang, J., Shi, Y., et al. 2018, *A&A*, **613**, A3
- Rangwala, N., Maloney, P. R., Glenn, J., et al. 2011, *ApJ*, **743**, 94
- Ray, B. S. 1932, *ZPhy*, **78**, 74
- Raymonda, J. W. 1970, *JChPh*, **52**, 3458
- Reichle Jr., H. G., & Young, C. 1972, *CalPh*, **50**, 2662
- Remijan, A. J., Hollis, J. M., Lovas, F. J., et al. 2007, *ApJL*, **664**, L47
- Remijan, A. J., Hollis, J. M., Lovas, F. J., Plusquellic, D. F., & Jewell, P. R. 2005, *ApJ*, **632**, 333
- Remijan, A. J., Hollis, J. M., Lovas, F. J., et al. 2008a, *ApJL*, **675**, L85
- Remijan, A. J., Hollis, J. M., Snyder, L. E., Jewell, P. R., & Lovas, F. J. 2006, *ApJL*, **643**, L37
- Remijan, A. J., Leigh, D. P., Markwick-Kemper, A. J., & Turner, B. E. 2008b, *arXiv:0802.2273*
- Remijan, A. J., Snyder, L. E., McGuire, B. A., et al. 2014, *ApJ*, **783**, 77
- Requena-Torres, M. A., Martín-Pintado, J., Rodríguez-Franco, A., et al. 2006, *A&A*, **455**, 971
- Ribeiro, F. D. A., Almeida, G. C., Garcia-Basabe, Y., et al. 2015, *PCCP*, **17**, 27473
- Rickard, L. J., Palmer, P., Morris, M., Zuckerman, B., & Turner, B. E. 1975, *ApJL*, **199**, L75
- Rickard, L. J., Palmer, P., Turner, B. E., Morris, M., & Zuckerman, B. 1977, *ApJ*, **214**, 390
- Ridgway, S. T., Hall, D. N. B., Kleinmann, S. G., Weinberger, D. A., & Wojslaw, R. S. 1976, *Natur*, **264**, 345
- Ring, H., Edwards, H., Kessler, M., & Gordy, W. 1947, *PhRv*, **72**, 1262
- Rivilla, V. M., Beltrán, M. T., Cesaroni, R., et al. 2017, *A&A*, **598**, A59
- Rivilla, V. M., Martín-Pintado, J., Jimenez-Serra, I., et al. 2020, *ApJL*, **899**, L28
- Robinson, J. S., Apponi, A. J., & Ziurys, L. M. 1997, *CPL*, **278**, 1
- Rodler, M. 1985, *JMoSp*, **114**, 23
- Rodler, M., Brown, R. D., Godfrey, P. D., & Kleibömer, B. 1986, *JMoSp*, **118**, 267
- Rodler, M., Brown, R. D., Godfrey, P. D., & Tack, L. M. 1984, *CPL*, **110**, 447
- Rodríguez-Almeida, L. F., Jimenez-Serra, I., Rivilla, V. M., et al. 2021, *ApJL*, **912**, L11
- Rubin, R. H., Swenson, G. W. J., Benson, R. C., Tigelaar, H. L., & Flygare, W. H. 1971, *ApJL*, **169**, L39
- Rydbeck, O. E. H., Ellder, J., & Irvine, W. M. 1973, *Natur*, **246**, 466
- Sage, L. J., & Ziurys, L. M. 1995, *ApJ*, **447**, 625
- Saito, S. 1972, *ApJL*, **178**, L95
- Saito, S. 1977, *JMoSp*, **65**, 229
- Saito, S., & Amano, T. 1970, *JMoSp*, **34**, 383
- Saito, S., Endo, Y., & Hirota, E. 1983, *JChPh*, **78**, 6447
- Saito, S., Endo, Y., & Hirota, E. 1984, *JChPh*, **80**, 1427
- Saito, S., Kawaguchi, K., Yamamoto, S., et al. 1987, *ApJL*, **317**, L115
- Saito, S., & Takagi, K. 1973, *JMoSp*, **47**, 99
- Saito, S., Yamamoto, S., Irvine, W. M., et al. 1988, *ApJL*, **334**, L113
- Saito, S., Yamamoto, S., Kawaguchi, K., et al. 1989, *ApJ*, **341**, 1114
- Sakaizumi, T., Kikuchi, H., Ohashi, O., & Yamaguchi, I. 1987, *Bull. Chem. Soc. Japan*, **60**, 3903
- Salinas, V. N., Hogerheijde, M. R., Bergin, E. A., et al. 2016, *A&A*, **591**, A122
- Salyk, C., Pontoppidan, K. M., Blake, G. A., et al. 2008, *ApJL*, **676**, L49
- Sargent, A. I., & Beckwith, S. 1987, *ApJ*, **323**, 294
- Sastry, K. V. L. N., Helminger, P., Charo, A., Herbst, E., & de Lucia, F. C. 1981a, *ApJL*, **251**, L119
- Sastry, K. V. L. N., Helminger, P., Herbst, E., & de Lucia, F. C. 1981b, *ApJL*, **250**, L91

- Sastry, K. V. L. N., Helminger, P., Plummer, G. M., Herbst, E., & de Lucia, F. C. 1984, *ApJS*, **55**, 563
- Saykally, R. J., Dixon, T. A., Anderson, T. G., Szanto, P. G., & Woods, R. C. 1976, *ApJL*, **205**, L101
- Scharpen, L. H., & Laurie, V. W. 1965, *JChPh*, **43**, 2765
- Schilke, P., Benford, D. J., Hunter, T. R., Lis, D. C., & Phillips, T. G. 2001, *ApJS*, **132**, 281
- Schlawin, E., Greene, T. P., Line, M., Fortney, J. J., & Rieke, M. 2018, *AJ*, **156**, 40
- Schmidt, R. E., & Quade, C. R. 1975, *JChPh*, **62**, 3864
- Schutte, W. A., & Greenberg, J. M. 1997, *A&A*, **317**, L43
- Schutte, W. A., Boogert, A. C. A., Tielens, A. G. G. M., et al. 1999, *A&A*, **343**, 966
- Schwahn, G., Schieder, R., Bester, M., & Winnewisser, G. 1986, *JMoSp*, **116**, 263
- Scoville, N. Z., & Solomon, P. M. 1978, *ApJL*, **220**, L103
- Scurlock, C. T., Steimle, T. C., Suenram, R. D., & Lovas, F. J. 1994, *JChPh*, **100**, 3497
- Sequist, E. R., & Bell, M. B. 1986, *ApJL*, **303**, L67
- Sedaghati, E., Boffin, H. M. J., MacDonald, R. J., et al. 2017, *Natur*, **549**, 238
- Sewilo, M., Indebetouw, R., Charney, S. B., et al. 2018, *ApJL*, **853**, L19
- Shigenari, T. 1967, *JPSJ*, **23**, 404
- Shklovskii, I. S. 1953, *Doklady Akademii Nauk SSSR*, **92**, 25
- Sinclair, M. W., Fourikis, N., Ribes, J. C., et al. 1973, *AuPh*, **26**, 85
- Smith, R. L., Pontoppidan, K. M., Young, E. D., Morris, M. R., & van Dishoeck, E. F. 2009, *ApJ*, **701**, 163
- Snow, T. P., & McCall, B. J. 2006, *ARA&A*, **44**, 367
- Snyder, L., Lovas, F., Hollis, J., et al. 2005, *ApJ*, **619**, 914
- Snyder, L. E., & Buhl, D. 1971, *ApJL*, **163**, L47
- Snyder, L. E., & Buhl, D. 1972a, *NYASA*, **194**, 17
- Snyder, L. E., & Buhl, D. 1972b, *ApJ*, **177**, 619
- Snyder, L. E., Buhl, D., Schwartz, P. R., et al. 1974, *ApJL*, **191**, L79
- Snyder, L. E., Buhl, D., Zuckerman, B., & Palmer, P. 1969, *PhRvL*, **22**, 679
- Snyder, L. E., Hollis, J. M., Jewell, P. R., Lovas, F. J., & Remijan, A. 2006, *ApJ*, **647**, 412
- Snyder, L. E., Hollis, J. M., & Ulich, B. L. 1976, *ApJL*, **208**, L91
- Snyder, L. E., Hollis, J. M., Ulich, B. L., et al. 1975, *ApJL*, **198**, L81
- Snyder, L. E., Kuan, Y.-J., Ziurys, L. M., & Hollis, J. M. 1993, *ApJL*, **403**, L17
- Sobolev, G. A., Shcherbakov, A. M., & Akishin, P. A. 1961, *OptSp*, **12**, 78
- Soifer, B. T., Puetter, R. C., Russell, R. W., et al. 1979, *ApJL*, **232**, L53
- Solomon, P. M., Jefferts, K. B., Penzias, A. A., & Wilson, R. W. 1971, *ApJL*, **168**, L107
- Sousa-Silva, C., Yurchenko, S. N., & Tennyson, J. 2013, *JMoSp*, **288**, 28
- Souter, C. E., & Wood, J. L. 1970, *JChPh*, **52**, 674
- Souza, S. P., & Lutz, B. L. 1977, *ApJL*, **216**, L49
- Stark, A. A., & Wolff, R. S. 1979, *ApJ*, **229**, 118
- Stark, G., Huber, K. P., Yoshino, K., et al. 2000, *ApJ*, **531**, 321
- Steber, A. L., Harris, B. J., Neill, J. L., & Pate, B. H. 2012, *JMoSp*, **280**, 3
- Steenbeckelers, G. 1968, *Ann. Soc. Sic. Brux.*, **82**, 331
- Steimle, T. C., Fletcher, D. A., Jung, K. Y., & Scurlock, C. T. 1992, *JChPh*, **97**, 2909
- Steimle, T. C., Saito, S., & Takano, S. 1993, *ApJL*, **410**, L49
- Stevenson, K. B., Bean, J. L., Madhusudhan, N., & Harrington, J. 2014, *ApJ*, **791**, 36
- Stevenson, K. B., Harrington, J., Nymeyer, S., et al. 2010, *Natur*, **464**, 1161
- Strahan, S. E., Mueller, R. P., & Saykally, R. J. 1986, *JChPh*, **85**, 1252
- Stratmann, R. E., Scuseria, G. E., & Frisch, M. J. 1998, *JRSp*, **29**, 483
- Stull, V. R., Wyatt, P. J., & Plass, G. N. 1962, *JChPh*, **37**, 1442
- Suenram, R. D., Golubiatnikov, G. Y., Leonov, I. I., et al. 2001, *JMoSp*, **208**, 188
- Suenram, R. D., & Lovas, F. J. 1980, *JChS*, **102**, 7180
- Suenram, R. D., Lovas, F. J., & Matsumura, K. 1989, *ApJL*, **342**, L103
- Sugie, M., Takeo, H., & Matsumura, C. 1985, *JMoSp*, **111**, 83
- Sutton, E. C., Blake, G. A., Masson, C. R., & Phillips, T. G. 1985, *ApJS*, **58**, 341
- Suzuki, H., Ohishi, M., Kaifu, N., Ishikawa, S.-I., & Kasuga, T. 1986, *PASJ*, **38**, 911
- Swain, M. R., Vasisht, G., & Tinetti, G. 2008, *Natur*, **452**, 329
- Swings, P., & Rosenfeld, L. 1937, *ApJ*, **86**, 483
- Tabor, W. J. 1957, *JChPh*, **27**, 974
- Takagi, K., & Kojima, T. 1973, *ApJL*, **181**, L91
- Takano, M., Sasada, Y., & Satoh, T. 1968, *JMoSp*, **26**, 157
- Tanaka, K., Sumiyoshi, Y., Ohshima, Y., Endo, Y., & Kawaguchi, K. 1997, *JChPh*, **107**, 2728
- Tang, J., Sumiyoshi, Y., & Endo, Y. 1999, *CPL*, **315**, 69
- Tanimoto, M., Klaus, T., Müller, H. S. P., & Winnewisser, G. 2000, *JMoSp*, **199**, 73
- Tenenbaum, E. D., Woolf, N. J., & Ziurys, L. M. 2007, *ApJL*, **666**, L29
- Tenenbaum, E. D., & Ziurys, L. M. 2008, *ApJL*, **680**, L121
- Tenenbaum, E. D., & Ziurys, L. M. 2009, *ApJL*, **694**, L59
- Tenenbaum, E. D., & Ziurys, L. M. 2010, *ApJL*, **712**, L93
- Tercero, B., Cernicharo, J., Cuadrado, S., de Vicente, P., & Guélin, M. 2020, *A&A*, **636**, L7
- Tercero, B., Kleiner, I., Cernicharo, J., et al. 2013, *ApJL*, **770**, L13
- Tercero, B., Margulès, L., Carvajal, M., et al. 2012, *A&A*, **538**, A119
- Tercero, B., Cernicharo, J., López, A., et al. 2015, *A&A*, **582**, L1
- Thaddeus, P., Cummins, S. E., & Linke, R. A. 1984, *ApJL*, **283**, L45
- Thaddeus, P., Gottlieb, C. A., Gupta, H., et al. 2008, *ApJ*, **677**, 1132
- Thaddeus, P., Gottlieb, C. A., Hjalmarsen, Å., et al. 1985a, *ApJL*, **294**, L49
- Thaddeus, P., Guélin, M., & Linke, R. A. 1981, *ApJL*, **246**, L41
- Thaddeus, P., Kutner, M. L., Penzias, A. A., Wilson, R. W., & Jefferts, K. B. 1972, *ApJL*, **176**, L73
- Thaddeus, P., & Turner, B. E. 1975, *ApJL*, **201**, L25
- Thaddeus, P., Vrtilke, J. M., & Gottlieb, C. A. 1985b, *ApJL*, **299**, L63
- Thi, W.-F., van Dishoeck, E. F., Blake, G. A., van Zadelhoff, G.-J., & Hogerheijde, M. R. 1999, *ApJL*, **521**, L63
- Thi, W. F., Ménard, F., Meeus, G., et al. 2011, *A&A*, **530**, L2
- Thiel, V., Belloche, A., Menten, K. M., Garrod, R. T., & Müller, H. S. P. 2017, *A&A*, **605**, L6
- Thompson, R. I., Lebofsky, M. J., & Rieke, G. H. 1978, *ApJL*, **222**, L49
- Thomson, R., & Dalby, F. W. 1968, *CaJPh*, **46**, 2815
- Thorwirth, S., & Lichau, H. 2003, *A&A*, **398**, L11
- Thorwirth, S., McCarthy, M. C., Dudek, J. B., & Thaddeus, P. 2004a, *JMoSp*, **225**, 93
- Thorwirth, S., Müller, H. S. P., Lichau, H., Winnewisser, G., & Mellau, G. C. 2004b, *JMoSt*, **695**, 263
- Thorwirth, S., Müller, H. S. P., & Winnewisser, G. 2000, *JMoSp*, **199**, 116
- Thorwirth, S., Harding, M. E., Asvany, O., et al. 2020, *MolPh*, **118**, e1776409
- Tielens, A. G. G. M. 2005, *The Physics and Chemistry of the Interstellar Medium* (Cambridge: Cambridge Univ. Press)
- Tielens, A. G. G. M. 2008, *ARA&A*, **46**, 289
- Tinetti, G., Vidal-Madjar, A., Liang, M.-C., et al. 2007, *Natur*, **448**, 169
- Törring, T. 1968, *ZNatA*, **23**, 777
- Törring, T., Bekooy, J. P., Meerts, W. L., et al. 1980, *JChPh*, **73**, 4875
- Townes, C. H. 1946, *PhRv*, **70**, 665
- Townes, C. H., & Schawlow, A. L. 1975, *Microwave Spectroscopy* (New York: Dover)
- Trambarulo, R., & Gordy, W. 1950, *JChPh*, **18**, 1613
- Travers, M. J., McCarthy, M. C., Gottlieb, C. A., & Thaddeus, P. 1996a, *ApJL*, **465**, L77
- Travers, M. J., McCarthy, M. C., Gottlieb, C. A., & Thaddeus, P. 1997, *ApJL*, **483**, L135
- Travers, M. J., McCarthy, M. C., Kalmus, P., Gottlieb, C. A., & Thaddeus, P. 1996b, *ApJL*, **469**, L65
- Tsunekawa, S. 1972, *JPSJ*, **33**, 167
- Tucker, K. D., Kutner, M. L., & Thaddeus, P. 1974, *ApJL*, **193**, L115
- Tudorie, M., Kleiner, I., Hogen, J. T., et al. 2011, *JMoSp*, **269**, 211
- Turner, B. E. 1971, *ApJL*, **163**, L35
- Turner, B. E. 1974, *ApJL*, **193**, L83
- Turner, B. E. 1977, *ApJL*, **213**, L75
- Turner, B. E. 1989, *ApJS*, **70**, 539
- Turner, B. E. 1992a, *ApJL*, **396**, L107
- Turner, B. E. 1992b, *ApJL*, **388**, L35
- Turner, B. E., & Apponi, A. J. 2001, *ApJL*, **561**, L207
- Turner, B. E., & Bally, J. 1987, *ApJL*, **321**, L75
- Turner, B. E., Liszt, H. S., Kaifu, N., & Kisliakov, A. G. 1975, *ApJL*, **201**, L149
- Turner, B. E., Steimle, T. C., & Meerts, L. 1994, *ApJL*, **426**, L97
- Tyler, J. K., & Sheridan, J. 1963, *Trans. Faraday Soc.*, **59**, 2661
- Tyler, J. K., Sheridan, J., & Costain, C. C. 1972, *JMoSp*, **43**, 248
- Ulich, B. L., Hollis, J. M., & Snyder, L. E. 1977, *ApJL*, **217**, L105
- Usero, A., García-Burillo, S., Fuente, A., Martín-Pintado, J., & Rodríguez-Fernández, N. J. 2004, *A&A*, **419**, 897
- Vacherand, J. M., Van Eijck, B. P., Burie, J., & Demaison, J. 1986, *JMoSp*, **118**, 355
- Vala, M., Chandrasekhar, T. M., Szczepanski, J., Van Zee, R., & Weltner Jr, W. 1989, *JChPh*, **90**, 595
- van Broekhuizen, F. A., Pontoppidan, K. M., Fraser, H. J., & van Dishoeck, E. F. 2005, *A&A*, **441**, 249
- van der Tak, F. 2011, *IAU Symp. 280, The Molecular Universe* (San Francisco, CA: ASP), 449

- van der Tak, F. F. S., Aalto, S., & Meijerink, R. 2008, *A&A*, **477**, L5
- van der Werf, P. P., Isaak, K. G., Meijerink, R., et al. 2010, *A&A*, **518**, L42
- van Dishoeck, E. F., Jansen, D. J., Schilke, P., & Phillips, T. G. 1993, *ApJL*, **416**, L83
- van Dishoeck, E. F., Thi, W. F., & van Zadelhoff, G. J. 2003, *A&A*, **400**, L1
- van Dishoeck, E. F., Helmich, F. P., de Graauw, T., et al. 1996, *A&A*, **315**, L349
- van Vaals, J. J., Meerts, W. L., & Dymanus, A. 1984, *CP*, **86**, 147
- van Zadelhoff, G. J., van Dishoeck, E. F., Thi, W. F., & Blake, G. A. 2001, *A&A*, **377**, 566
- von Czarowski, A., & Meiwes-Broer, K. H. 1995, *CPL*, **246**, 321
- Vrtilek, J. M., Gottlieb, C. A., Gottlieb, E. W., Wang, W., & Thaddeus, P. 1992, *ApJL*, **398**, L73
- Vrtilek, J. M., Gottlieb, C. A., & Thaddeus, P. 1987, *ApJ*, **314**, 716
- Vrtilek, J. M., Thaddeus, P., Gottlieb, C. A., Gottlieb, E. W., & Killian, T. C. 1990, *ApJL*, **364**, L53
- Wagener, V., Winnewisser, M., & Bellini, M. 1995, *JMoSp*, **170**, 323
- Walker, G. A. H., Bohlender, D. A., Maier, J. P., & Campbell, E. K. 2015, *ApJL*, **812**, L8
- Wallström, S. H. J., Muller, S., Roueff, E., et al. 2019, *A&A*, **629**, A128
- Walmsley, C. M., Bachiller, R., Pineau des Forêts, G., & Schilke, P. 2002, *ApJL*, **566**, L109
- Walmsley, C. M., Jewell, P. R., Snyder, L. E., & Winnewisser, G. 1984, *A&A*, **134**, L11
- Walsh, C., Millar, T. J., Nomura, H., et al. 2014, *A&A*, **563**, A33
- Walsh, C., Vissapragada, S., & McGee, H. 2018, IAU Symp. 332, *Astrochemistry VII: Through the Cosmos from Galaxies to Planets* (Cambridge: Cambridge Univ. Press), 395
- Walsh, C., Loomis, R. A., Öberg, K. I., et al. 2016, *ApJL*, **823**, L10
- Wang, J., Li, D., Goldsmith, P. F., et al. 2020, *ApJ*, **889**, 129
- Weinreb, S., Barrett, A. H., Meeks, M. L., & Henry, J. C. 1963, *Natur*, **200**, 829
- Weiß, A., Requena-Torres, M. A., Güsten, R., et al. 2010, *A&A*, **521**, L1
- Weliachew, L. 1971, *ApJL*, **167**, L47
- Welty, D. E., Howk, J. C., Lehner, N., & Black, J. H. 2013, *MNRAS*, **428**, 1107
- Whiteoak, J. B., Gardner, F. F., & Hoglund, B. 1980, *MNRAS*, **190**, 17P
- Widicus Weaver, S. L., Laas, J. C., Zou, L., et al. 2017, *ApJS*, **232**, 3
- Willacy, K. 2003, *ApJL*, **600**, L87
- Wilson, R. W., Jefferts, K. B., & Penzias, A. A. 1970, *ApJL*, **161**, L43
- Wilson, R. W., Penzias, A. A., Jefferts, K. B., Kutner, M., & Thaddeus, P. 1971, *ApJL*, **167**, L97
- Wilson, S., & Green, S. 1977, *ApJL*, **212**, L87
- Winnewisser, G. 1973, *JMoSp*, **46**, 16
- Winnewisser, G., & Churchwell, E. 1975, *ApJL*, **200**, L33
- Winnewisser, G., & Walmsley, C. M. 1978, *A&A*, **70**, L37
- Winnewisser, M., Sastry, K. V. L. N., Cook, R. L., & Gordy, W. 1964, *JChPh*, **41**, 1687
- Winnewisser, M., & Schäfer, E. 1980, *ZNatA*, **35**, 483
- Winnewisser, M., Seibert, J. W. G., & Yamada, K. M. T. 1992, *JMoSp*, **153**, 635
- Winnewisser, M., & Winnewisser, B. P. 1971, *ZNatA*, **26**, 128
- Winnewisser, M., Winnewisser, G., Honda, T., & Hirota, E. 1975, *Z. Naturforsch.*, **30**, 1001
- Włodarczak, G., Boucher, D., Bocquet, R., & Demaison, J. 1986, *JMoSp*, **116**, 251
- Włodarczak, G., & Demaison, J. 1988, *A&A*, **192**, 313
- Włodarczak, G., Demaison, J., Heineking, N., & Császár, A. G. 1994, *JMoSp*, **167**, 239
- Wohlhart, K., Schnell, M., Grabow, J.-U., & Küpper, J. 2008, *JMoSp*, **247**, 119
- Wong, M., Ozier, I., & Meerts, W. L. 1983, *JMoSp*, **102**, 89
- Woods, R. C., Dixon, T. A., Saykally, R. J., & Szanto, P. G. 1975, *PhRvL*, **35**, 1269
- Woods, R. C., Gudeman, C. S., Dickman, R. L., et al. 1983, *ApJ*, **270**, 583
- Woon, D. E. 2002, *ApJ*, **569**, 541
- Wootten, A., Boulanger, F., Bogey, M., et al. 1986, *A&A*, **166**, L15
- Wootten, A., Turner, B. E., Mangum, J. G., et al. 1991, *ApJL*, **380**, L79
- Wyrowski, F., Menten, K. M., Güsten, R., & Belloche, A. 2010, *A&A*, **518**, A26
- Wyse, F. C., Gordy, W., & Pearson, E. F. 1970, *JChPh*, **52**, 3887
- Wyse, F. C., Manson, E. L., & Gordy, W. 1972, *JChPh*, **57**, 1106
- Xue, C., Willis, E. R., Loomis, R. A., et al. 2020, *ApJL*, **900**, L9
- Yamada, C., Cohen, E. A., Fujitake, M., & Hirota, E. 1990, *JChPh*, **92**, 2146
- Yamada, C., Hirota, E., & Kawaguchi, K. 1981, *JChPh*, **75**, 5256
- Yamada, C., Saito, S., Kanamori, H., & Hirota, E. 1985, *ApJL*, **290**, L65
- Yamamoto, S., & Saito, S. 1992, *JChPh*, **96**, 4157
- Yamamoto, S., Saito, S., Kawaguchi, K., et al. 1987a, *ApJL*, **317**, L119
- Yamamoto, S., Saito, S., Ohishi, M., et al. 1987b, *ApJL*, **322**, L55
- Zack, L. N., Halfen, D. T., & Ziurys, L. M. 2011, *ApJL*, **733**, L36
- Zaleski, D. P., Seifert, N. A., Steber, A. L., et al. 2013, *ApJL*, **765**, L10
- Zeng, S., Quenard, D., Jimenez-Serra, I., et al. 2019, *MNRAS*, **484**, L43
- Zhang, K., Bergin, E. A., Blake, G. A., et al. 2017, *NatAs*, **1**, 0130
- Zhou, Y., Quan, D.-H., Zhang, X., & Qin, S.-L. 2020, *RAA*, **20**, 125
- Ziurys, L. M. 1987, *ApJL*, **321**, L81
- Ziurys, L. M., & Apponi, A. J. 1995, *ApJL*, **455**, L73
- Ziurys, L. M., Apponi, A. J., Guélin, M., & Cernicharo, J. 1995, *ApJL*, **445**, L47
- Ziurys, L. M., Apponi, A. J., Hollis, J. M., & Snyder, L. E. 1994a, *ApJL*, **436**, L181
- Ziurys, L. M., Apponi, A. J., & Phillips, T. G. 1994b, *ApJ*, **433**, 729
- Ziurys, L. M., Hollis, J. M., & Snyder, L. E. 1994c, *ApJ*, **430**, 706
- Ziurys, L. M., Savage, C., Highberger, J. L., et al. 2002, *ApJL*, **564**, L45
- Ziurys, L. M., & Turner, B. E. 1986, *ApJL*, **302**, L31
- Zuckerman, B., Ball, J. A., & Gottlieb, C. A. 1971, *ApJL*, **163**, L41
- Zuckerman, B., Morris, M., Palmer, P., & Turner, B. E. 1972, *ApJL*, **173**, L125
- Zuckerman, B., Turner, B. E., Johnson, D. R., et al. 1975, *ApJL*, **196**, L99